

LARGE-SCALE GALACTIC DYNAMICS

THE PERSPECTIVE FROM SIMULATIONS

FLORENT RENAUD | LUND OBSERVATORY

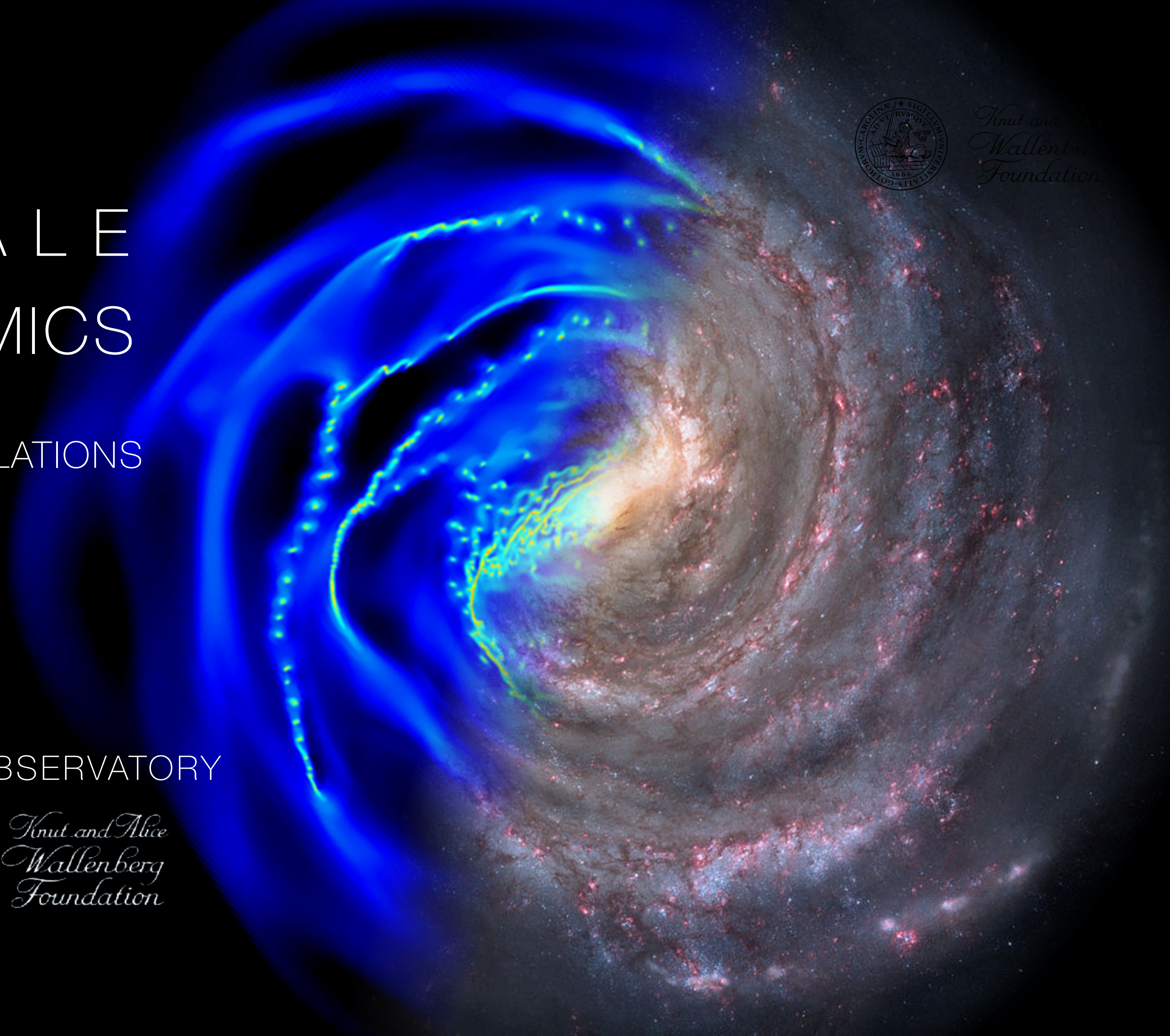
florent@astro.lu.se
@renaudflo



*Knut and Alice
Wallenberg
Foundation*



*Knut and Alice
Wallenberg
Foundation*



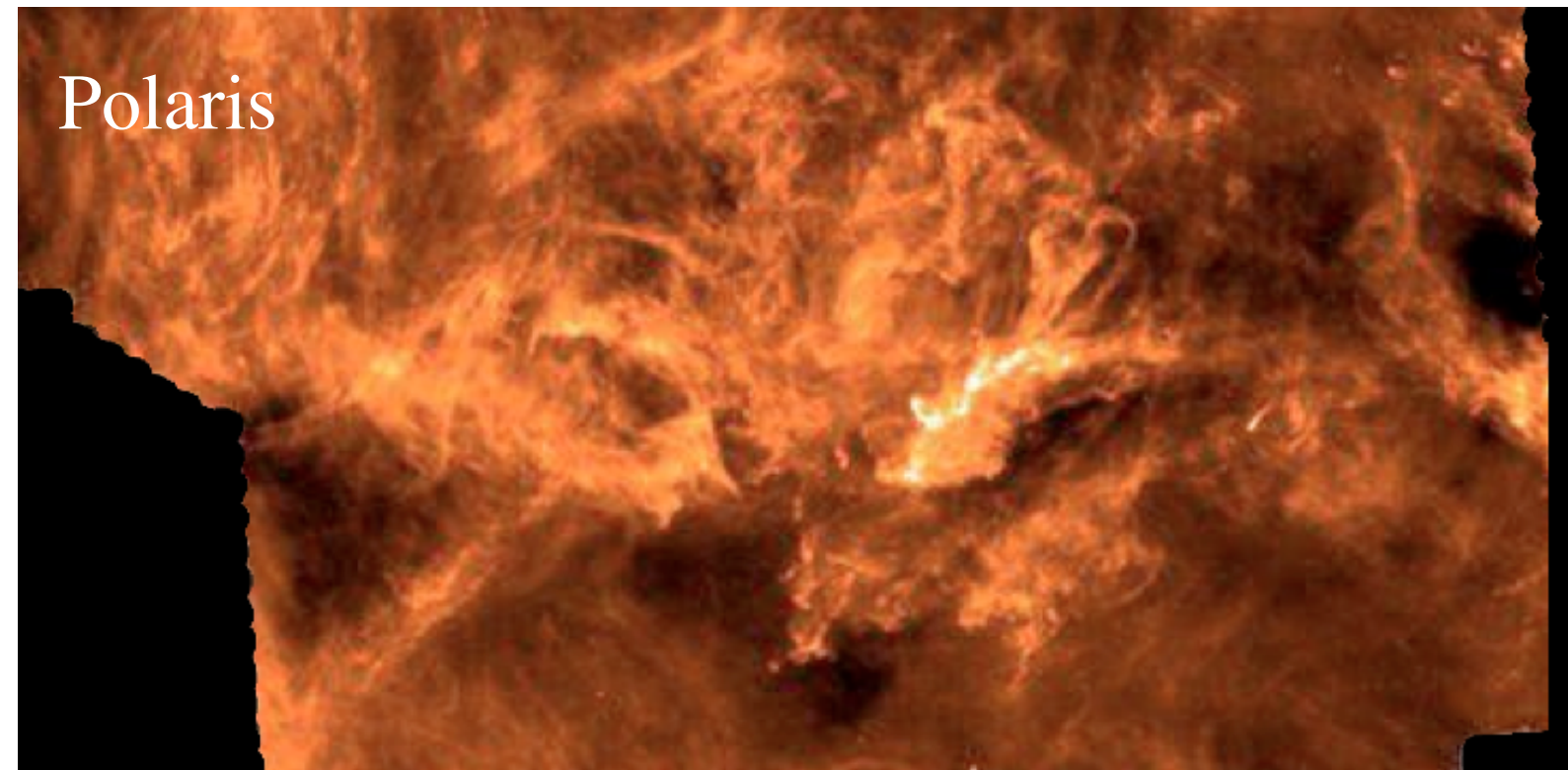
DISCLAIMER

It is impossible to fully cover this topic in 2 hours.

This lecture aims at being a starting point to explore this field in more details.

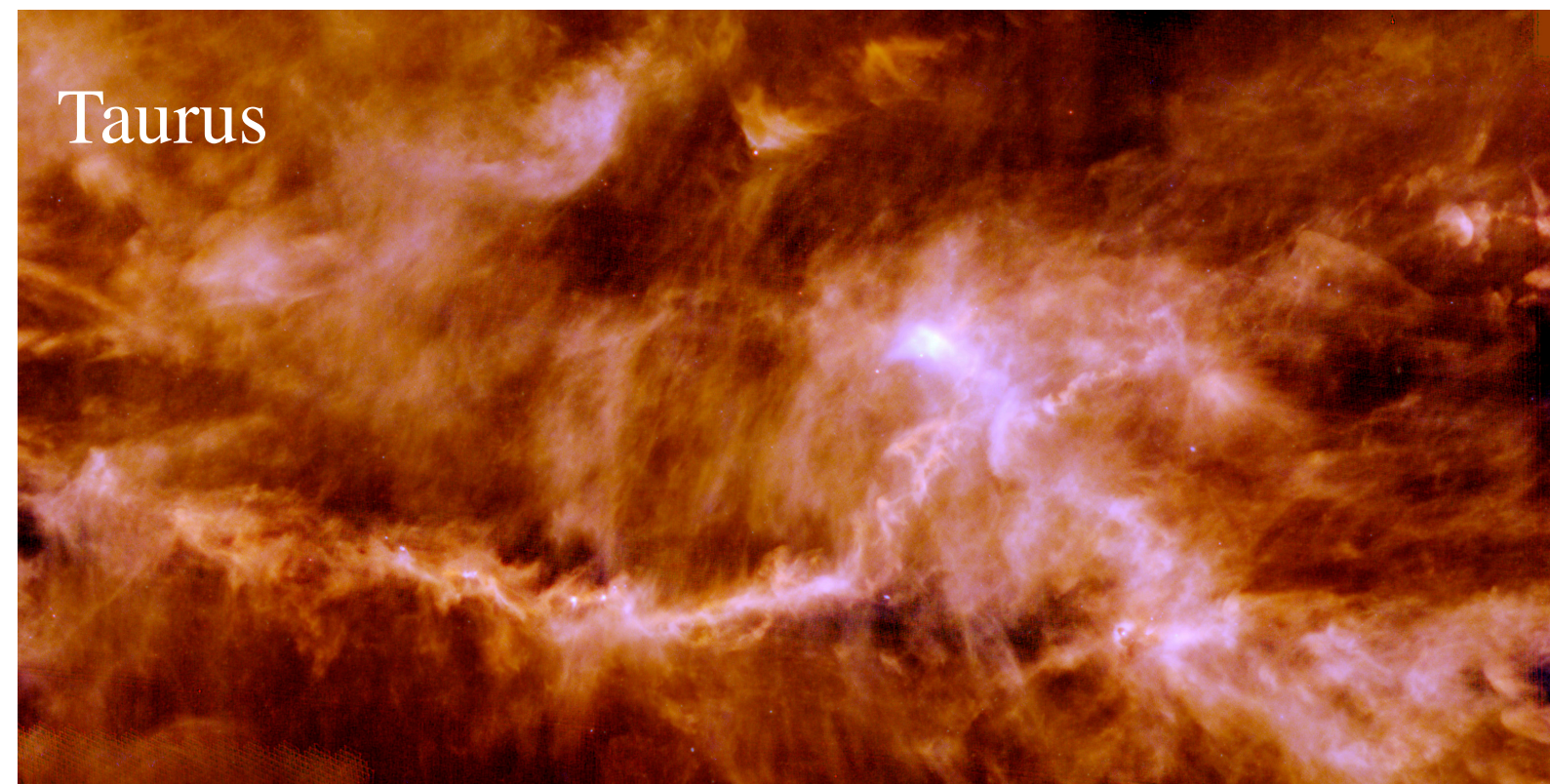
It is biased towards my personal interests and own work.

UNIVERSAL(?) STAR FORMATION IN A DIVERSITY OF ENVIRONMENTS

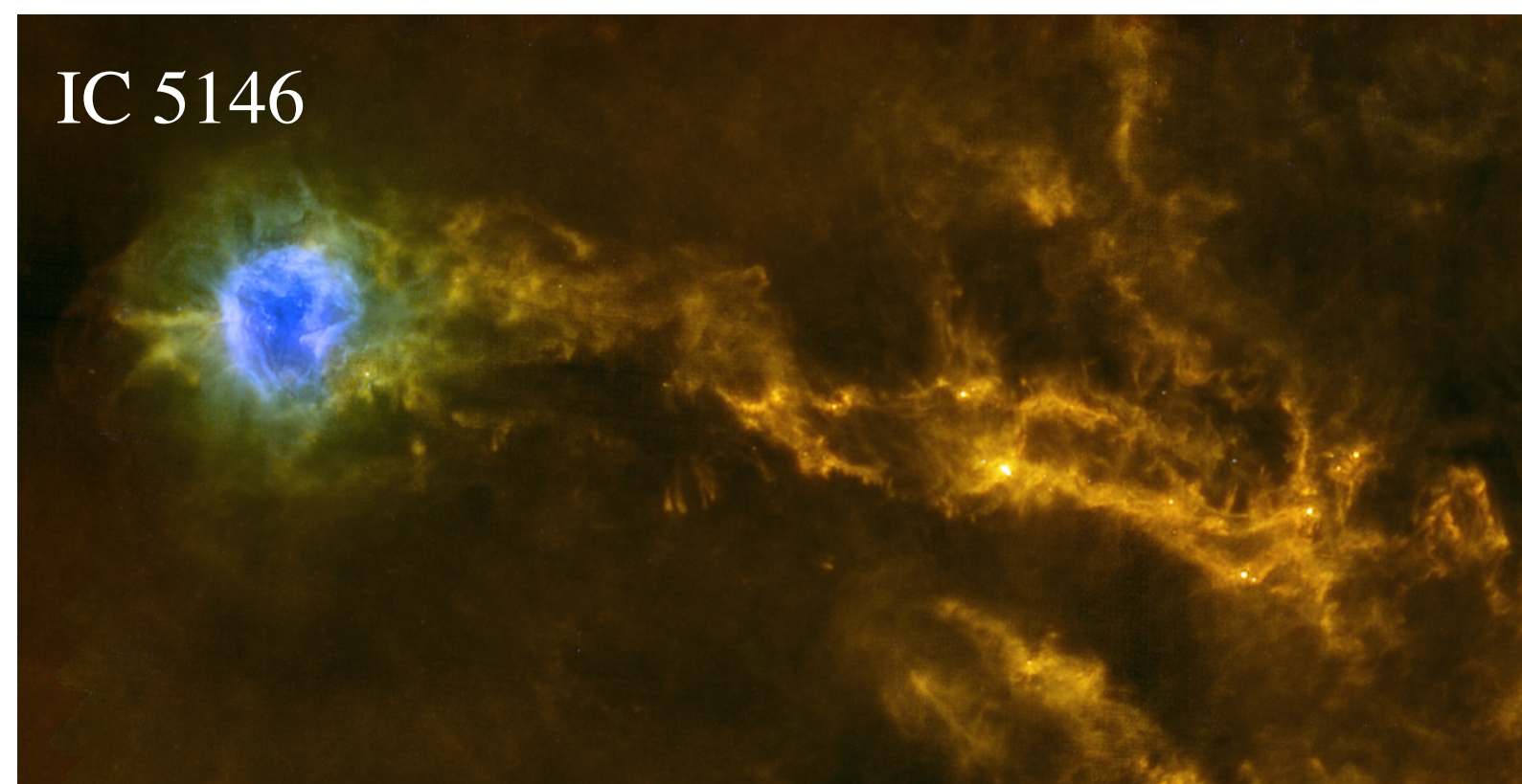


Star formation appears to be universal:

- filamentary structure
- diameter of ~ 0.1 pc
- extinction threshold of $A_v > 7$
- pre-stellar cores in knots
- cluster formation at intersections
- universal initial mass function (IMF)

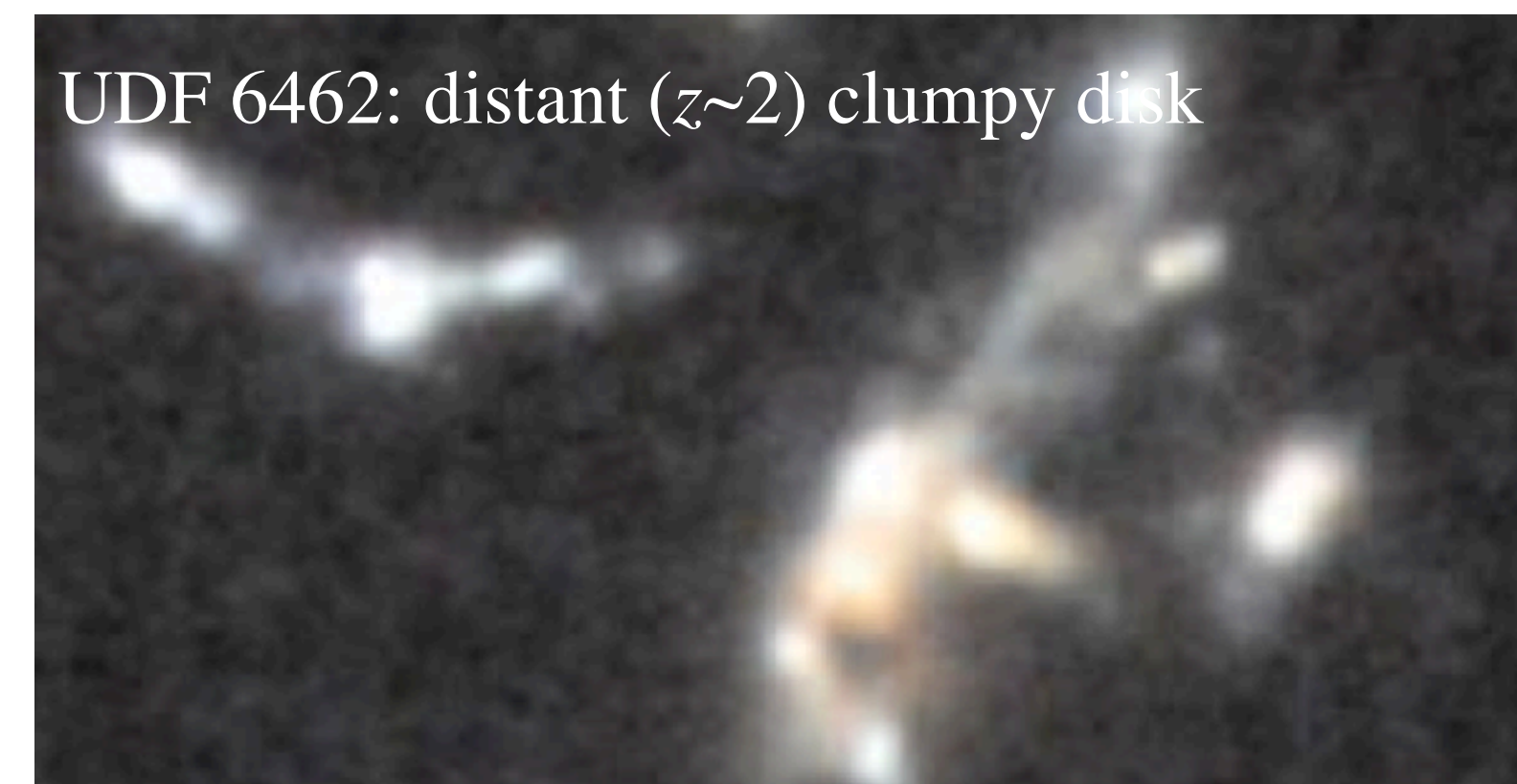


This universality is observed ...
where it can be resolved!
i.e. in the solar neighborhood,
i.e. in 1 single environment



But looking further reveals:

- different cluster formation
- variations of the IMF
- role of disk structures (spirals, bars)
- impact of interactions and mergers
- evolution with redshift
- ...



COSMIC EVOLUTION OF STAR FORMATION

The evolution of the conditions in the ISM, along galaxy formation/evolution, impacts star formation

- galaxy mergers (triggering starbursts)
(density of the Universe $\propto (1+z)^3$)
- formation of the disks
- formation of substructures (spirals, bars)
- lowering of the gas fraction
- lowering of the turbulence

The peak of SFR occurred at redshift ~ 2
(statistically speaking, not for all galaxies)

On average, most galaxies form less and less stars

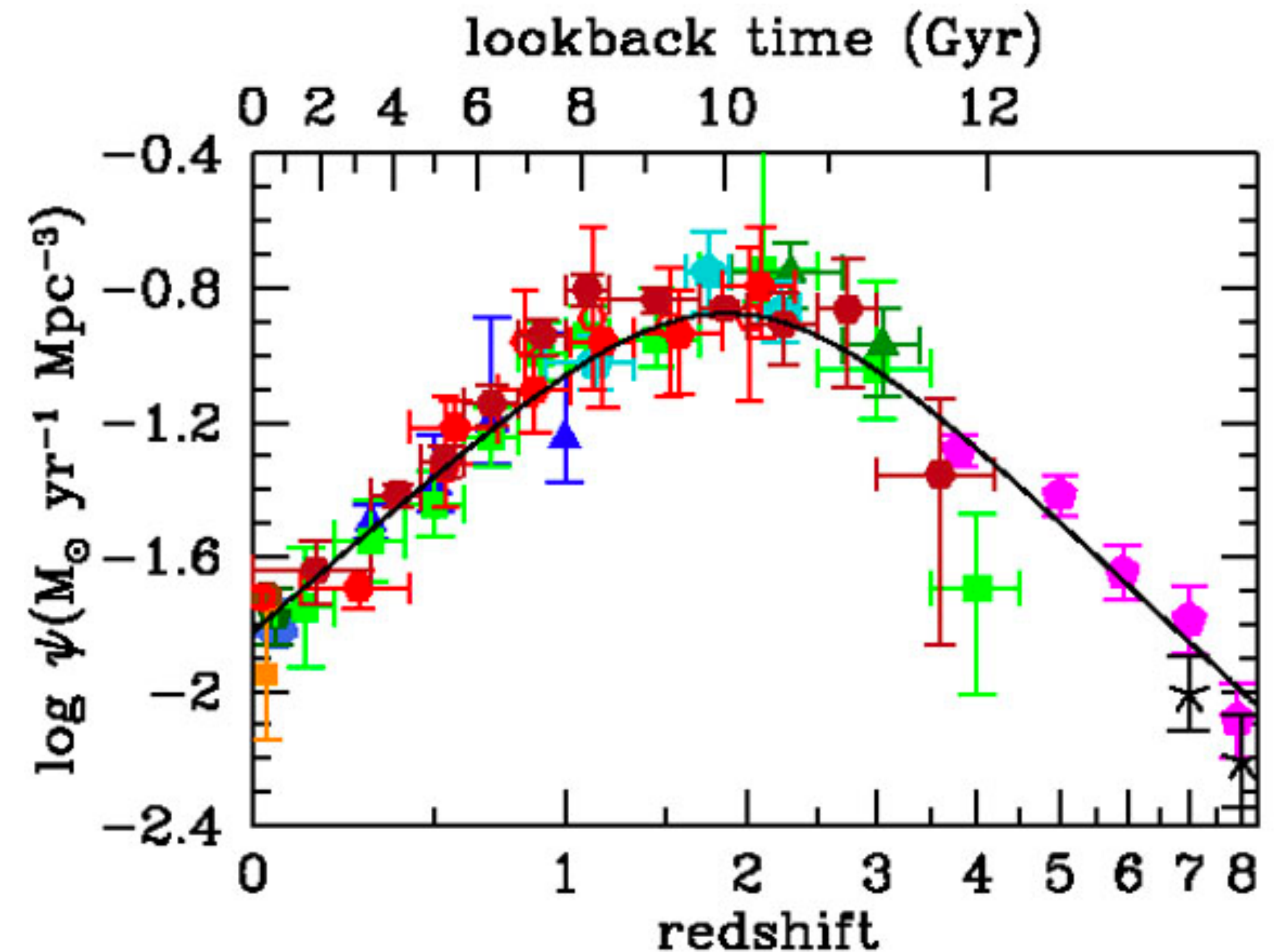


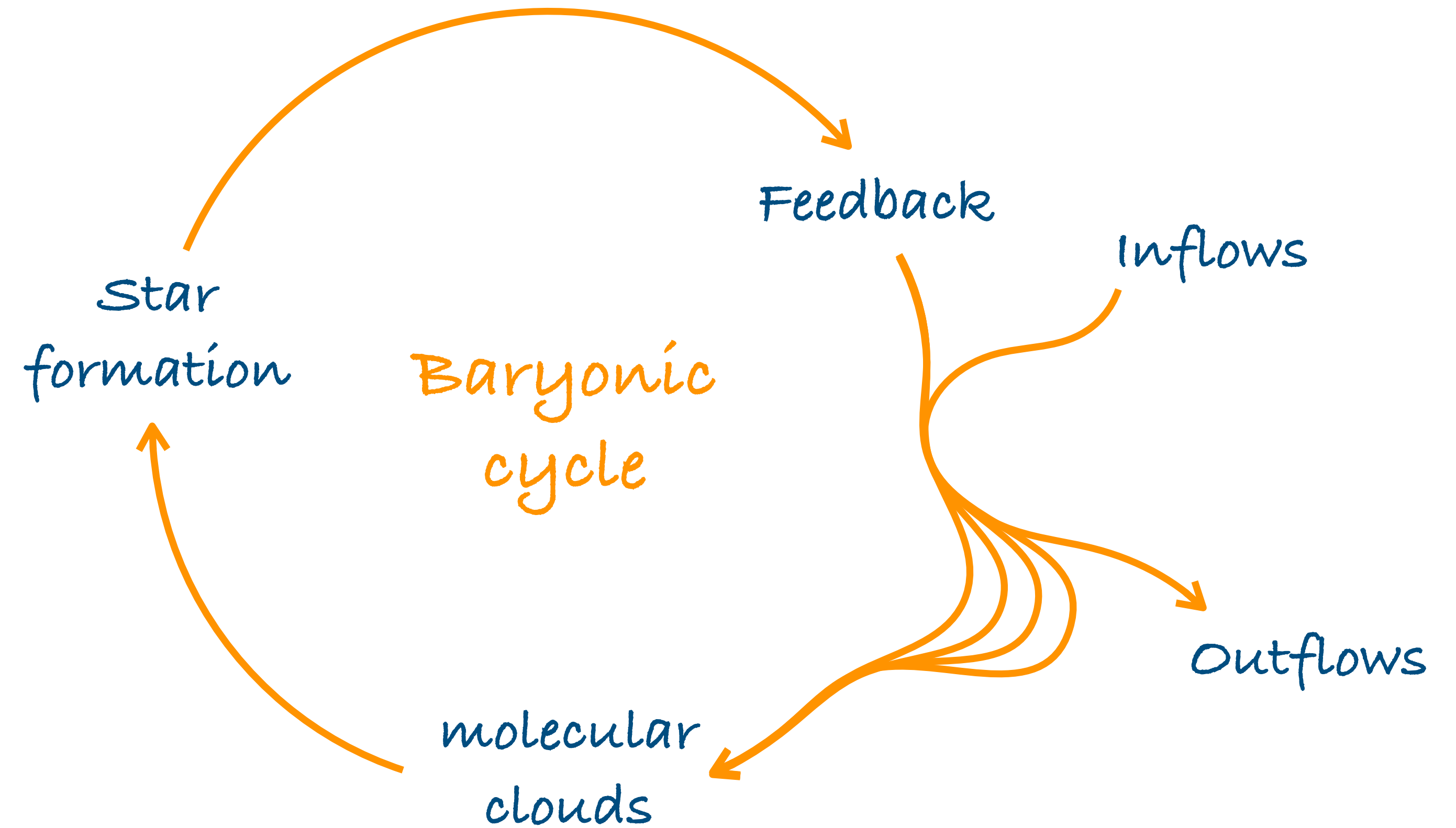
Fig: SFR density (per unit comoving volume) as function of redshift (Madau & Dickinson 2014)

BARYONIC CYCLE

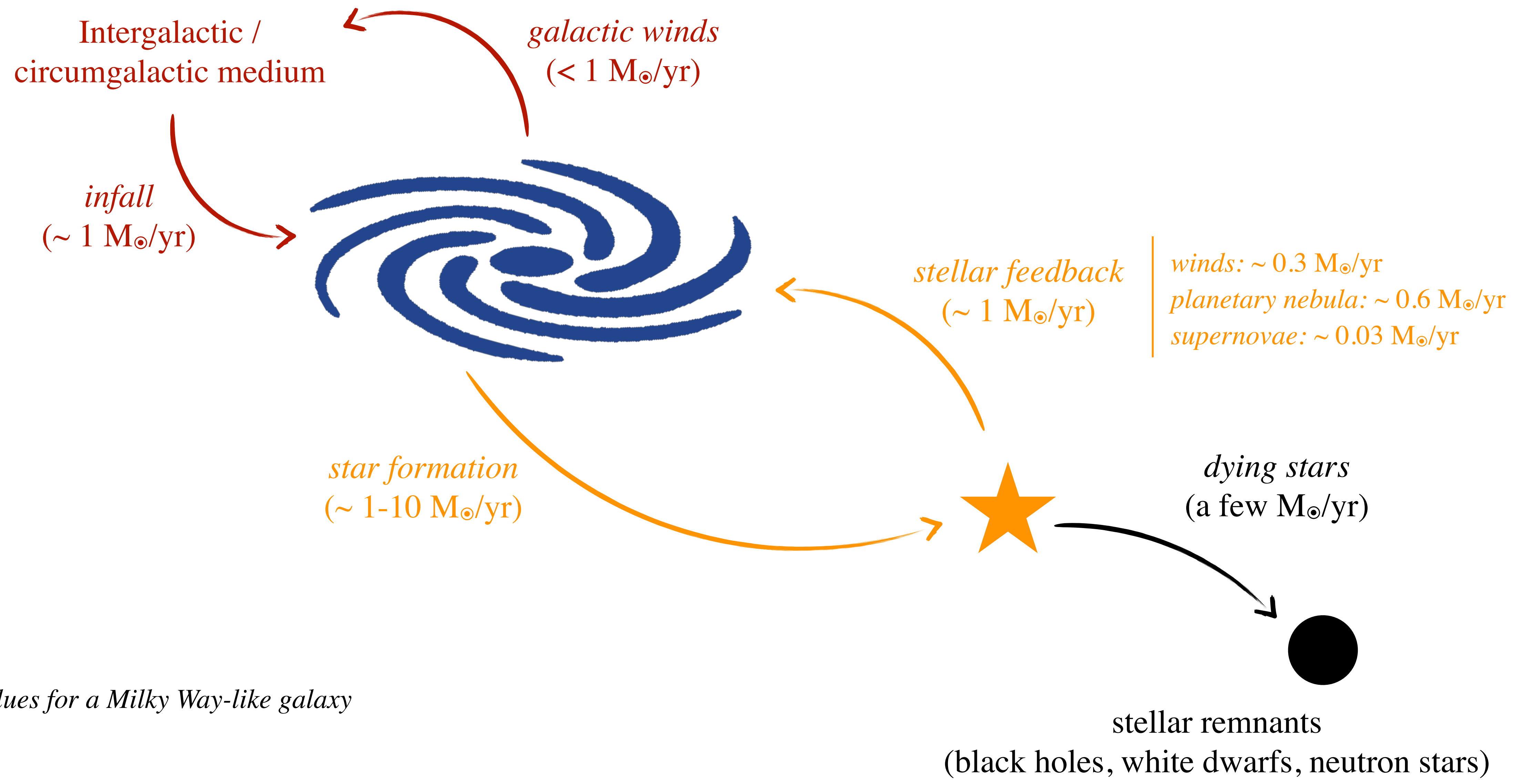
The recycling of gas is set at galactic scale

To understand galaxy formation and the ISM in galaxies, we first need to answer these questions:

- how much gas is available in the galaxy?
- where is this gas (corona, inter-arm, clouds ...)?
- in which physical state (density, temperature) this gas is?
- how / how fast does this change?



GAS FLOWS



typical values for a Milky Way-like galaxy

PHASE DIAGRAM

Phase diagrams can be plotted from simulations. They depend on the physics considered and resolution and can vary a lot. Only generic features are presented here.

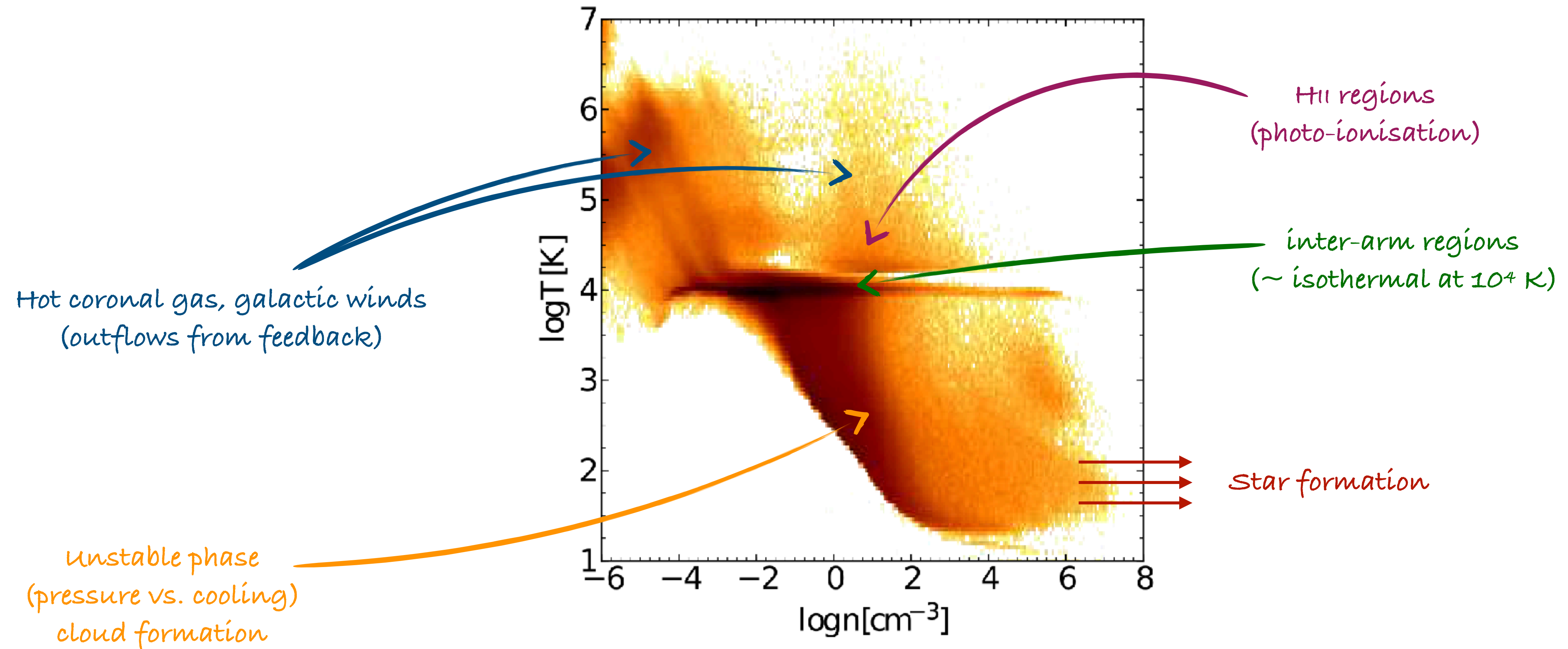
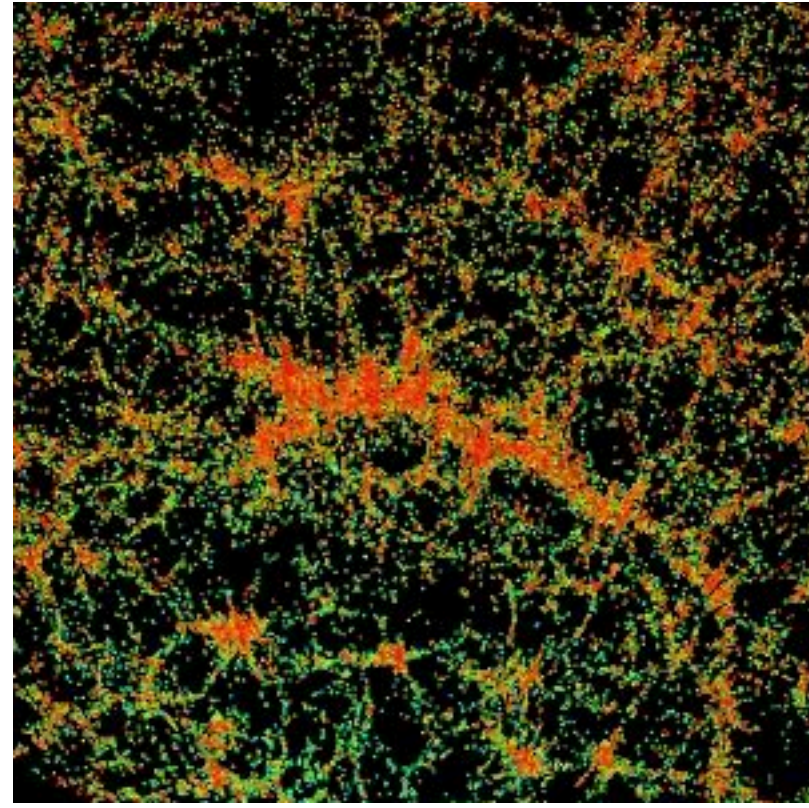


*Fig: phase diagram
(adapted from Marinacci et al. 2019)*

A MULTI-SCALE AND MULTI-PHYSICS TOPIC



cosmological

10 Mpc
1 Gyr

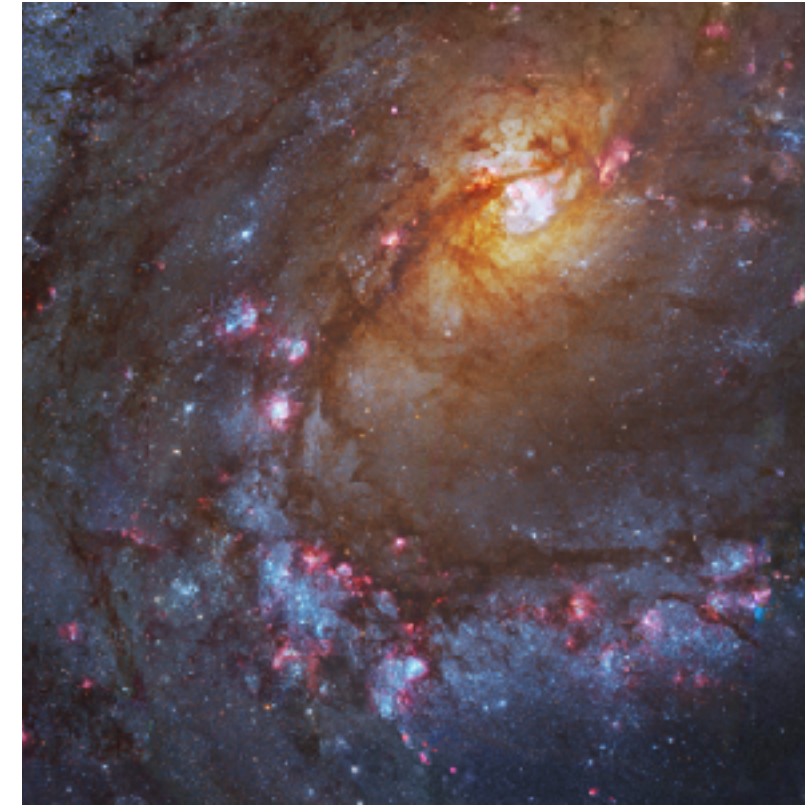
structures

100 kpc
100 Myr



galaxy

formation



galactic

dynamics

1 kpc
10 Myr



star

formation

10 pc
1 Myr



star cluster

evolution

0.1 pc
0.1 Myr

gas inflows

mergers

outflows, galactic winds

turbulence

shear

magnetic fields

stellar evolution

stellar feedback

gravitation, tides

WHY SIMULATIONS?

Compared to observations, simulations can provide:

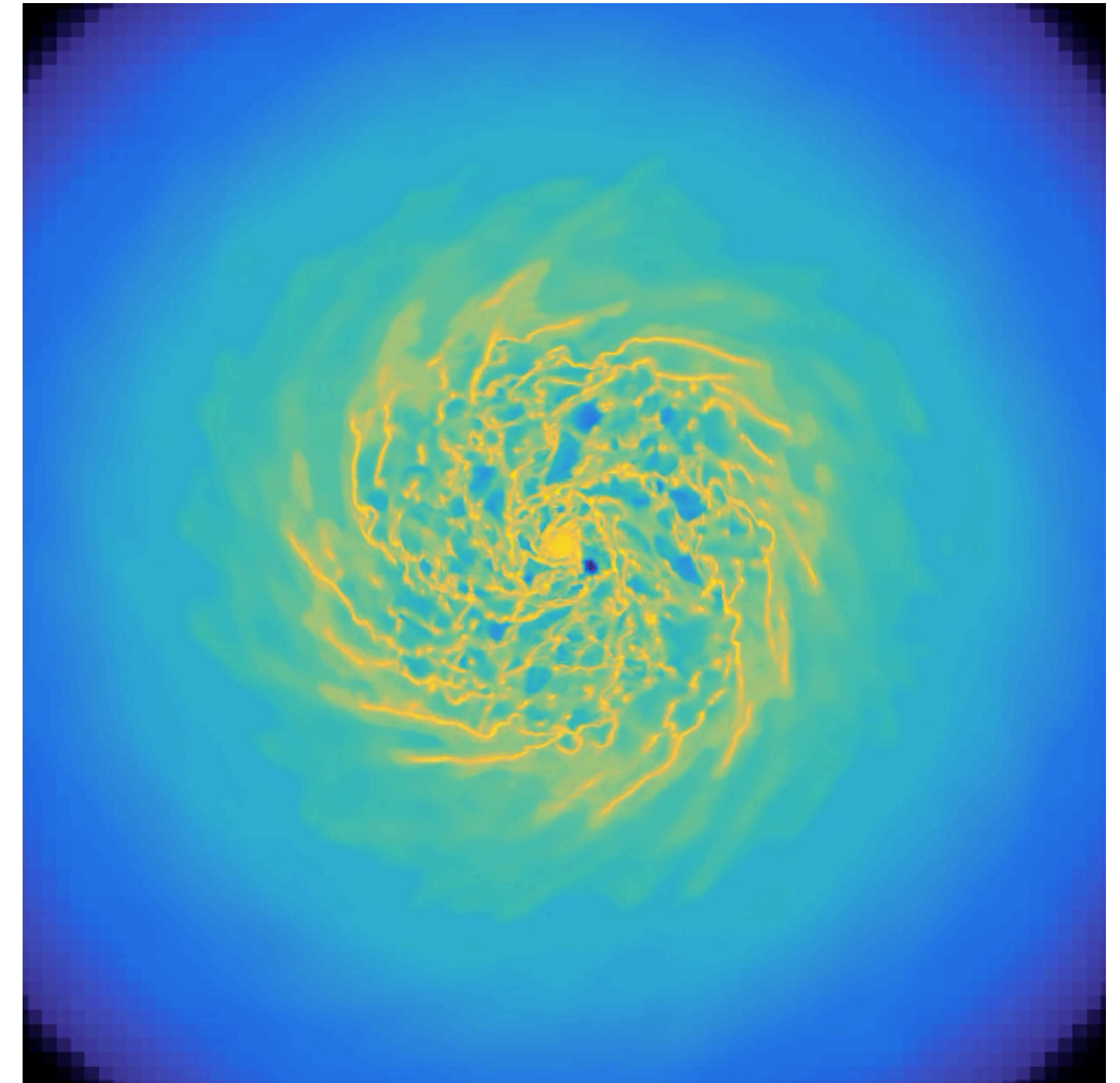
- access to time, evolution
- 3D structure
- easier measurements of dynamical quantities (mass, acceleration)
- higher resolution (except in the Milky Way)
- control on the initial and boundary conditions

Simulations are (and should be considered as) expensive *experiments*

They are used to simplify the reality, and help the interpretation of complex physical phenomena, and of their interplay

Linking simulation results back to reality is difficult

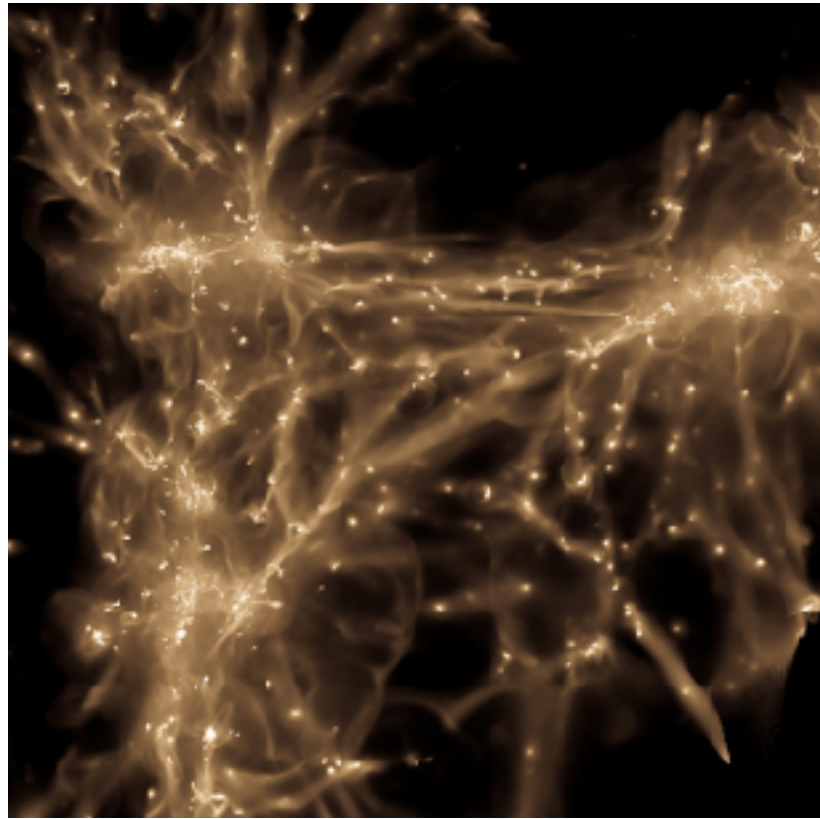
Never trust a computer!



Movie: gas density in a simulation of a local disk galaxy (Renaud et al. 2021c)

SEVERAL TYPES OF GALAXY SIMULATIONS

New Horizon
Dubois et al. (2021)



cosmological volume

size: > 10 Mpc
res.: ~100-500 pc

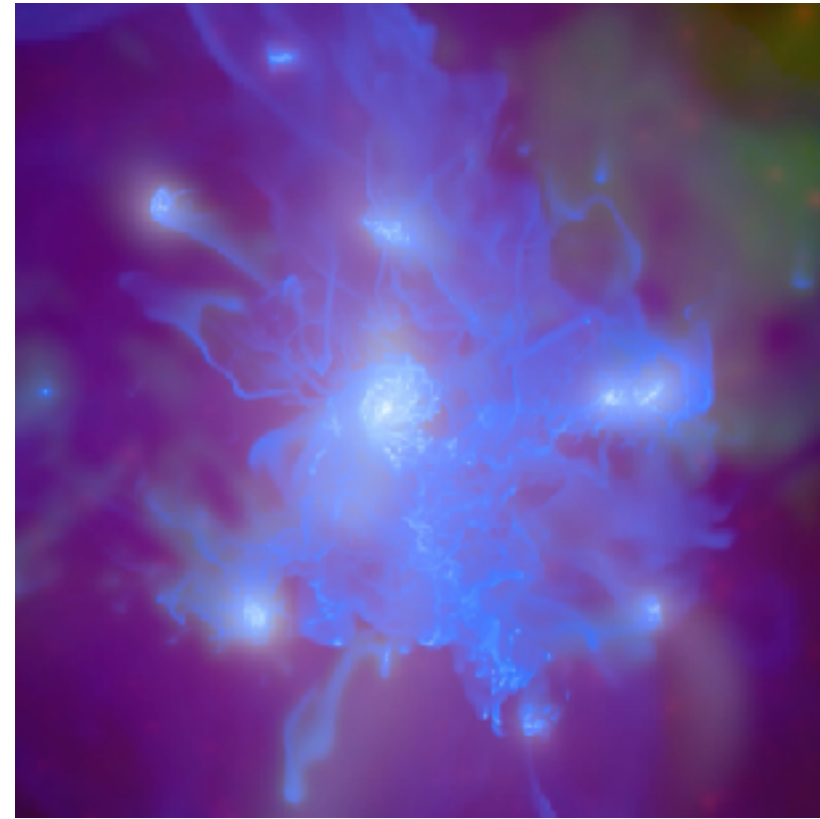


- initial conditions (CMB)
- statistics on galaxy pop.



- poor resolution for describing star formation and feedback
- barely resolves galactic disks

Vintergatan
Agertz et al. (2021)
Renaud et al. (2021a,b)



cosmological zoom-in

size: ~1 Mpc
res.: ~10-100 pc

- initial conditions (CMB)
- some can capture GMCs

- only one galaxy
- do not resolve internal GMC physics
- very expensive to run

Renaud et al. (2021c)



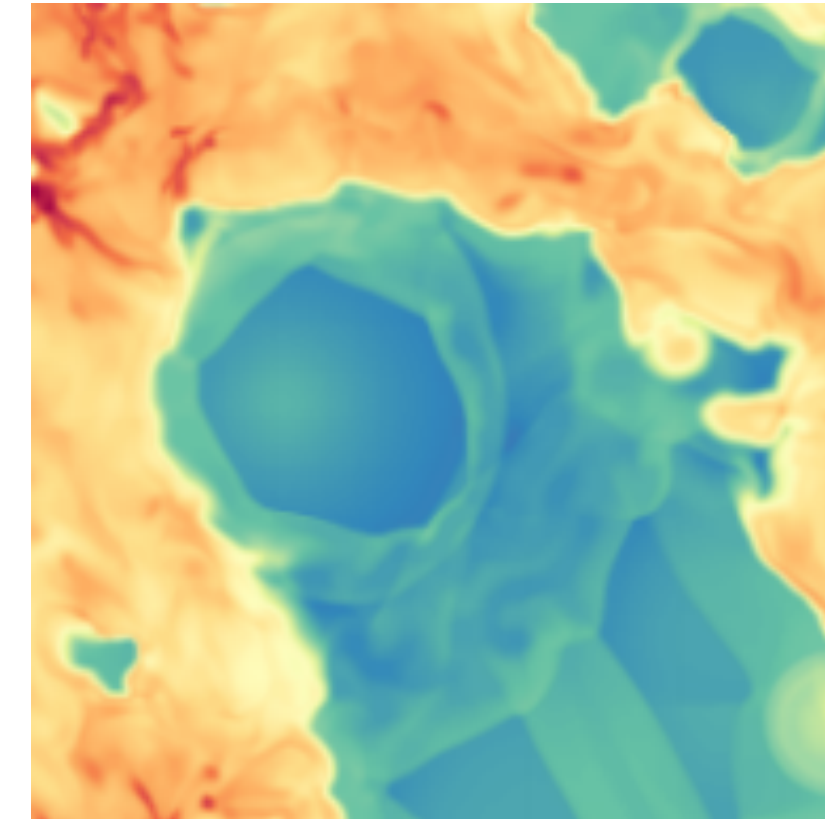
isolated galaxy

size: ~100 kpc
res.: ~0.1-10 pc

- control on the parameters
- can be cheap to run

- not realistic environment (mergers and gas accretion missing)
- relies on artificial initial conditions
- can be very expensive to run

Tigress
Kim et al. (2017)



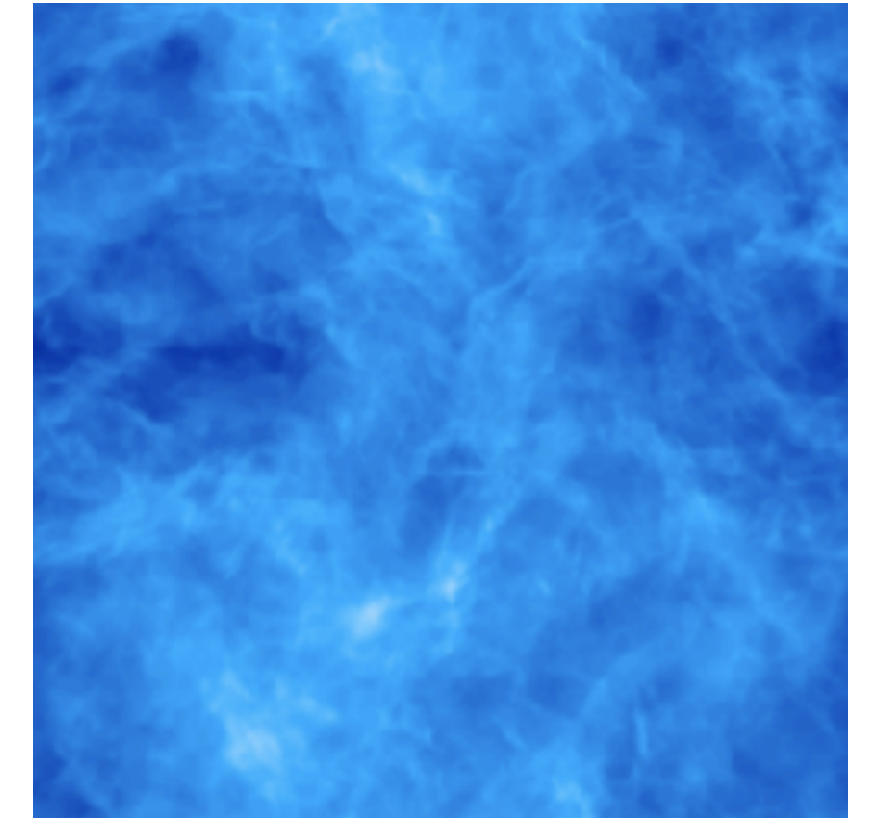
galaxy patch

size: ~0.1-1 kpc
res.: ~0.1-10 pc

- easy to setup
- relatively cheap to run

- misses several aspects of disk dynamics
- imposed instabilities
- not a huge advantage compared to isolated galaxies

Federrath et al. (2008)



ISM box

size: < 100 pc
res.: < 0.1 pc

- very high resolution
- control on the parameters

- no realistic gas recycling
- no effect of galaxy (e.g. potential, turbulence, tides, shear etc.)

WHY DO LARGE-SCALES MATTER FOR THE SMALL-SCALE ISM?

Several evidences that properties of the ISM are tightly connected to $>$ kpc scales:

- Young stars and star clusters are preferentially found along spiral arms
- Special physical conditions in the bar induce a diversity of star formation activity
 - Giant molecular associations at the tips (e.g. W43) \rightarrow possibly the formation sites of massive clusters
 - Weak star formation in the Central Molecular Zone (i.e. the central ~ 300 pc)
 - Assembly of the nuclear star cluster
- Molecular clouds are turbulent
 - Turbulence dissipates over a few Myr within a typical cloud
 - Feedback from young stars (winds, supernovae) is a source of turbulence, but ...
 - Star-free clouds (i.e. before star formation) are also turbulent \rightarrow turbulence must be injected at larger scales
 - Possible sources: differential rotation of the disk, gas accretion ...

DENSITY INCREASE AND NEED FOR SUPPORT

Stars ($\sim 10^{-7}$ pc, 10^{24} cm $^{-3}$) form in giant molecular clouds (GMC, $\sim 10 - 100$ pc, 100 cm $^{-3}$)

Density increase by 22 orders of magnitude!


Only stars younger than 10 Myr are observed in GMCs \rightarrow lifetime of GMCs: $t_{\text{GMC}} \sim 10$ Myr

(but maybe not for all of GMCs!
e.g. inter-arm clouds,
mergers, high redshift)

$$\text{Free-fall time: } t_{\text{ff}} = \sqrt{\frac{3\pi}{32G\rho}} \approx 3.6 \text{ Myr} \sqrt{\frac{100 \text{ cm}^{-3}}{n_H}}$$

$t_{\text{GMC}} > t_{\text{ff}} \rightarrow$ clouds are not in free-fall \rightarrow need for support against collapse

Another argument from stability criterion: $M_{\text{GMC}} \gg M_{\text{Jeans}} \sim M_{\text{Bonort-Ebert}} \rightarrow$ clouds should collapse, unless supported...


definitions and
derivations at the end

TURBULENCE AND THE REYNOLDS NUMBER IN SIMULATIONS

The Reynolds number quantifies the nature of a flow:

$$R_e = \frac{VL}{\nu} = \frac{\text{inertial forces}}{\text{viscous forces}}$$

velocity \rightarrow V
scale-length of the flow (e.g. diameter of the pipe) \rightarrow L
kinematic viscosity \rightarrow ν

High R_e ($\lesssim 100 - 1000$) = turbulent flow, low R_e = laminar flow

The cold ISM is highly compressible and supersonic: $R_e \sim 10^{5-7}$

In the intergalactic medium: $R_e \sim 10^{1-10}$ (uncertainties from magnetic viscosity)

Hard to estimate in simulations, but $R_e \approx \frac{2L}{\Delta x} \sim 10^{2-4} \rightarrow$ much smaller than reality
see Teyssier (2015) for details

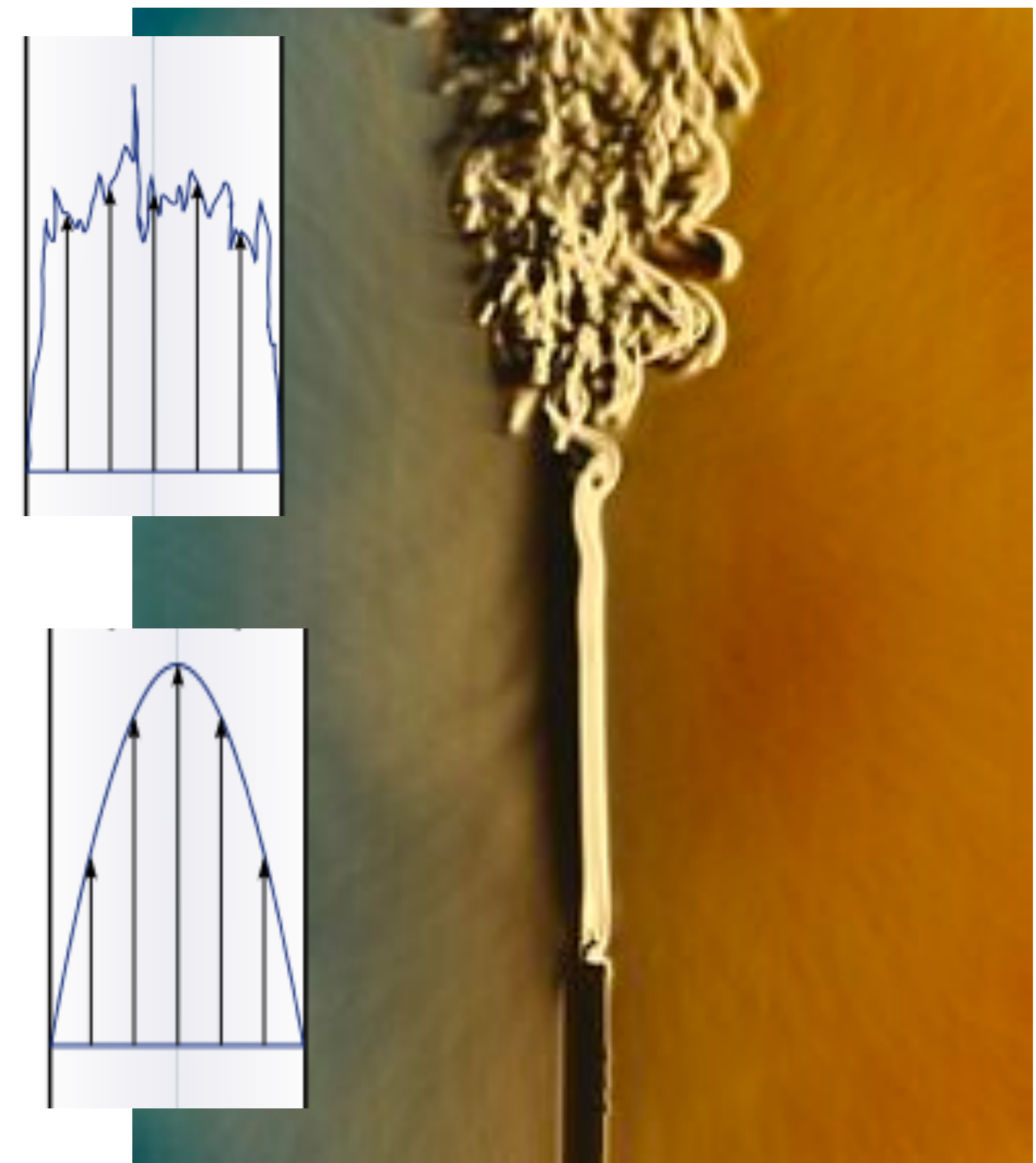


Fig: laminar to turbulent transition in candle smoke

TURBULENCE CASCADE

Definition of turbulence: instability of laminar flows that develops as soon as the inertial forces greatly exceed the viscous forces
(from Hennebelle & Falgarone 2012)

Turbulent energy is transferred to smaller scales until dissipation
(dissipation = conversion into heat due to particle viscosity)

Injection scale: $\sim 1-10$ kpc

Dissipation scale: probably milliparsec ~ 1000 AU

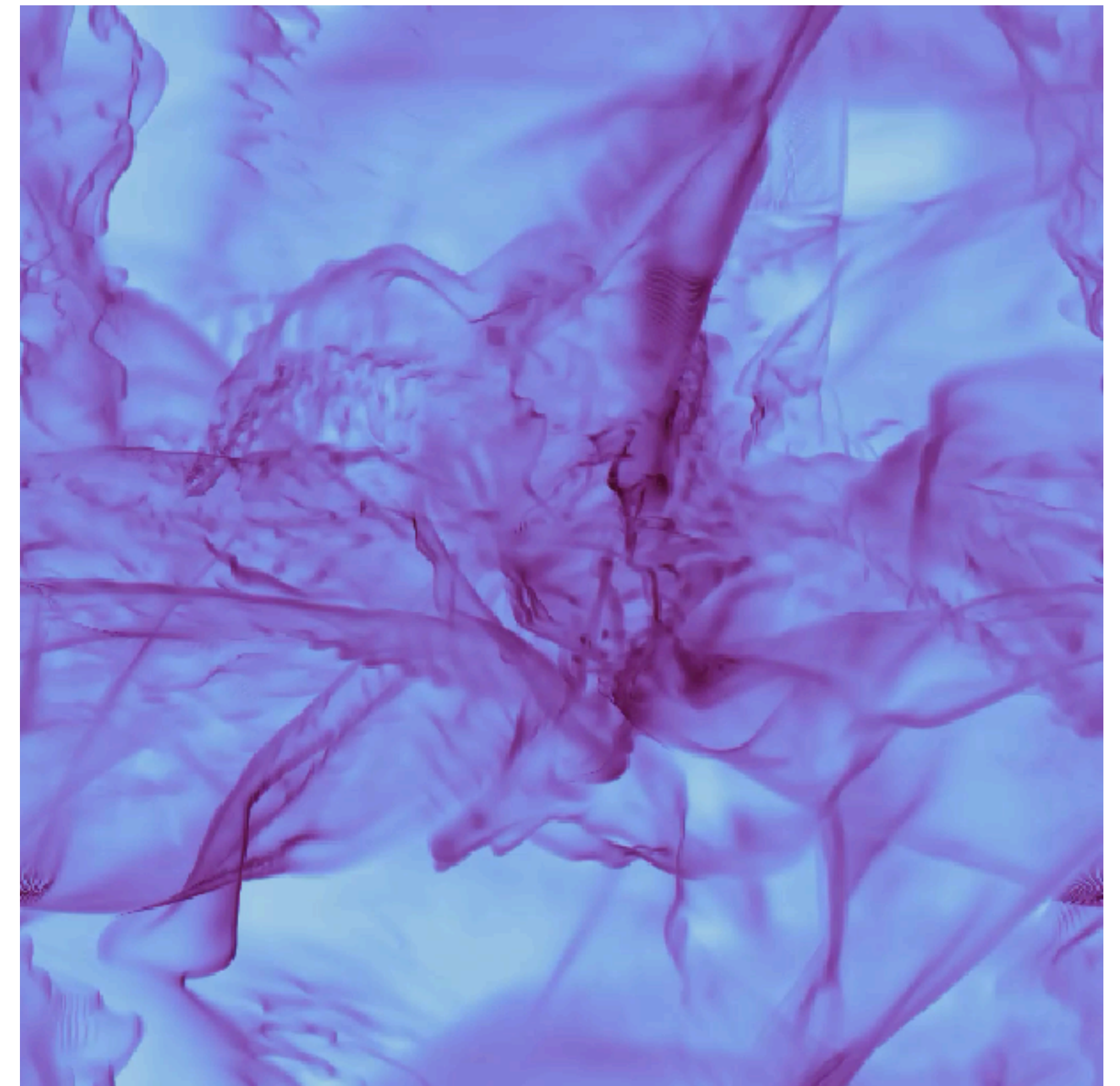
Scales in between are called the inertial range

Kolmogorov's cascade: self-similarity of the velocity field in incompressible turbulence \rightarrow energy spectrum $E \propto k^{-5/3}$

wavenumber
($=1/\text{scale}$)

But the ISM is highly compressible!

Turbulence is key in setting the density structure of the ISM



*Movie: simulation of turbulence gas
(Ohlin et al. 2019)*

2 MODES OF TURBULENCE

Turbulence leads to complex density and velocity structures, and fluctuations

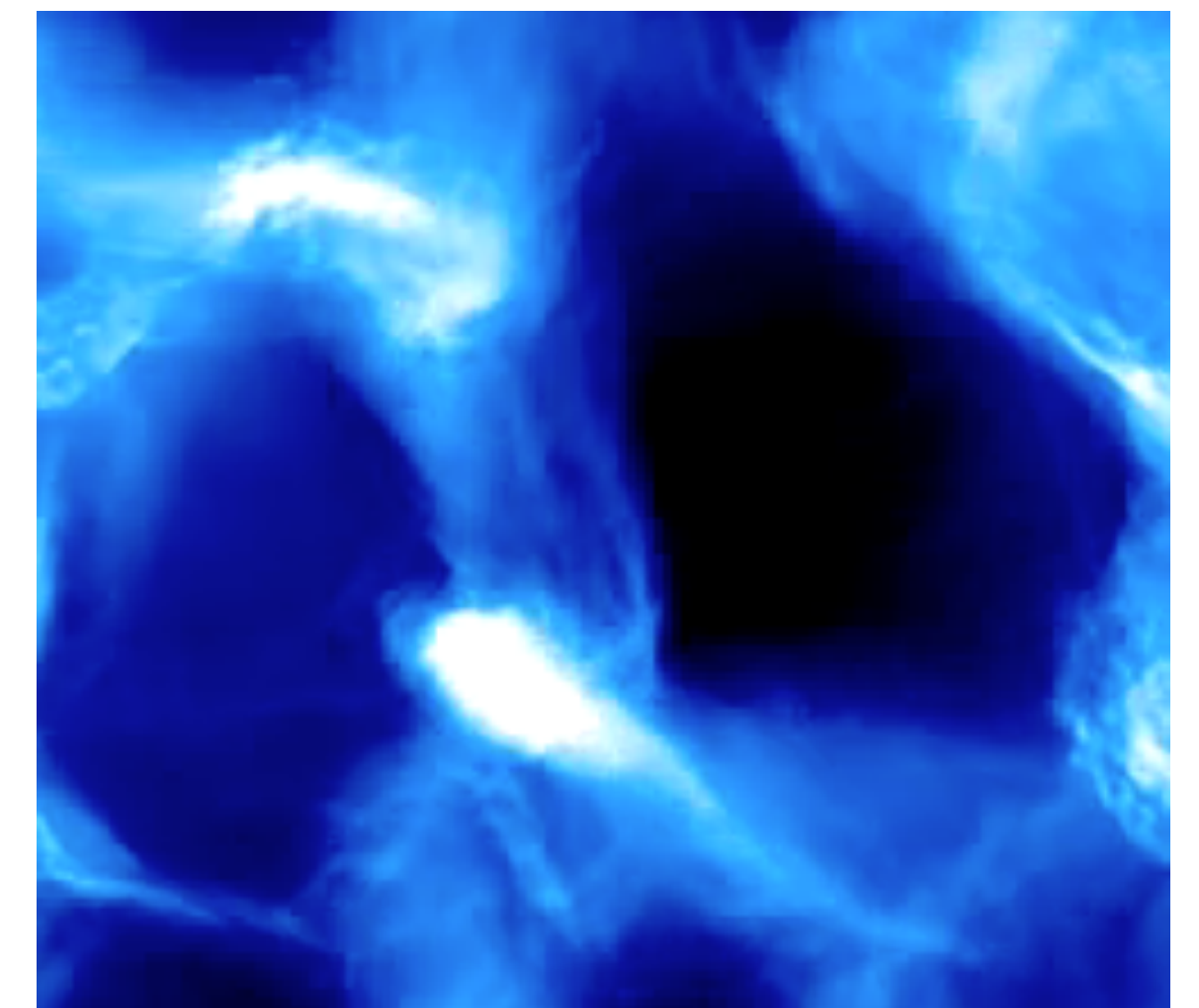
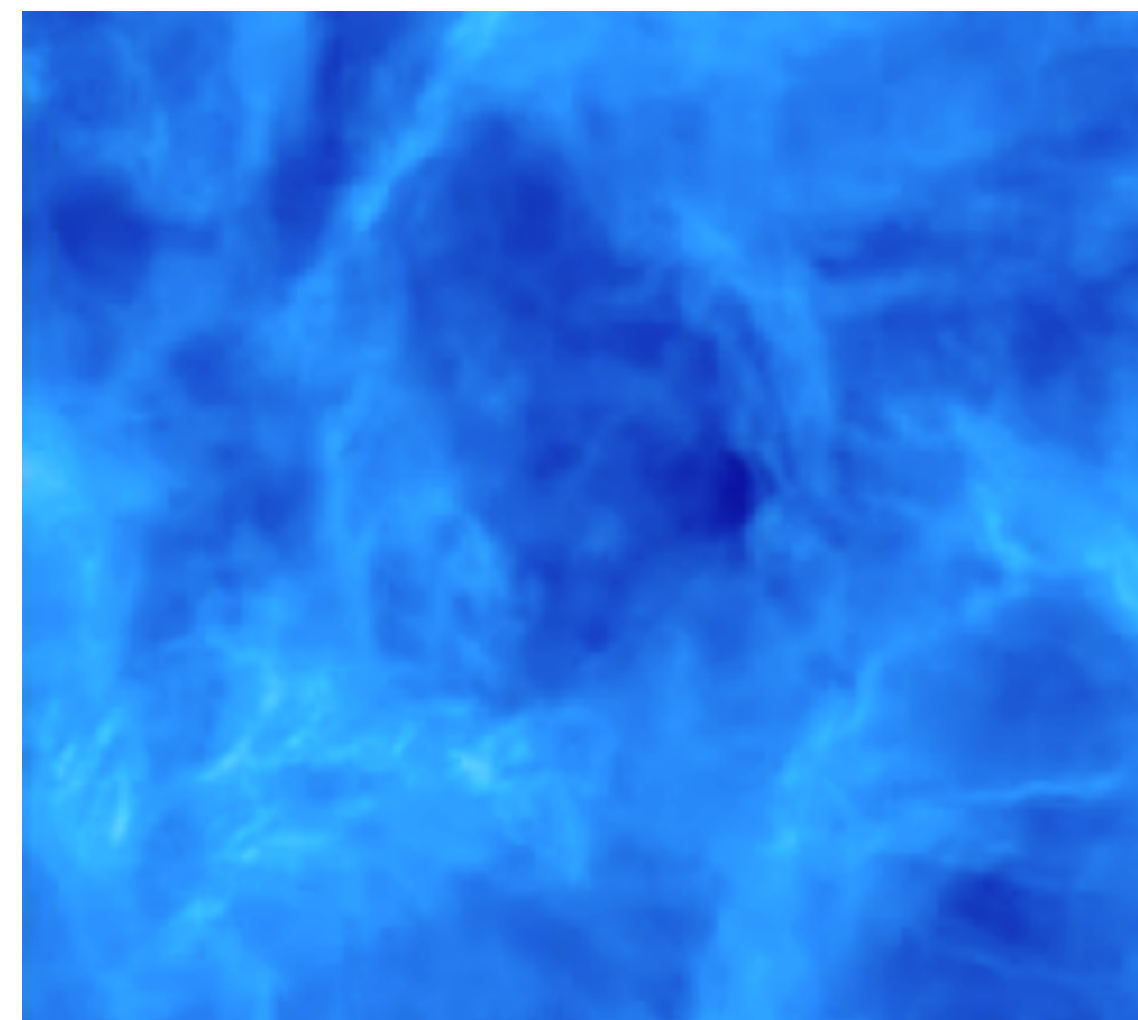
Measurement through the velocity dispersion (e.g. line broadening): $\Delta\nu = \nu \left(\underbrace{\frac{2k_{\text{B}}T}{m_{\text{H}}c^2}}_{\text{thermal}} + \underbrace{\frac{2v^2}{3c^2}}_{\text{turbulent}} \right)^{1/2}$

Turbulence is a (non-thermal) pressure term \rightarrow it acts against collapse

Fluctuations can also increase the density locally \rightarrow it acts with collapse

Galaxies host the 2 modes of turbulence, but their relative importance changes (e.g. in mergers, see Renaud et al. 2014)

Movies: simulations of 2 types of turbulences. The left one is mostly mixing the gas while the right one leads to more compression. Both modes exist in galaxies. (from C. Federrath)



DENSITY PROBABILITY DISTRIBUTION FUNCTION (PDF)

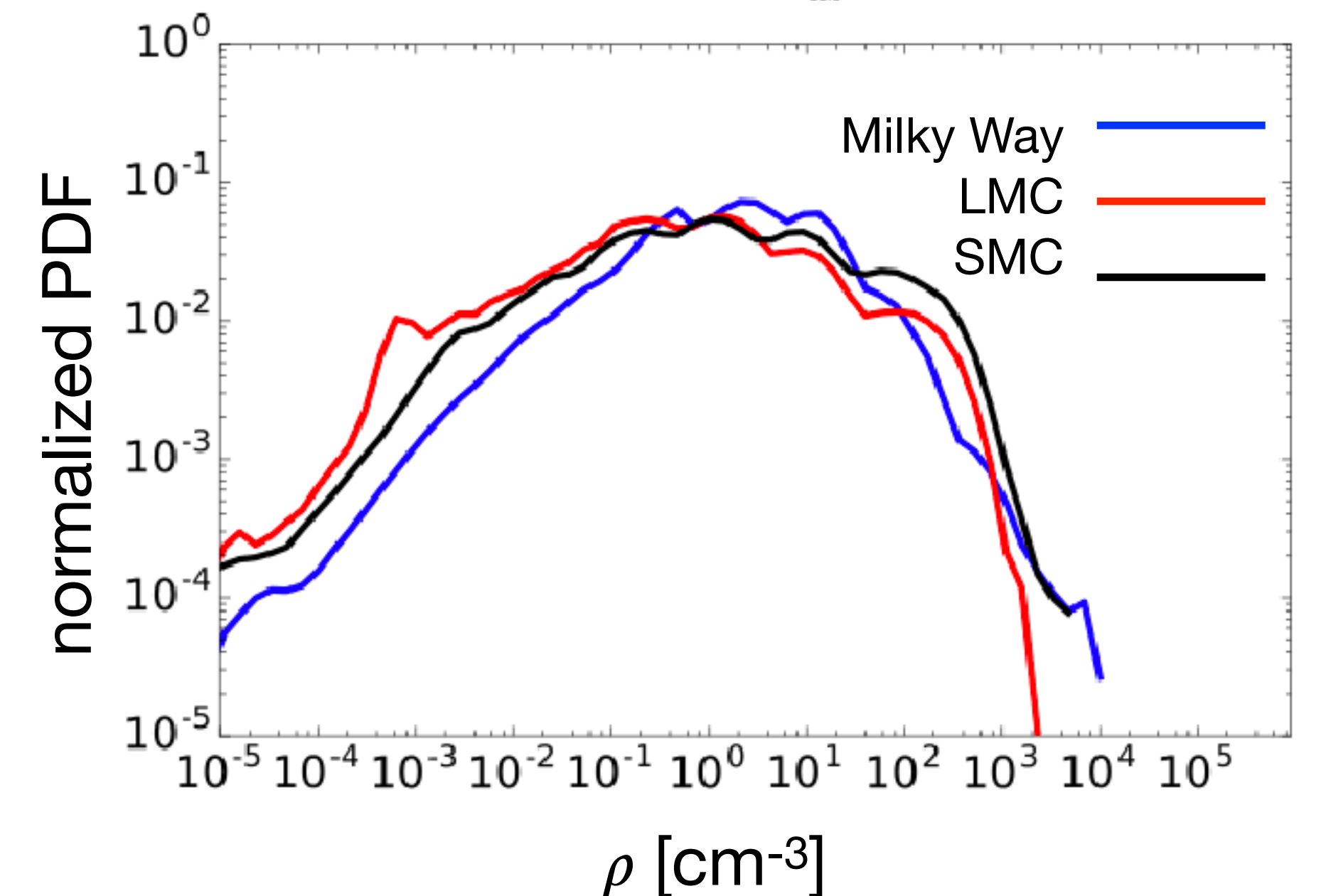
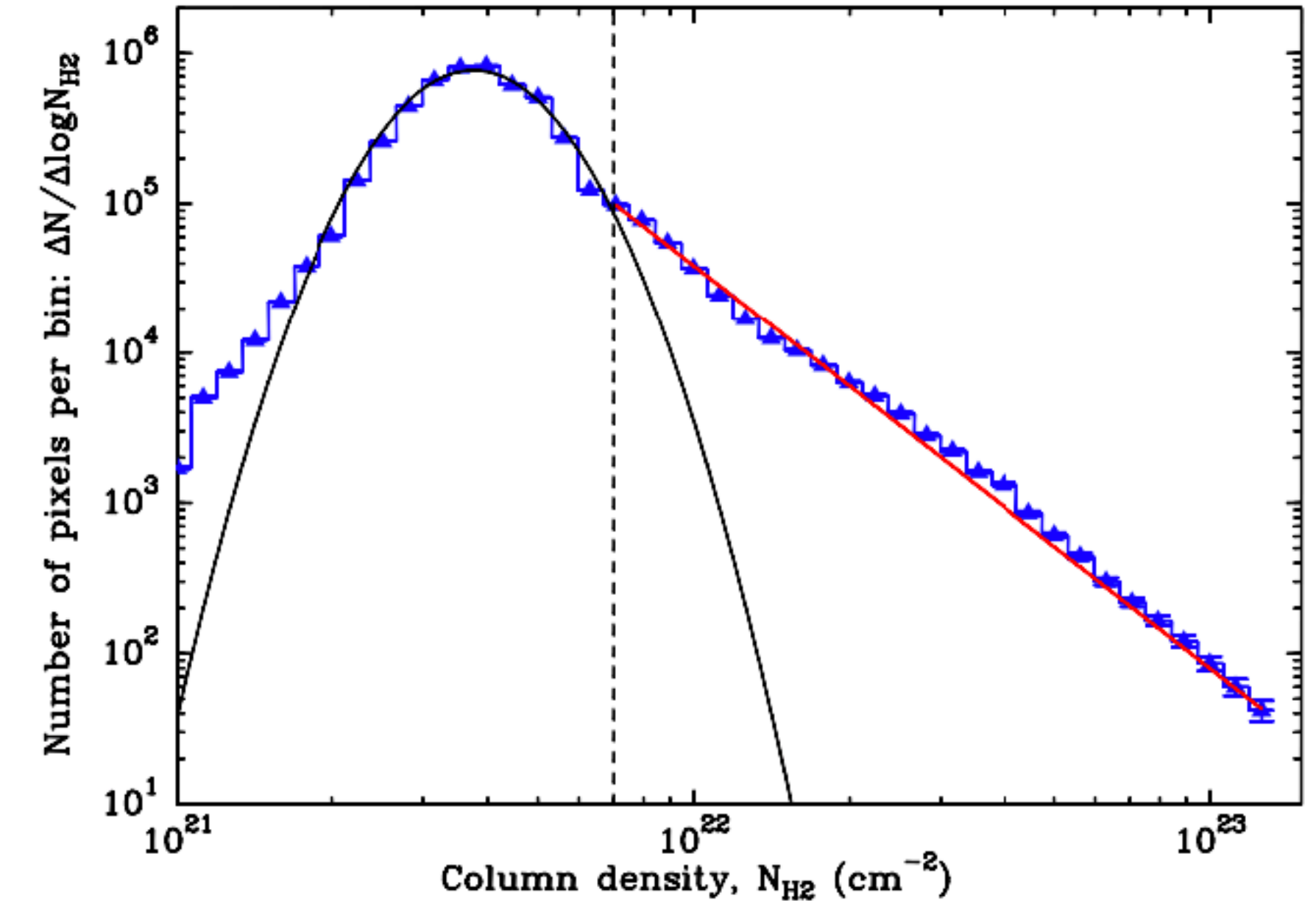
The result of the interplay between turbulence, gravitation, shocks etc. is a wide distribution of gas densities

In galaxies, the PDF is a log-normal (set by turbulence), with a power-law tail (set by self-gravity)

The shape is rather universal, except in extreme cases (e.g. high redshift, interactions)

Knowing the distribution of gas density is very important since it is the ingredient for star formation

*Fig: top: column density PDF in observations (André et al. 2010).
Bottom: volume density PDF from galaxy simulations. The power-law tail is not captured because of limited resolution. (Grisdale et al. 2017)
(For an example capturing the power tail, see Renaud et al 2013)*



GALACTIC POWER SPECTRUM DENSITY (1/2)

The power spectrum density (PSD) quantifies the relative representativity of scales

$$P = \lim_{N \rightarrow \infty} \frac{(\Delta x)^2}{N} \left| \sum_{n=1}^N x_n \exp\left(-\frac{i2\pi n \Delta x}{N}\right) \right|^2$$

where x_n is the signal (e.g. a gas density map) sampled over N points at the resolution Δx

In other words: $P = \mathcal{F} \mathcal{F}^* = |\mathcal{F}|^2$ where \mathcal{F} is the Fourier transform and \mathcal{F}^* is its complex conjugate

Expect a change of slope at the scale-height of the galactic disk: turbulence switches from 2D to 3D

Other features can be seen (feedback effects, large-scale structures), but are mostly averaged-out.

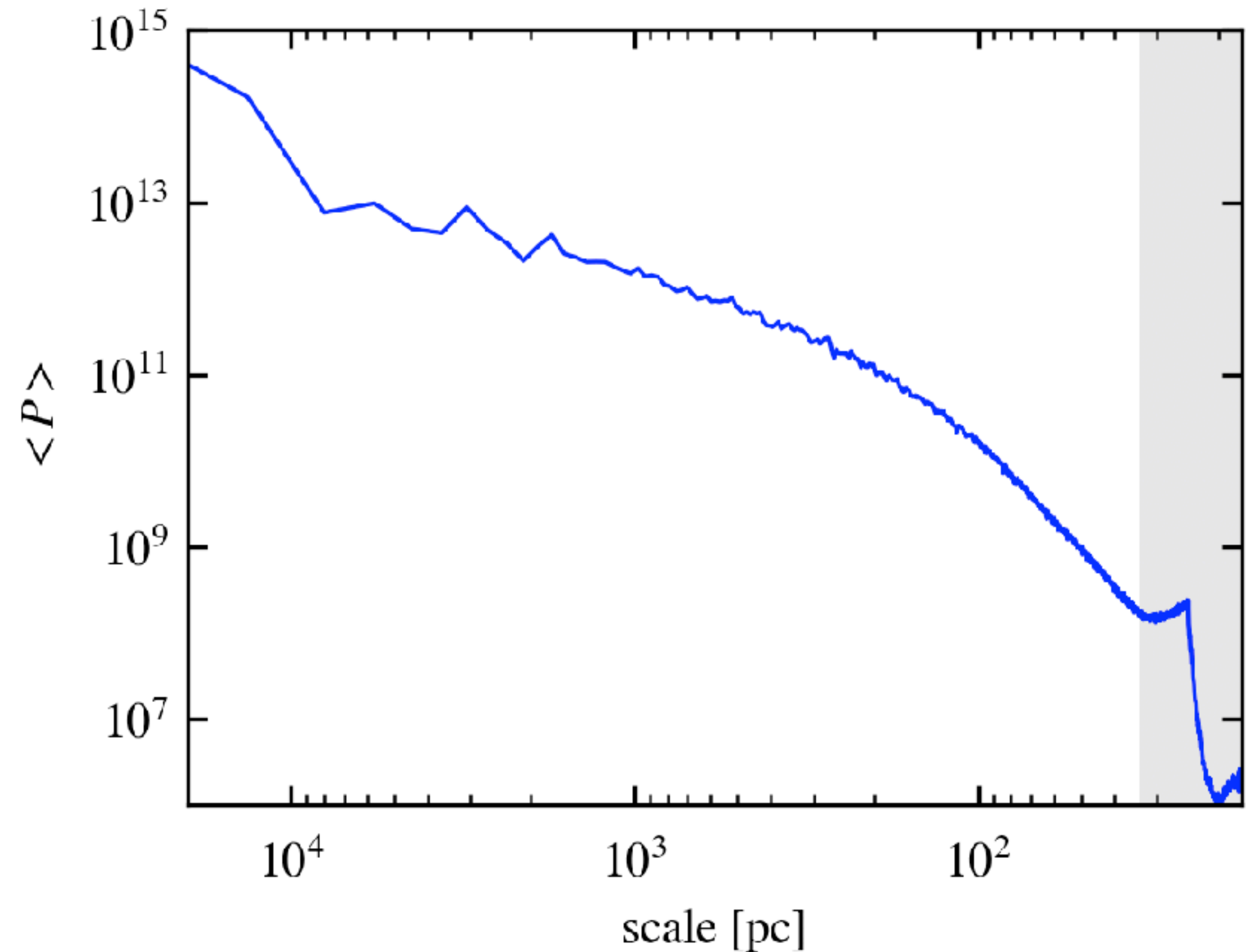
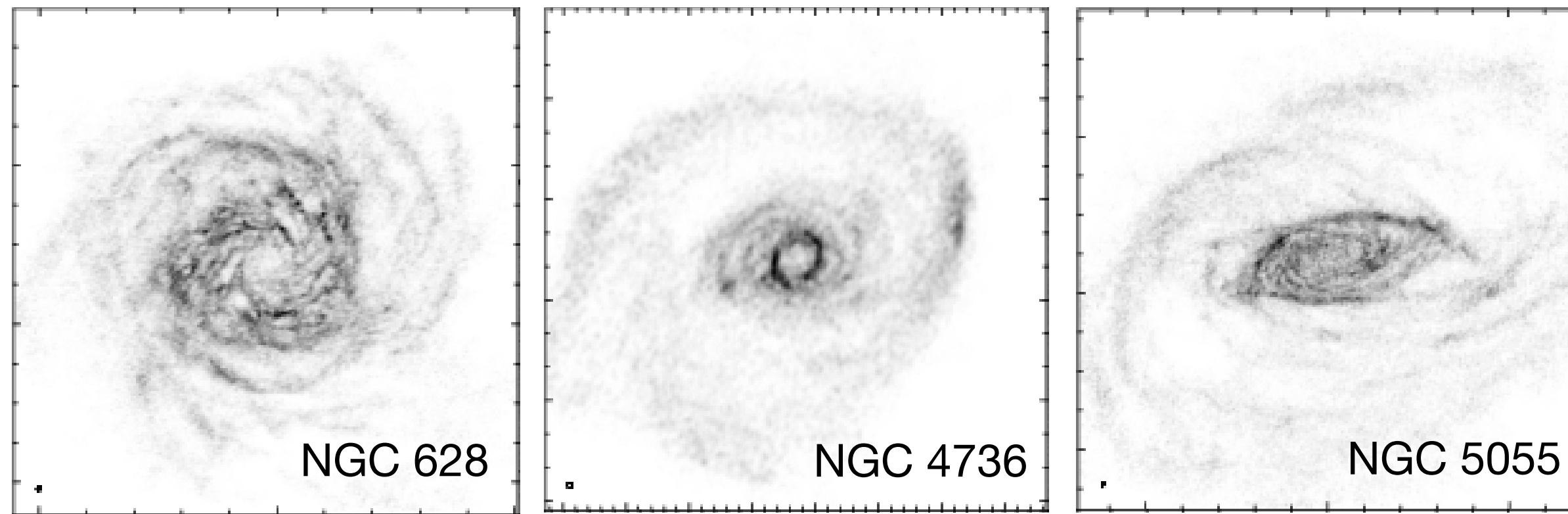


Fig: Power spectrum density of a simulation of a Milky Way-like disk galaxy. The change of slope at ~ 100 pc corresponds to the transition to 3D turbulence, at the scale-height of the disk. The shaded area is affected by finite resolution (Renaud et al. 2021c)

GALACTIC POWER SPECTRUM DENSITY (2/2)

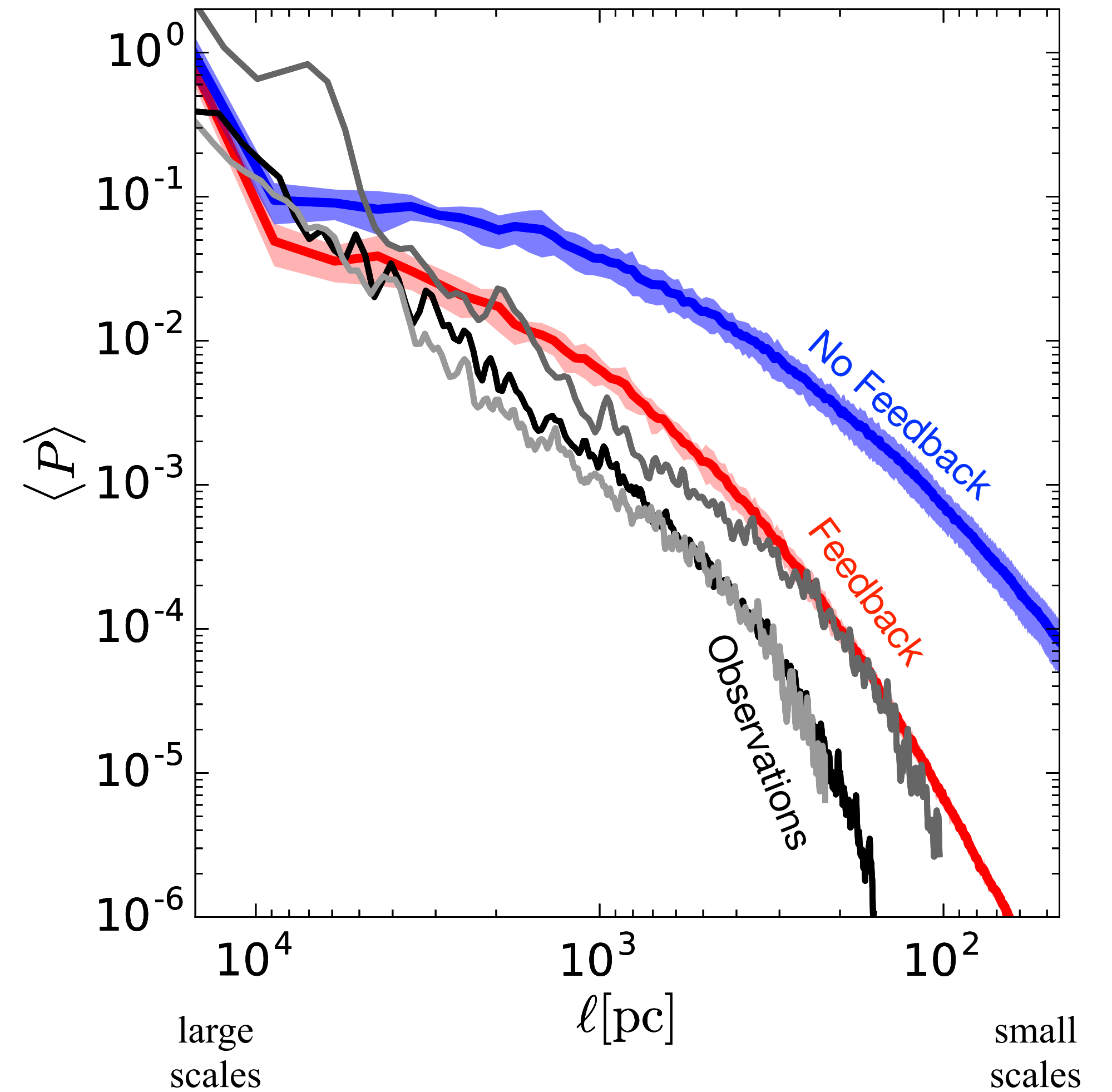


Without feedback: largest discrepancies at small scales

Feedback is needed to *statistically* match real galaxies

Fig: Top: observations of disk galaxies from the THINGS survey (Walter et al. 2008).

Right: Power Spectrum Density of simulated disk galaxies, with and without feedback (Grisdale et al. 2017)



INJECTION SCALE OF TURBULENCE

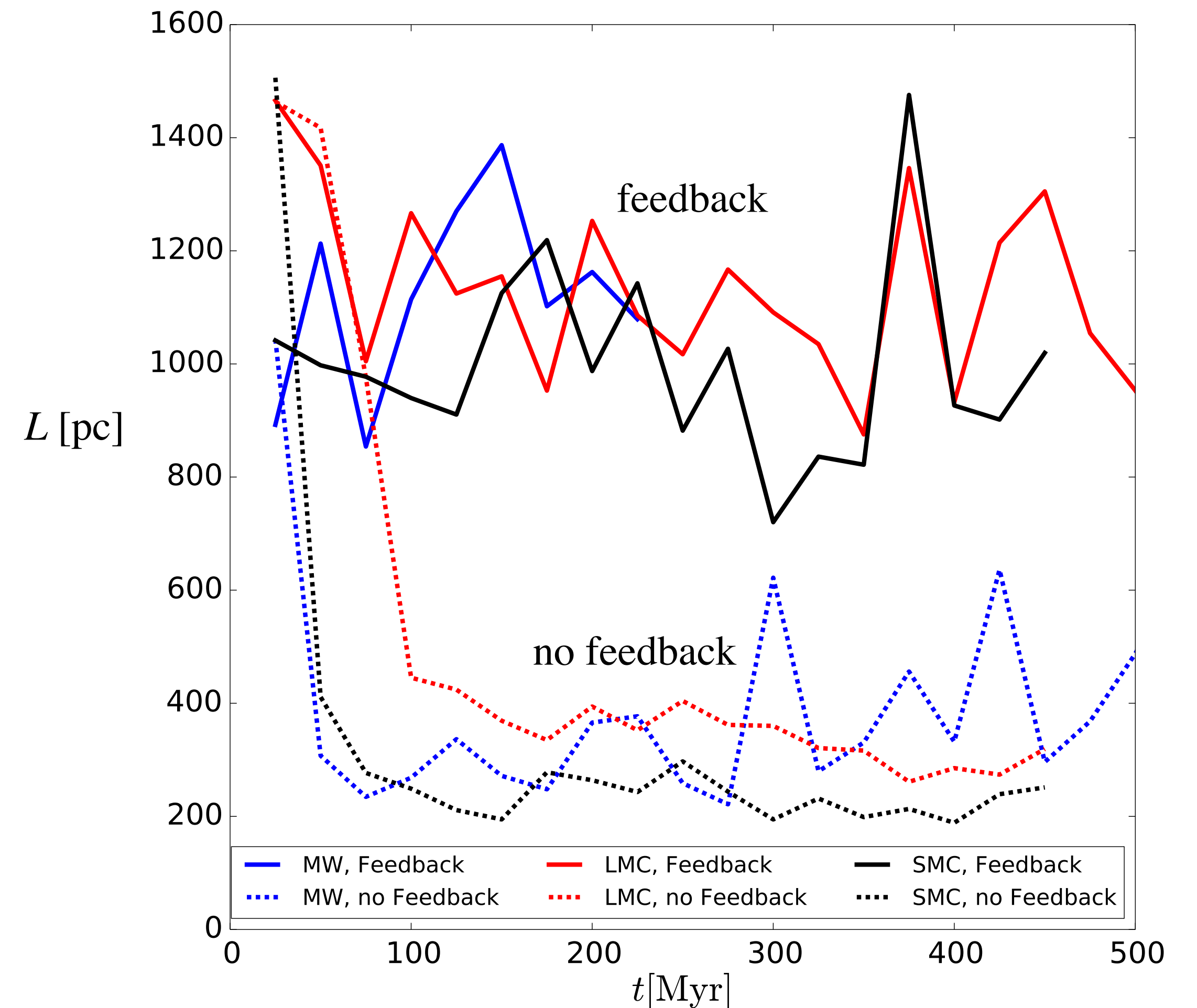
Because of dissipation, turbulence needs a continuous energy injection to be maintained

$$L = 2\pi \frac{\int k^{-1} E_k dk}{\int E_k dk} \quad \text{where } k \text{ is the wavenumber}$$

see Joung, Mac Low and Bryan (2009) for details

Feedback participates in turbulence injection to scales much larger than molecular clouds (\sim kpc)

Coupling of feedback to large scales is the key



COMPLEX PROPAGATION OF FEEDBACK

The deposition of energy and momentum by stellar feedback is well understood

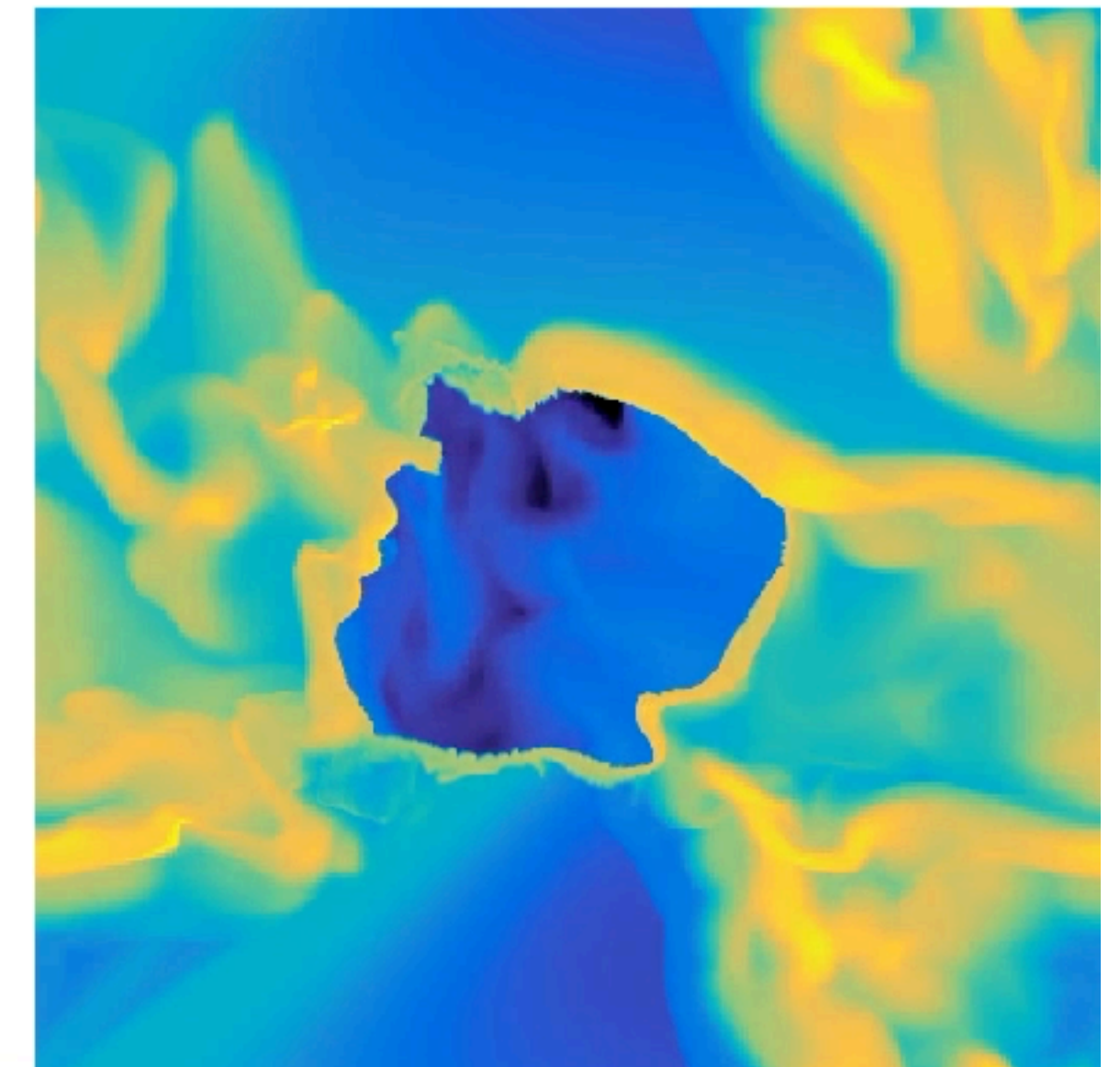
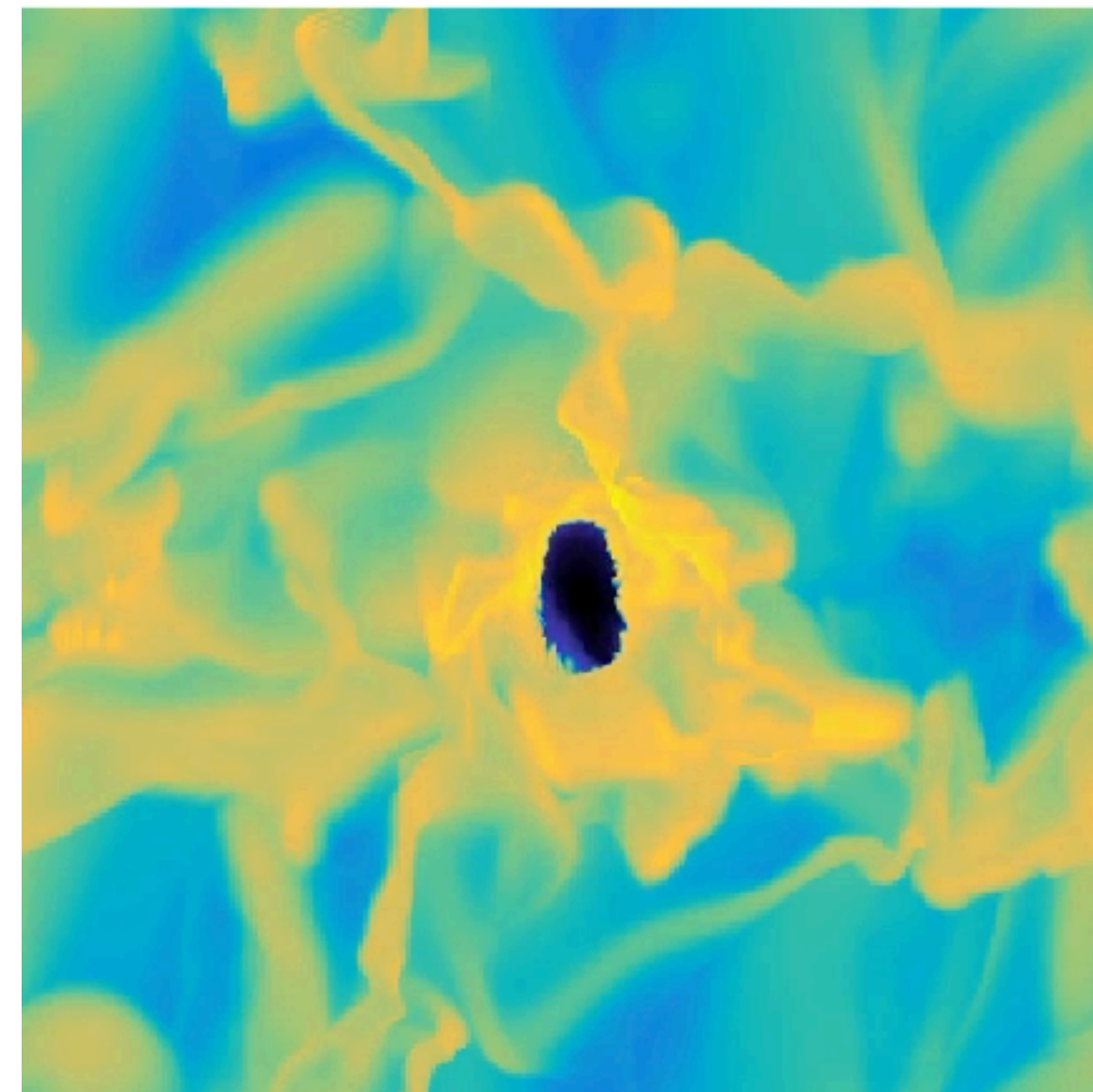
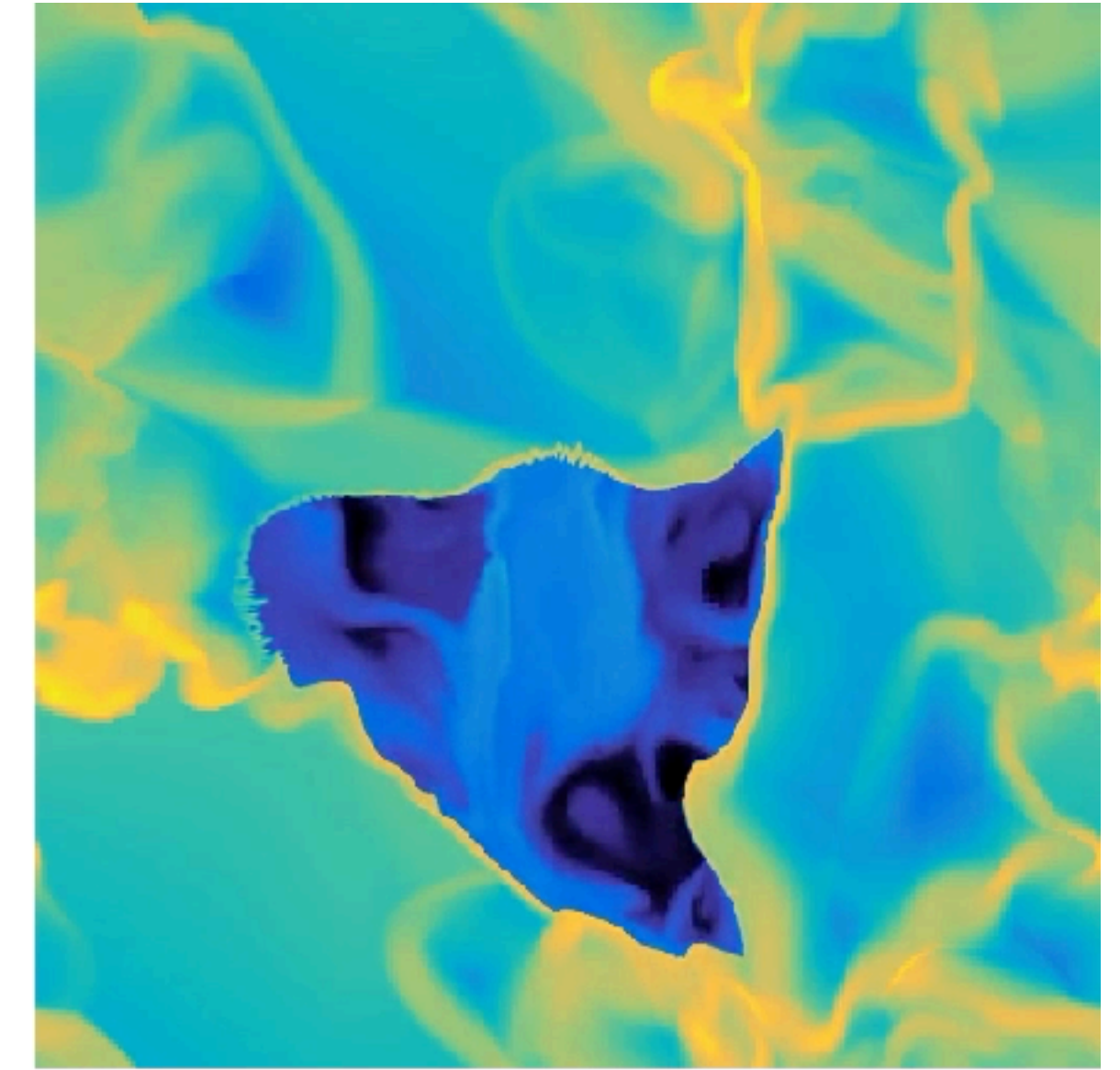
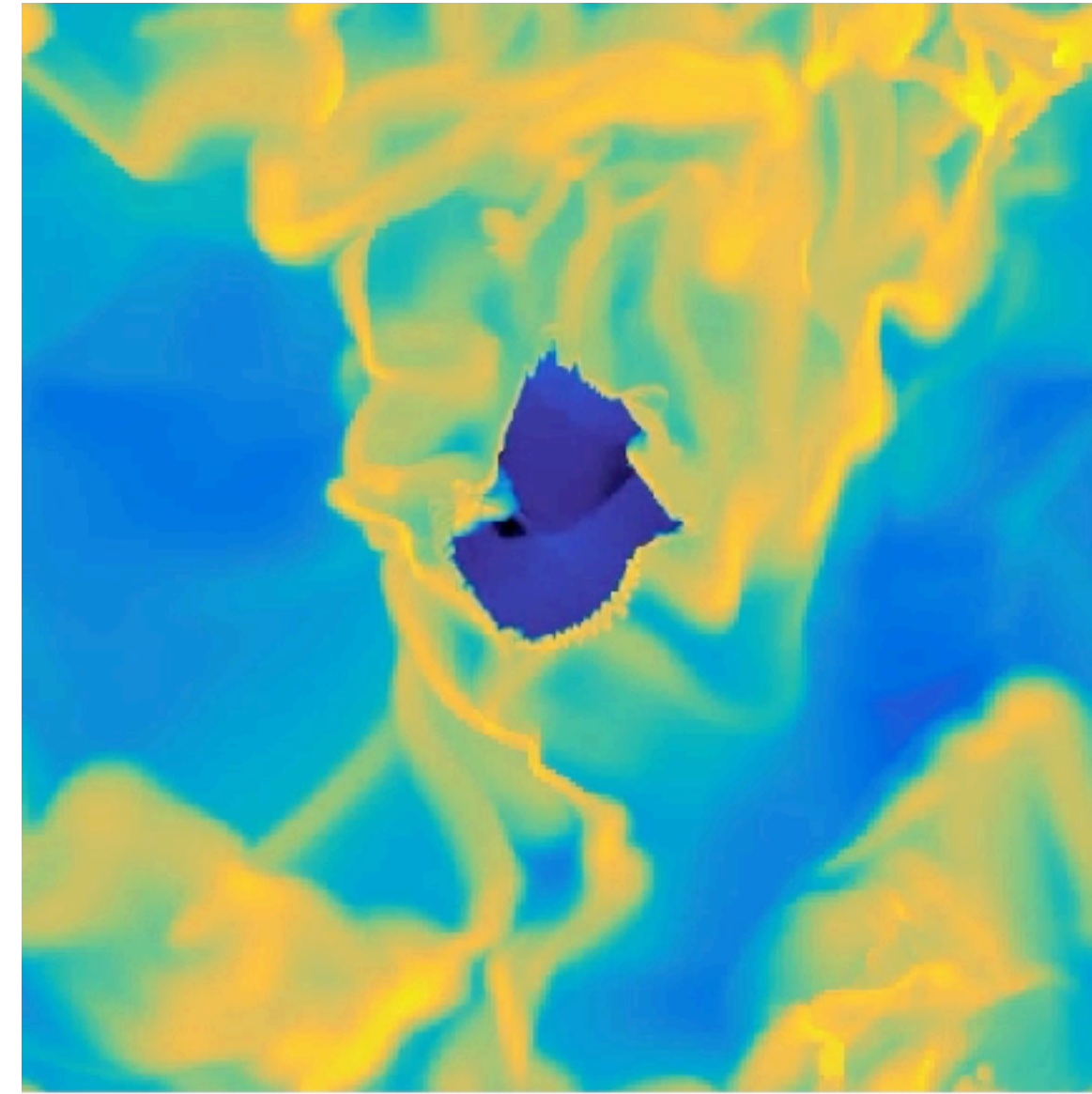
How feedback couples to galactic scales is very complex

Example: consider a box of gas (100 pc, 10 km/s, 100 cm⁻³)

Make different realizations of the turbulence keeping the average quantities unchanged

(i.e. these are *strictly* identical if the resolution is > 100 pc)

Movies: propagation of one supernova bubble in 4 different realizations. Every case is different (scale, speed, coupling). (Ohlin et al. 2019)



EXPANSION RATE AND VOLUME OF SN BUBBLES

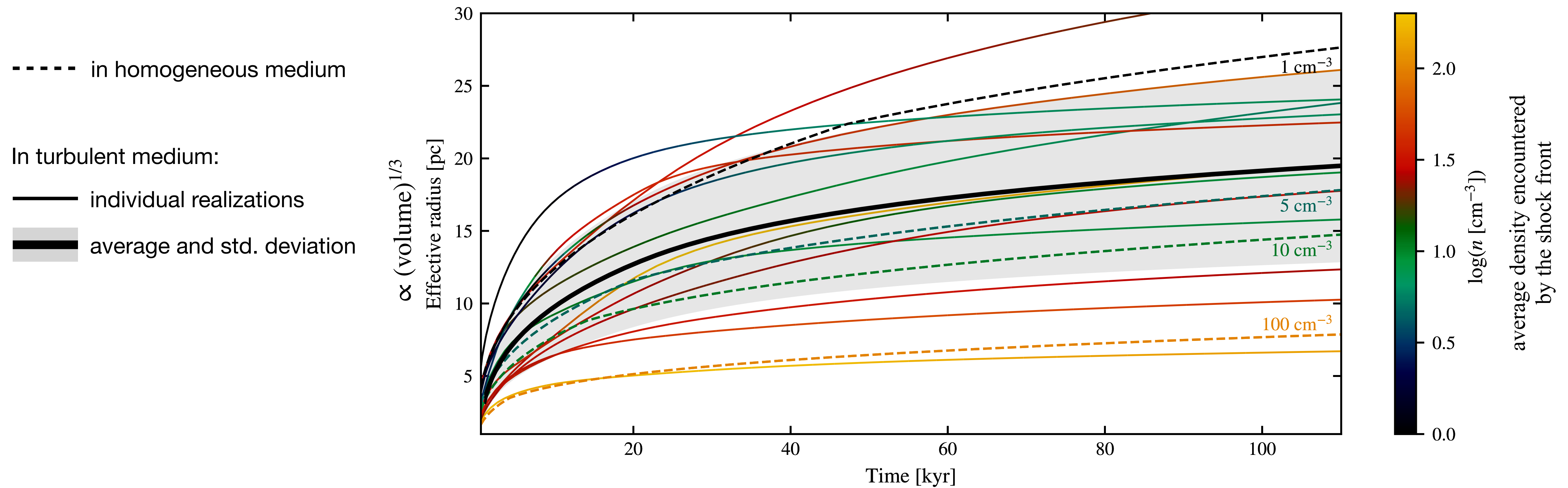


Fig: time evolution of the size of supernova bubble in different realizations of the same medium, with different turbulence realizations. The average solution (solid black) is far from that in the average medium (dashed orange). (Ohlin et al. 2019)

The coupling to large scale depends on the fine details of the ISM structure: highly anisotropic!

Impossible to resolve in cosmological simulations ... Is feedback wrong in large-scales simulations?

DRIFT AND RUNAWAYS

Where stars inject feedback is very important!
But stars can move significantly away from their formation sites

- Asymmetric drift:

$$\text{Velocity in the galaxy: } v^2 = v_{\text{circ}}^2 - \sigma^2$$

$$\text{At formation: } \sigma_{\star} = \sigma_{\text{cloud}} \approx 10 \text{ km s}^{-1}$$

$$\sim 10 \text{ Myr later: } \sigma_{\star} \approx 15 \text{ km s}^{-1} \text{ (because of relaxation)}$$

$$\sigma_{\text{cloud}} \approx 9 \text{ km s}^{-1} \text{ (because of dissipation)}$$

→ stars lag behind their clouds

- Runaways:

Some stars get kicked out clusters (by star-star interactions)
with velocities $\sim 30 - 500 \text{ km/s}$

→ can reach low density ISM
and the circum-galactic medium

→ less efficient (or less rapid) cloud destruction

*Movie: simulation of a disk galaxy without (left) and
with (right) runaway stars (Andersson et al. 2020)*

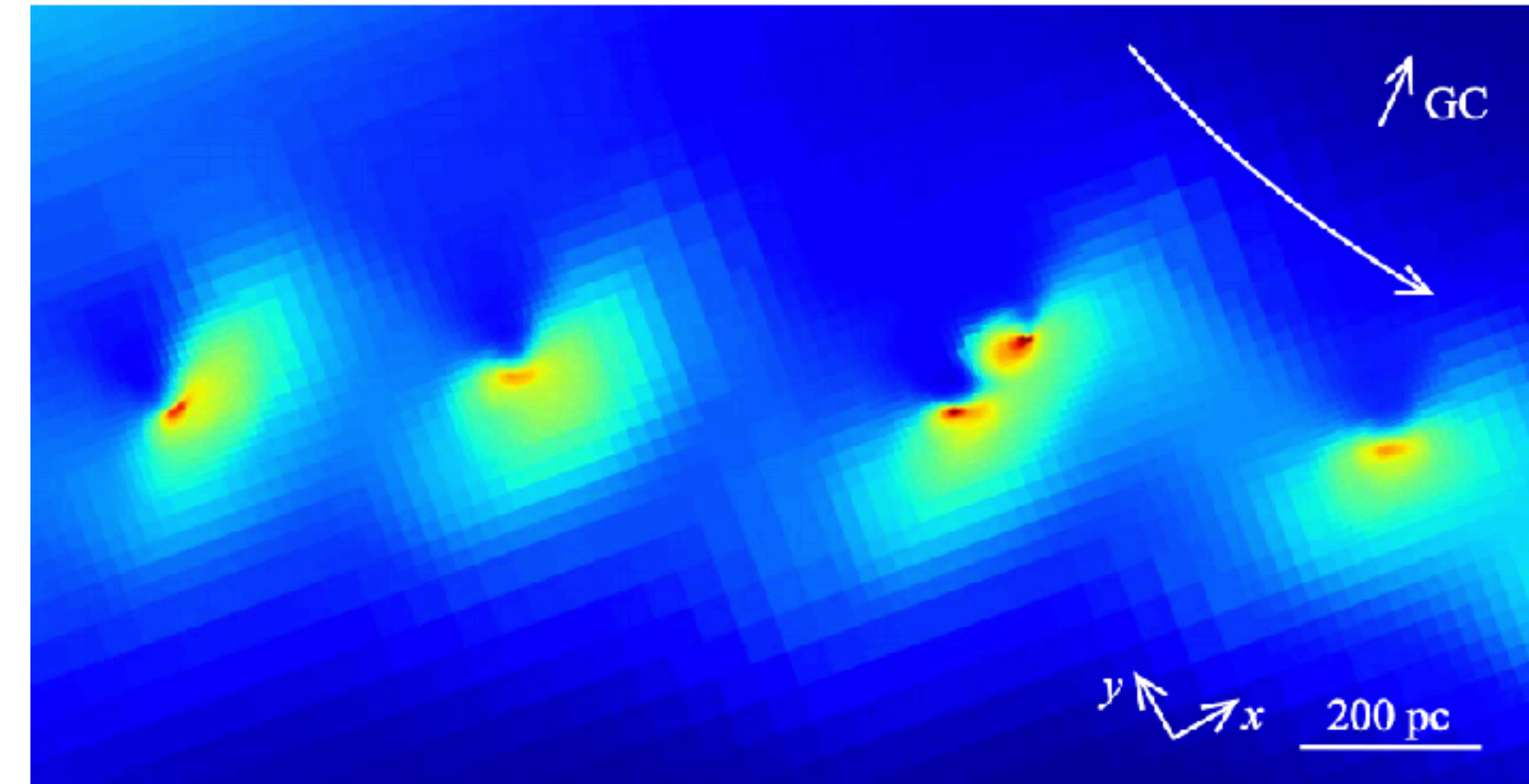
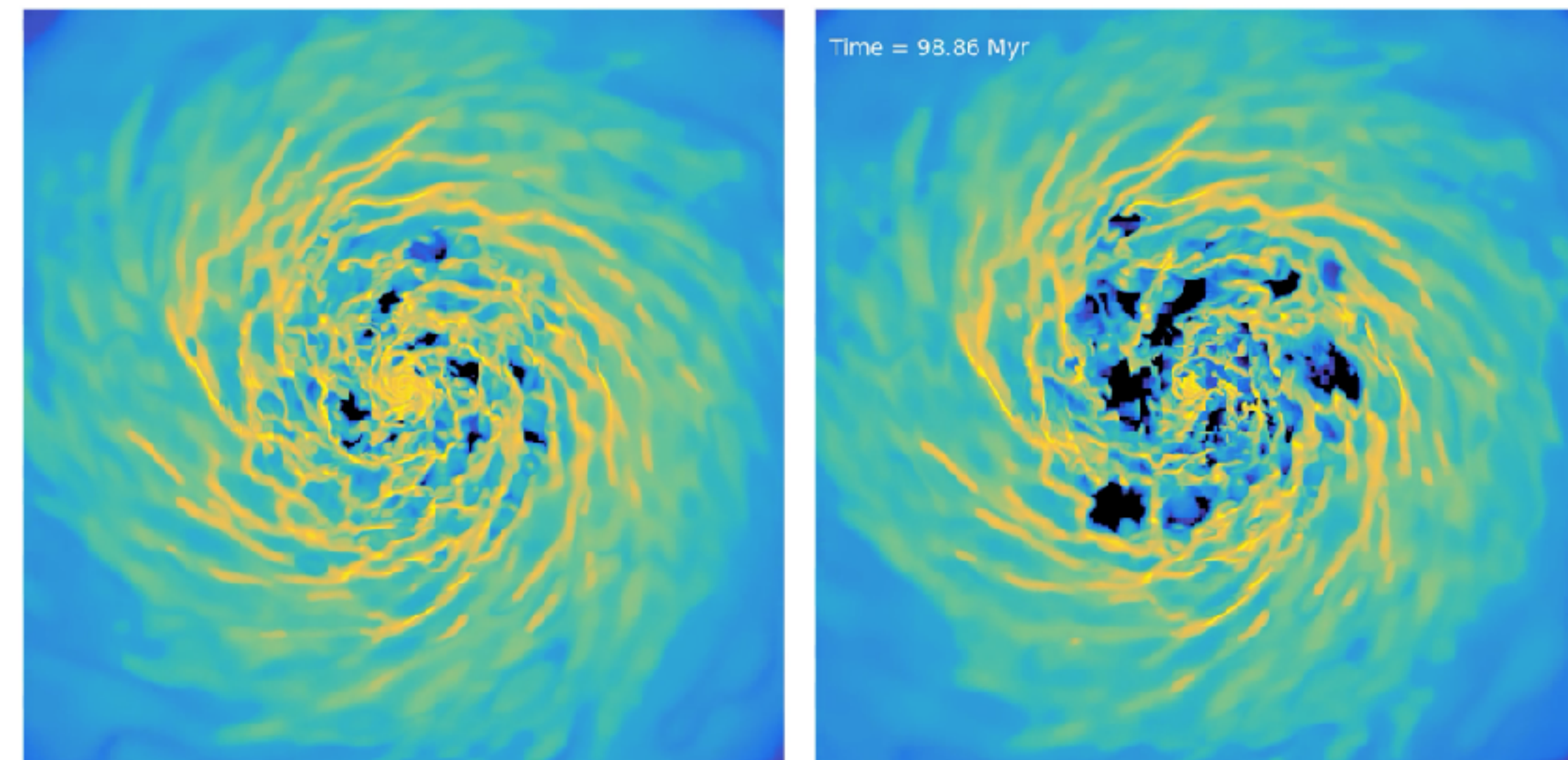


Fig: asymmetric shapes of GMCs due to explosions of SNe behind the clouds in a galaxy simulation (Renaud et al. 2013)



FEEDBACK IS NEEDED TO REGULATE GALAXY FORMATION

Efficient suppression of star formation by stellar feedback in the first ~ 3 Gyr

The regulation depends on:

- how much feedback is injected (energy, momentum)
- how the galaxy reacts to it (e.g. escape velocity)

It is highly non-linear and time-dependent

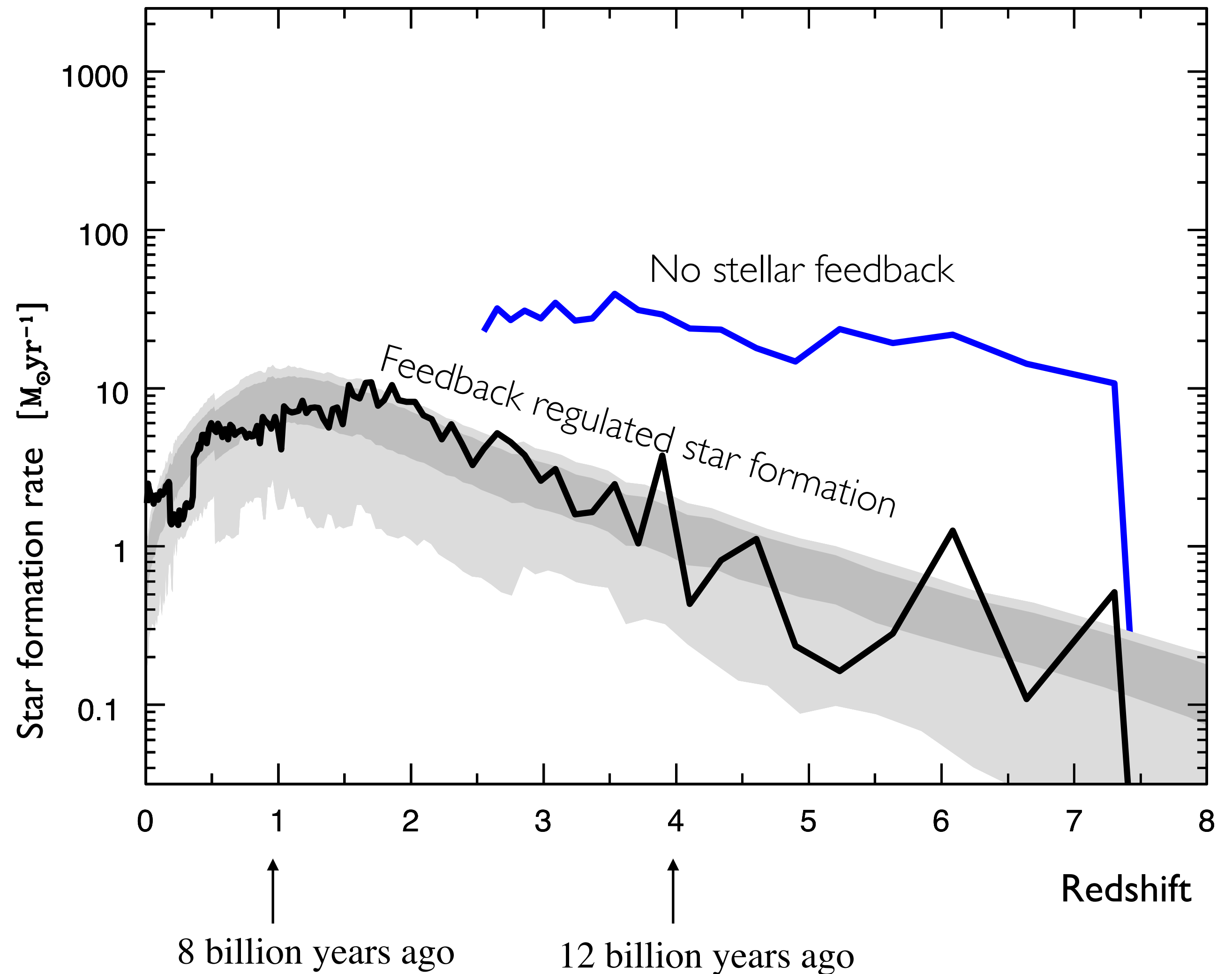


Fig: star formation history of a simulated Milky Way-like galaxy (Agertz & Kravtsov 2015)

FEEDBACK DOES NOT EXPLAINS EVERYTHING

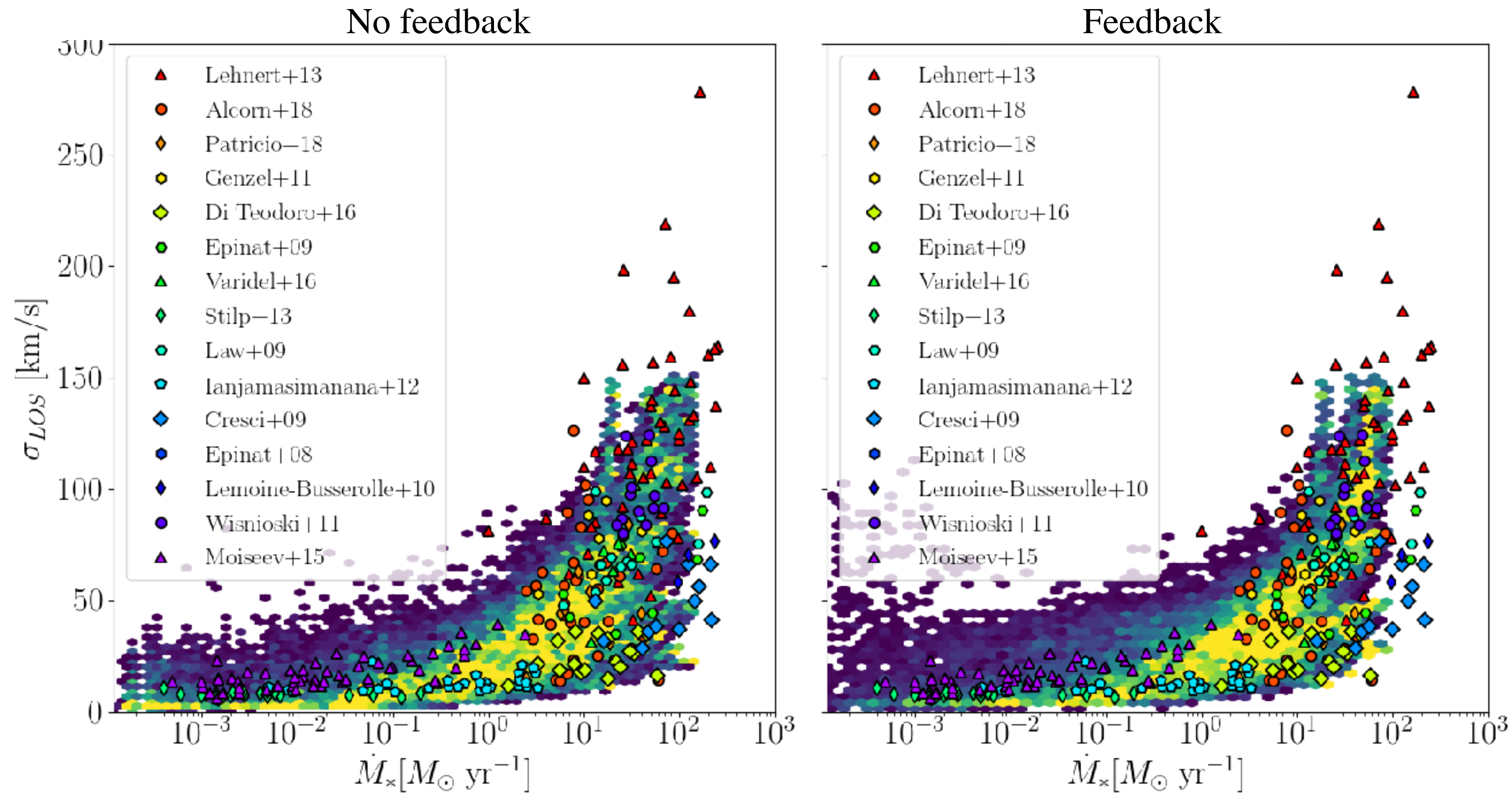
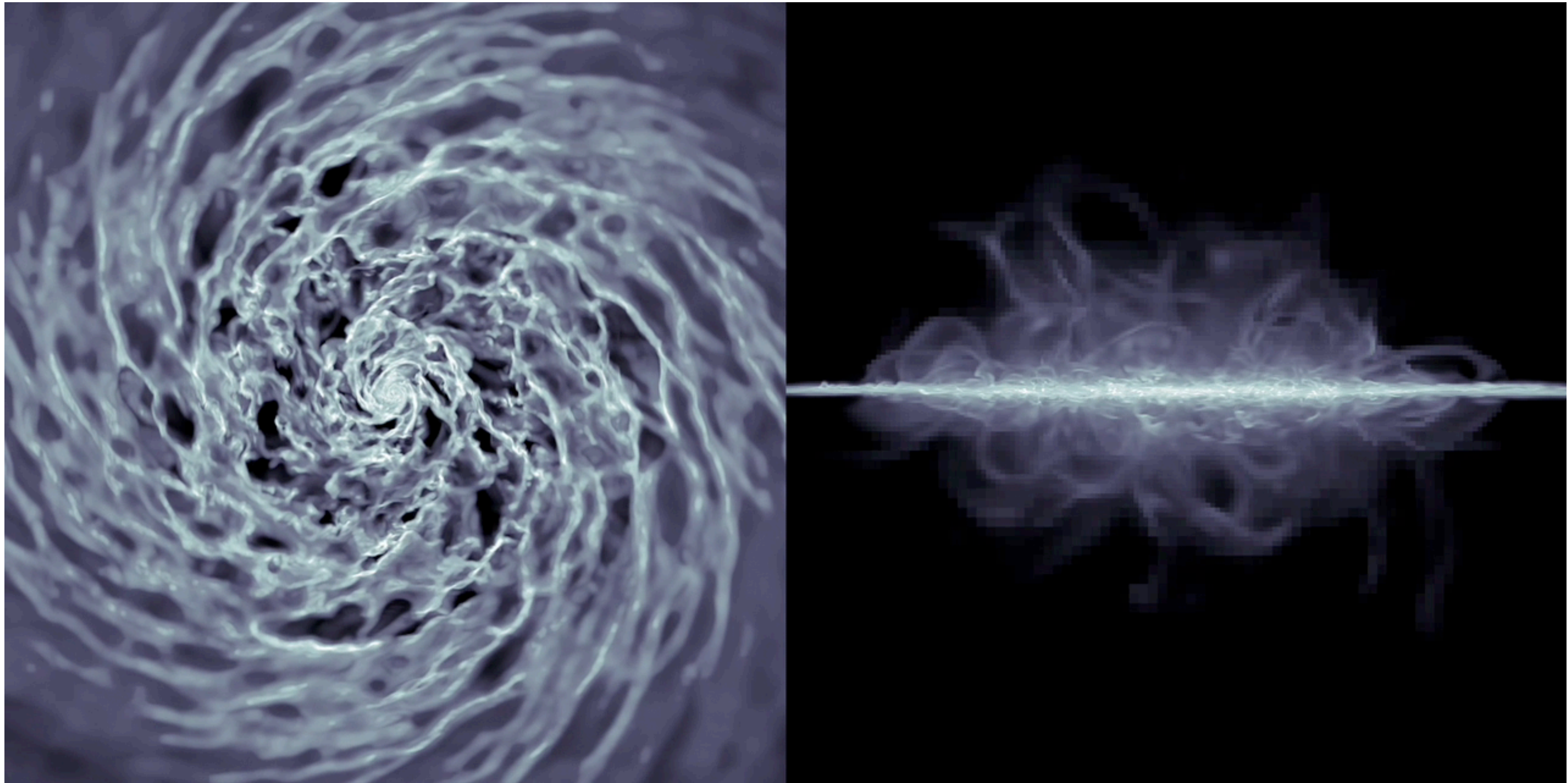


Fig: velocity dispersion vs. SFR. Symbols = observations; Background = simulation of an isolated disk. Similar behaviors are found with and without feedback \rightarrow The observed dispersion originate mostly from large-scale disk dynamics, not feedback. (From Ejdetjärn et al., submitted)

FEEDBACK NEEDED TO FEED THE STIRRING BY THE GALACTIC STRUCTURE

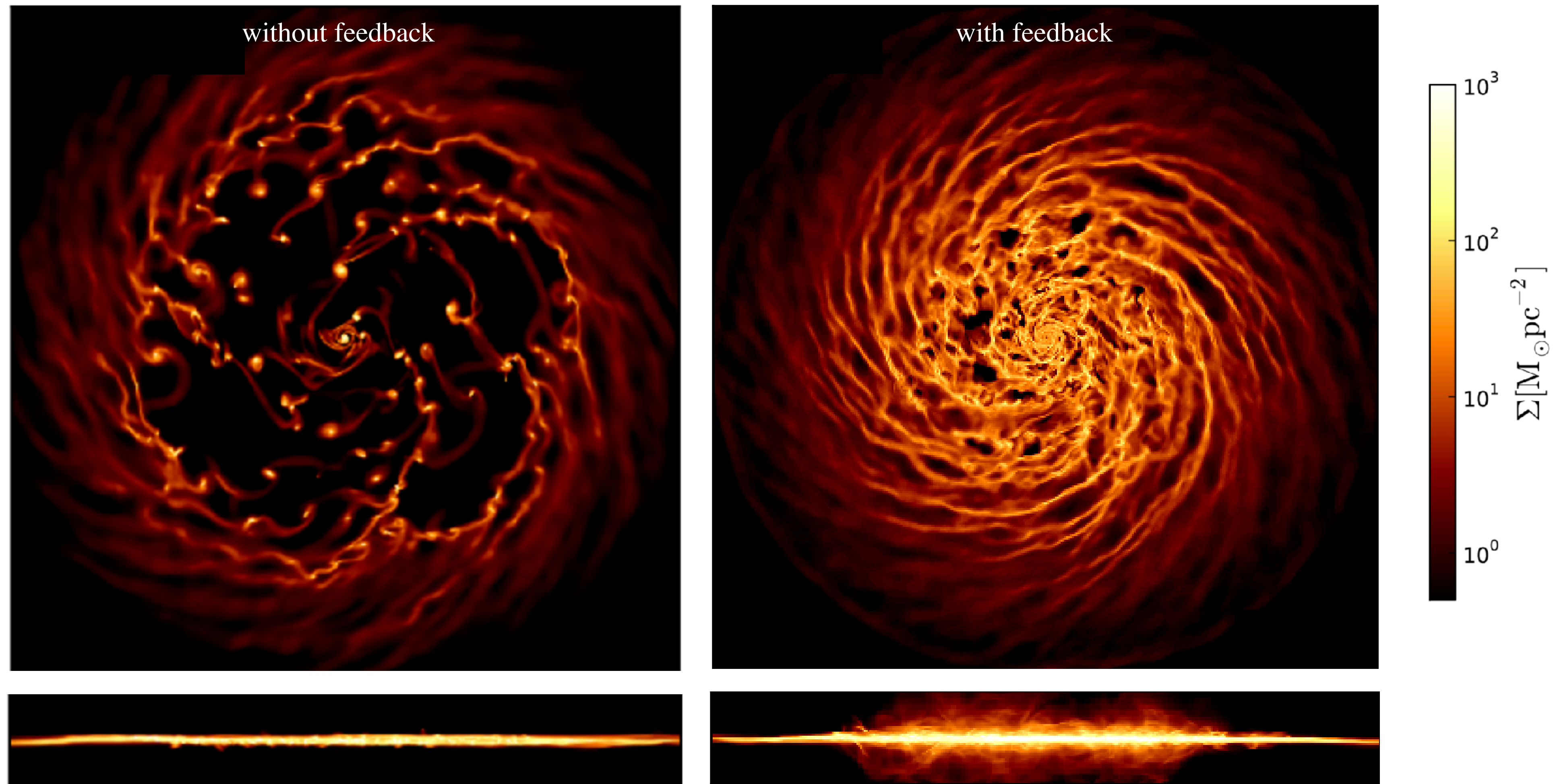
Grisdale et al. (2017)



FEEDBACK NEEDED TO FEED THE STIRRING BY THE GALACTIC STRUCTURE

Without feedback, unstable regions collapse and make unrealistic clumps

Grisdale et al. (2017)



ROLE OF THE SPIRALS

The role of spiral arms in organizing / regulating the ISM is not completely clear yet

Spiral arms are density waves, not material waves, trapped in between resonances



Fig: the grand-design spiral galaxy M83. A lot of star (cluster) formation activity occurs along the spiral arms.

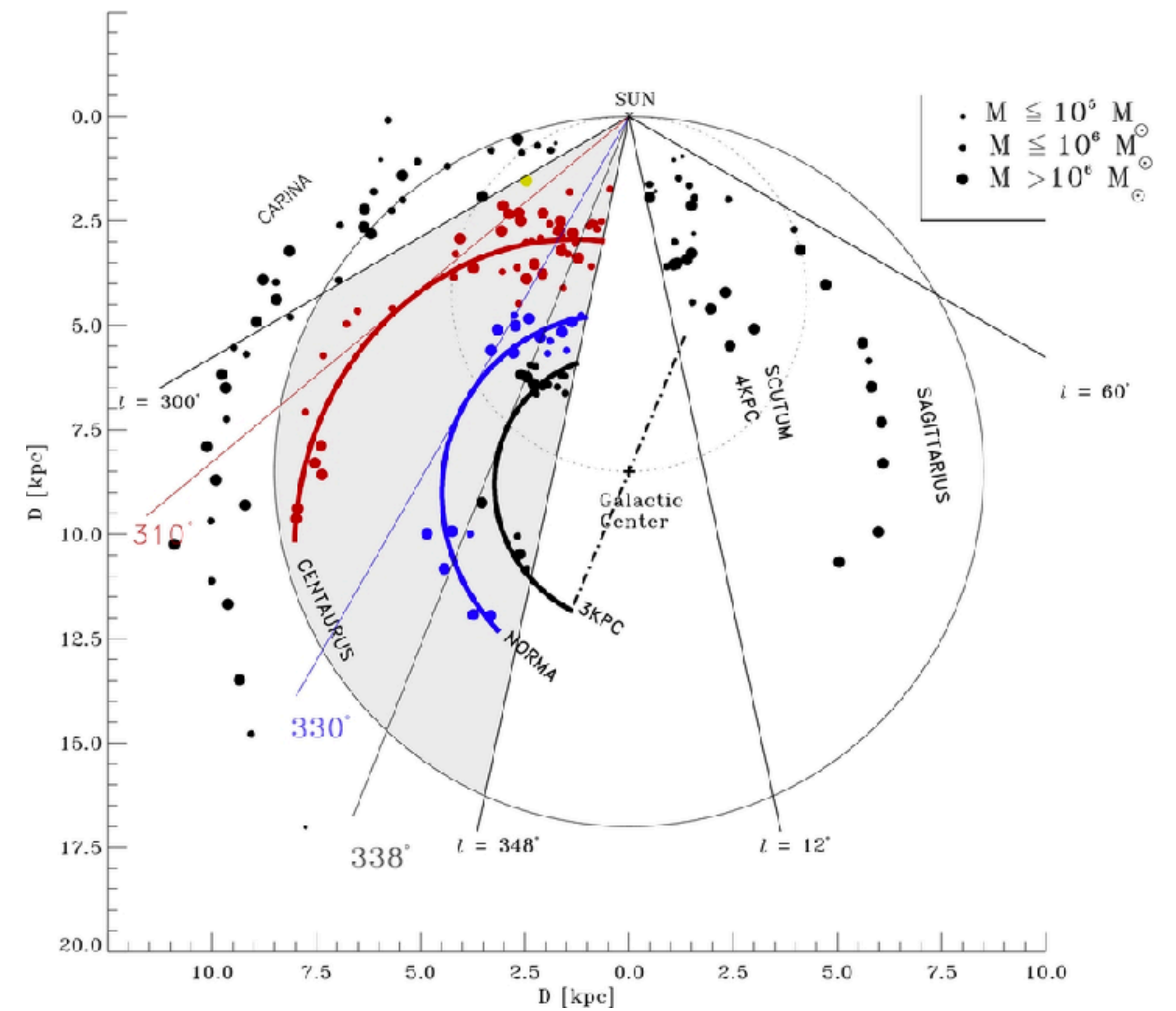


Fig: Distribution of clouds in the Milky Way. Most but not all clouds are found along spirals. (Garcia Fuentes et al. 2014)

SPIRAL ARMS AND THE WINDING PROBLEM

The basic idea for spiral formation is differential rotation:

A flat rotation curve implies a differential rotation: $\Omega \propto R^{-1}$

→ matter gets sheared into a spiral

But quickly, the spiral would be very tightly wound, and thus short-lived (unlike grand-design spirals) = winding problem

Simplistic solution: re-formation of the spiral.

Problem: spirals are also seen in NIR (= old stars), so they must be old

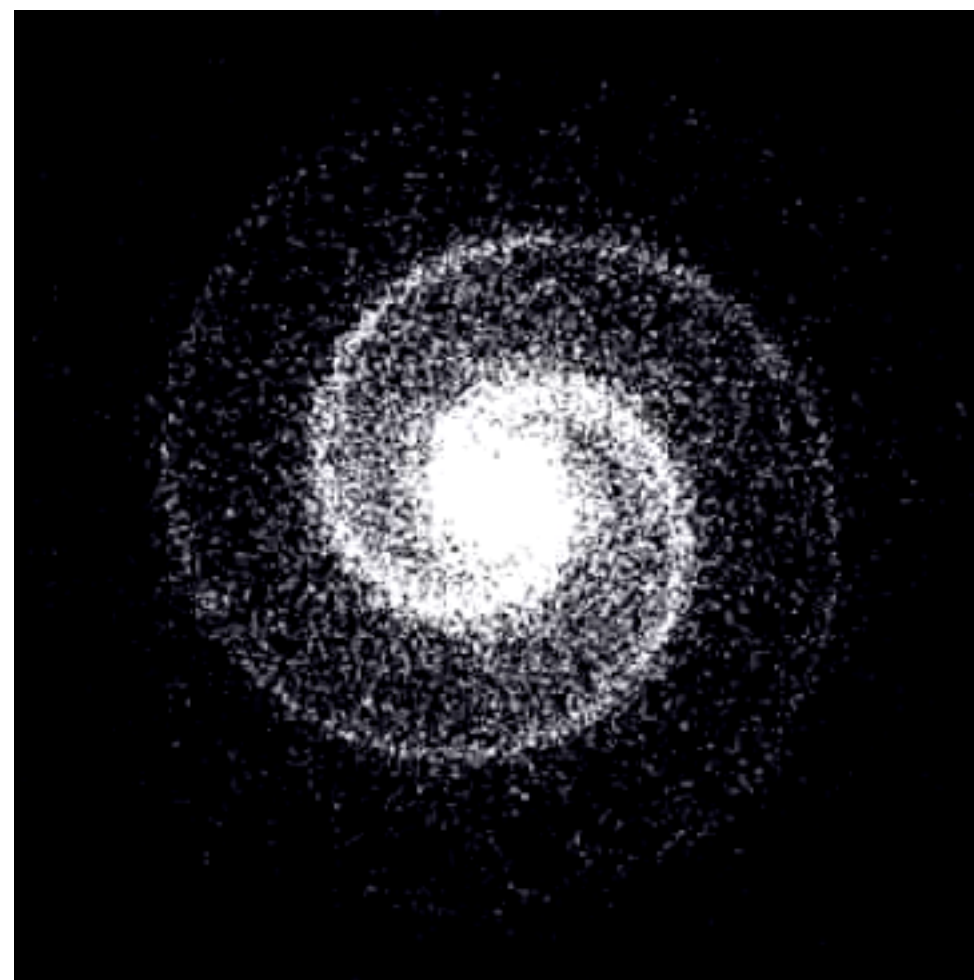


Fig: example of a winding spiral

Movie: the winding problem

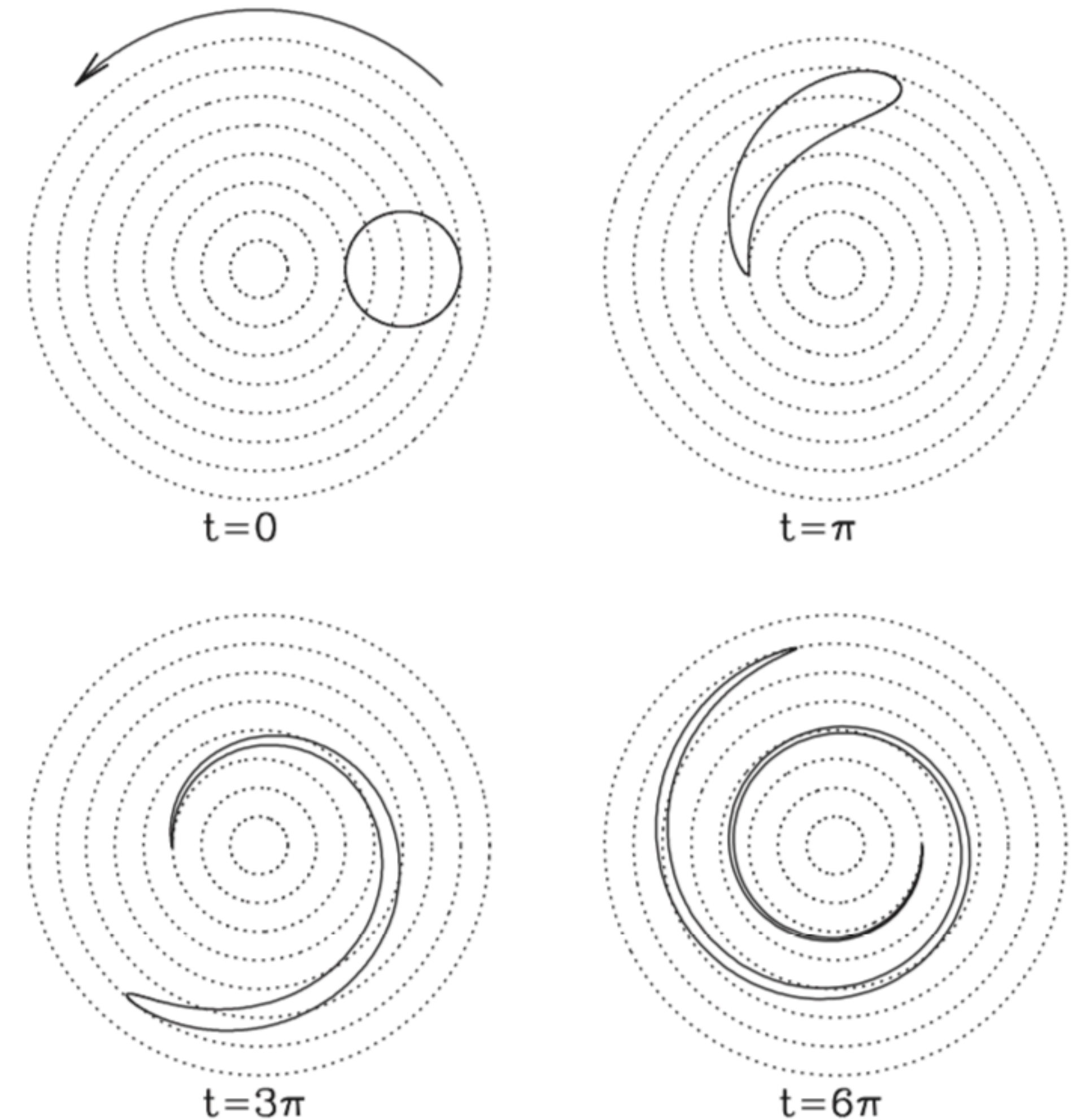


Fig: spiral formation via differential rotation (Mo et al. 2010)

SPIRAL DENSITY WAVE

The solution to the winding problem: spirals are not material structures, but density waves

→ Density wave theory (Lin & Shu 1964)

A spiral structure has a pattern speed Ω_p

→ Almost all stars have a $\Omega \neq \Omega_p$

(except at the radius where $V/R = \Omega_p$, which is the co-rotation)

*needs an instability to trigger it
(e.g. tidal interaction with a
companion, but not in all cases)
This is still not understood!*

The passage of the wave increases local density → favors star formation

Clouds are expected to be destroyed when leaving the arm, but we observe inter-arm clouds... (this is not fully understood and relates to uncertainties on the lifetime of clouds)

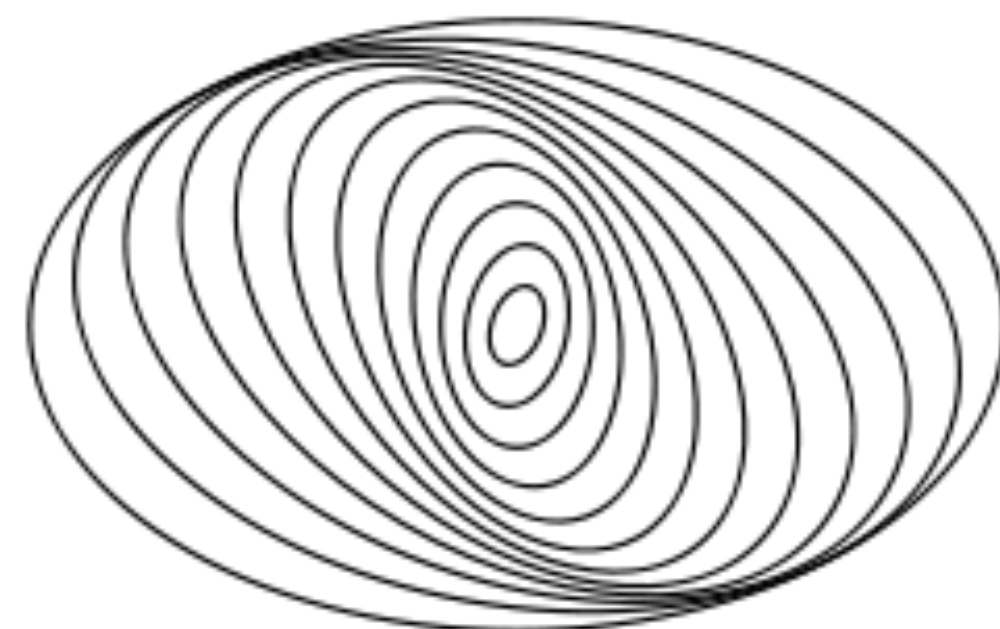


Fig: misaligned elliptical orbits lead to the formation of orbital over-densities = spiral waves



*Movie: density wave, in the reference frame of the spiral: matter enters and leaves the spiral
= no shearing from diff. rotation
(from I. Berg)*

GAS ACCUMULATION, OR COMPRESSION?

Cloud formation is more efficient along spiral arms

Simulations show that clouds are destroyed when they leave the spirals arms: shallower potential, stronger shear (e.g. Dobbs et al. 2006, Roman-Duval et al. 2010)

Arms have little effect on the star formation process itself

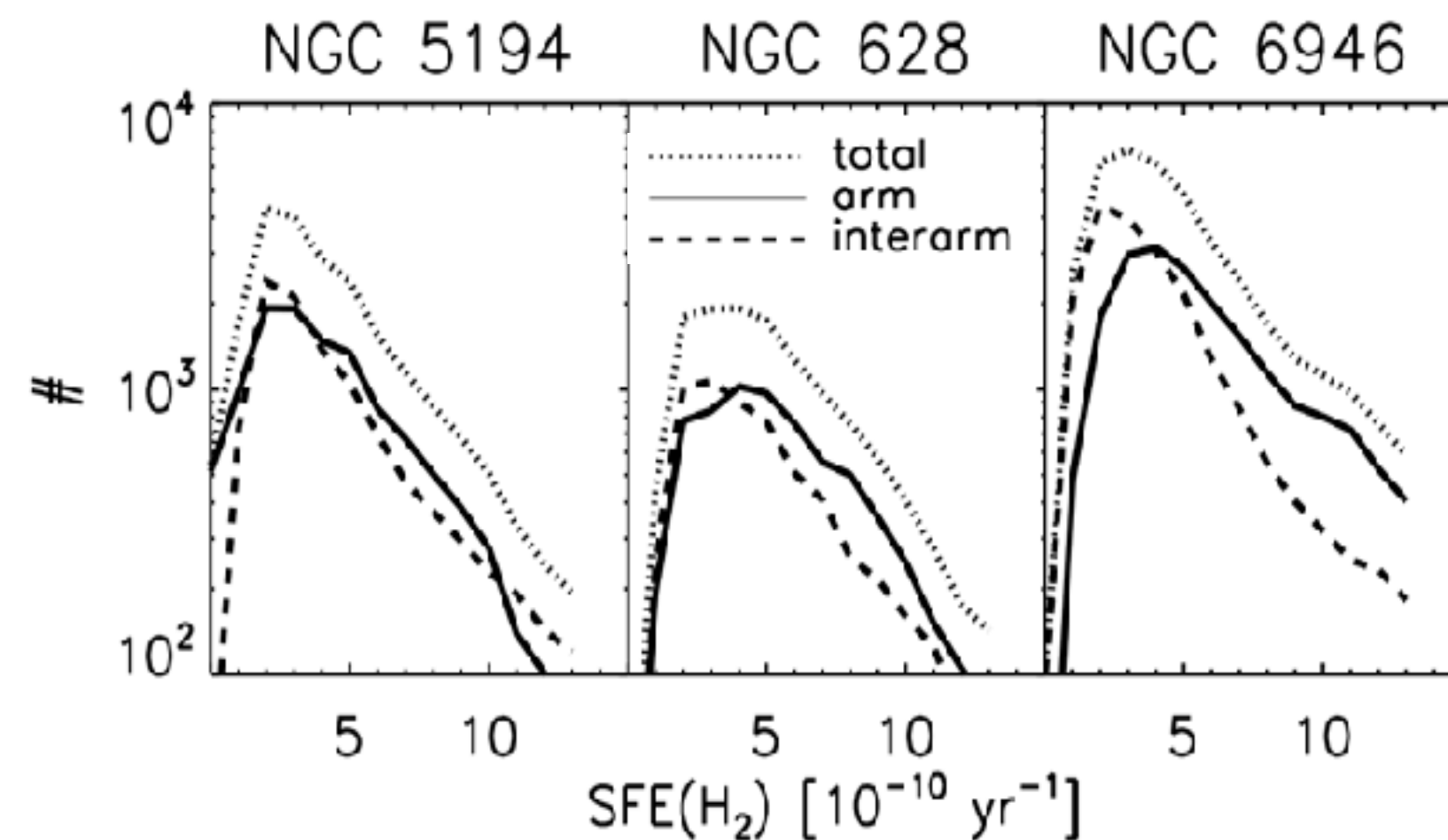
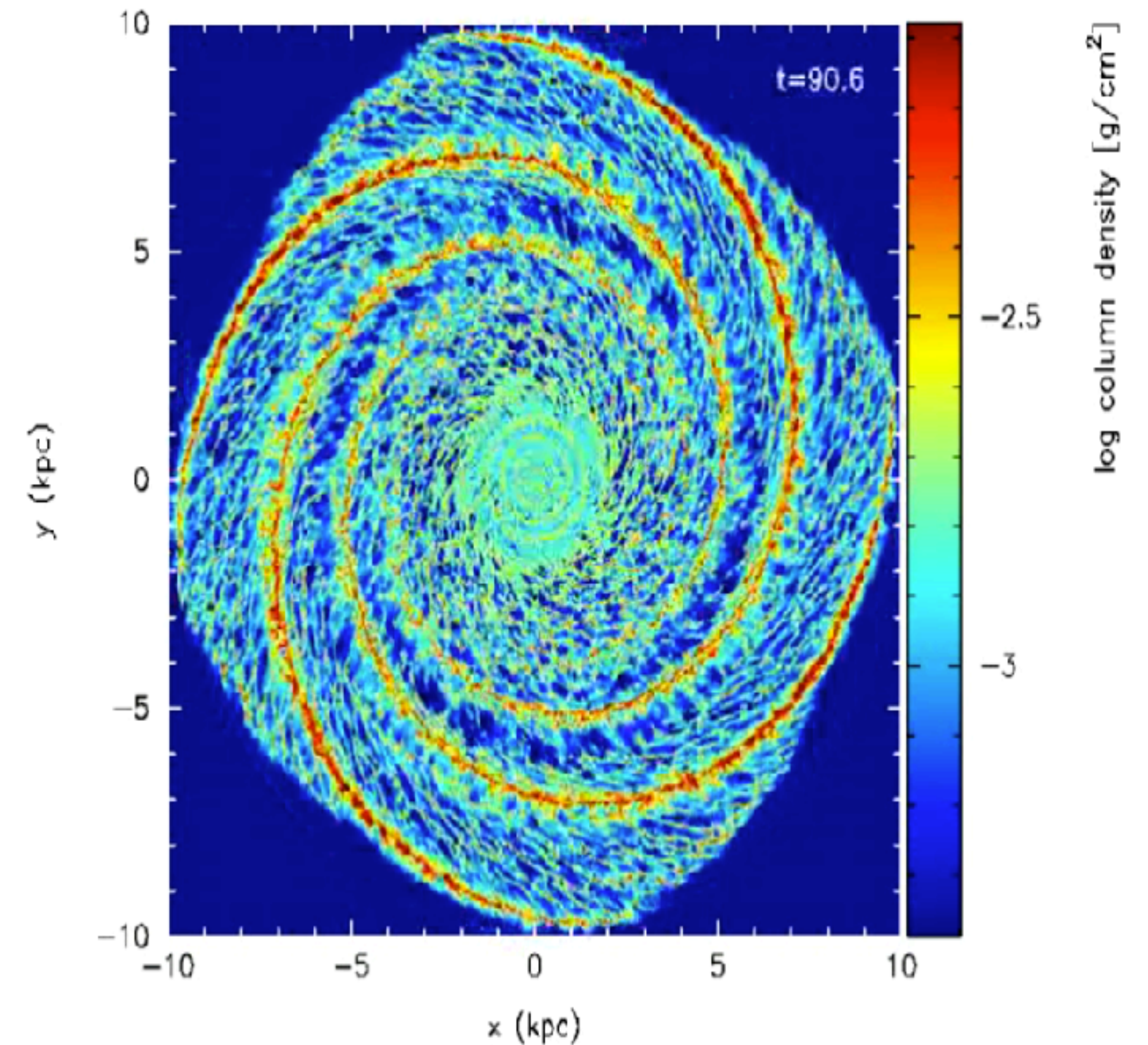
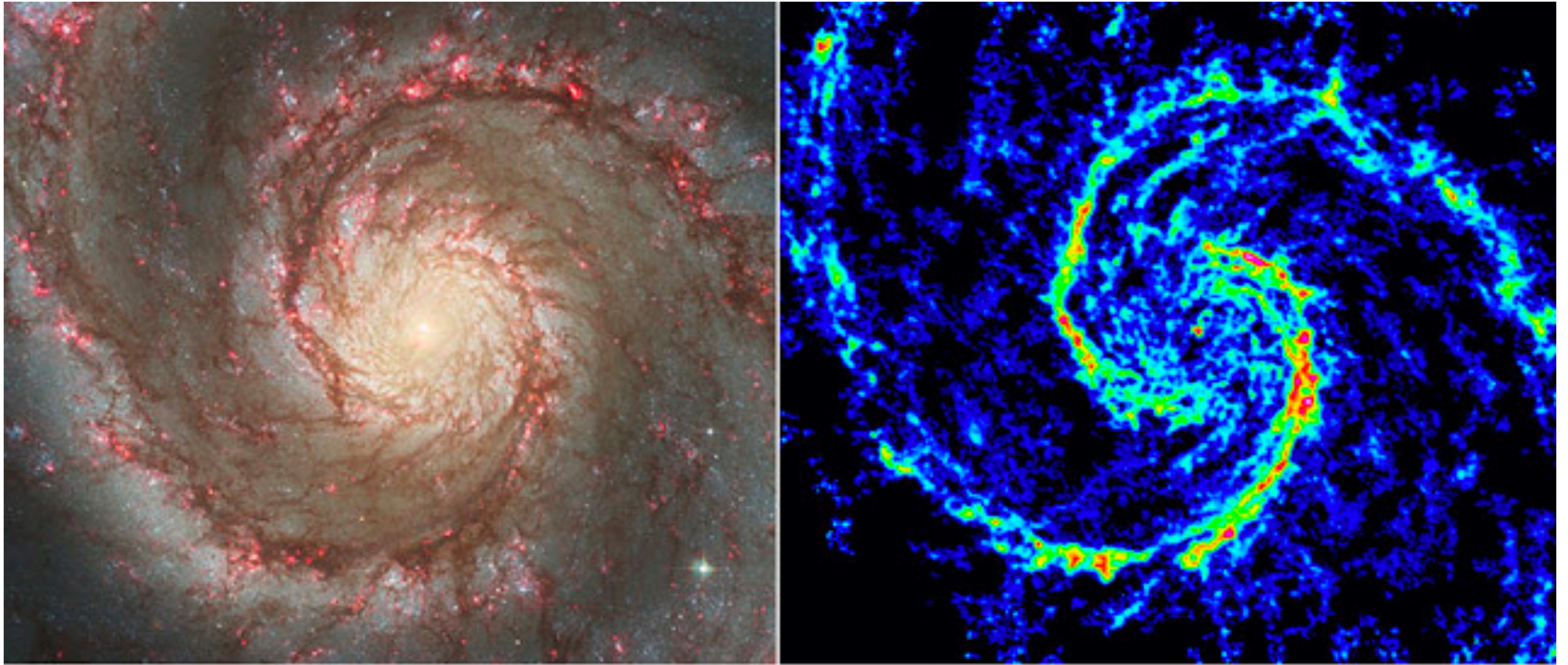


Fig: distribution of star formation efficiency in H₂ observed in different media in 3 galaxies. No big differences are found. (Foyle et al. 2010)



Movie: simulation of a disk with imposed spiral pattern. Overdensities are mostly found in the spirals, and dissolve when leaving the arms. (From C. Dobbs)

SPIRALS HOST A DIVERSITY OF STRUCTURES



*Fig: CO emission in the M51 galaxy
(Schinnerer et al. 2014)*

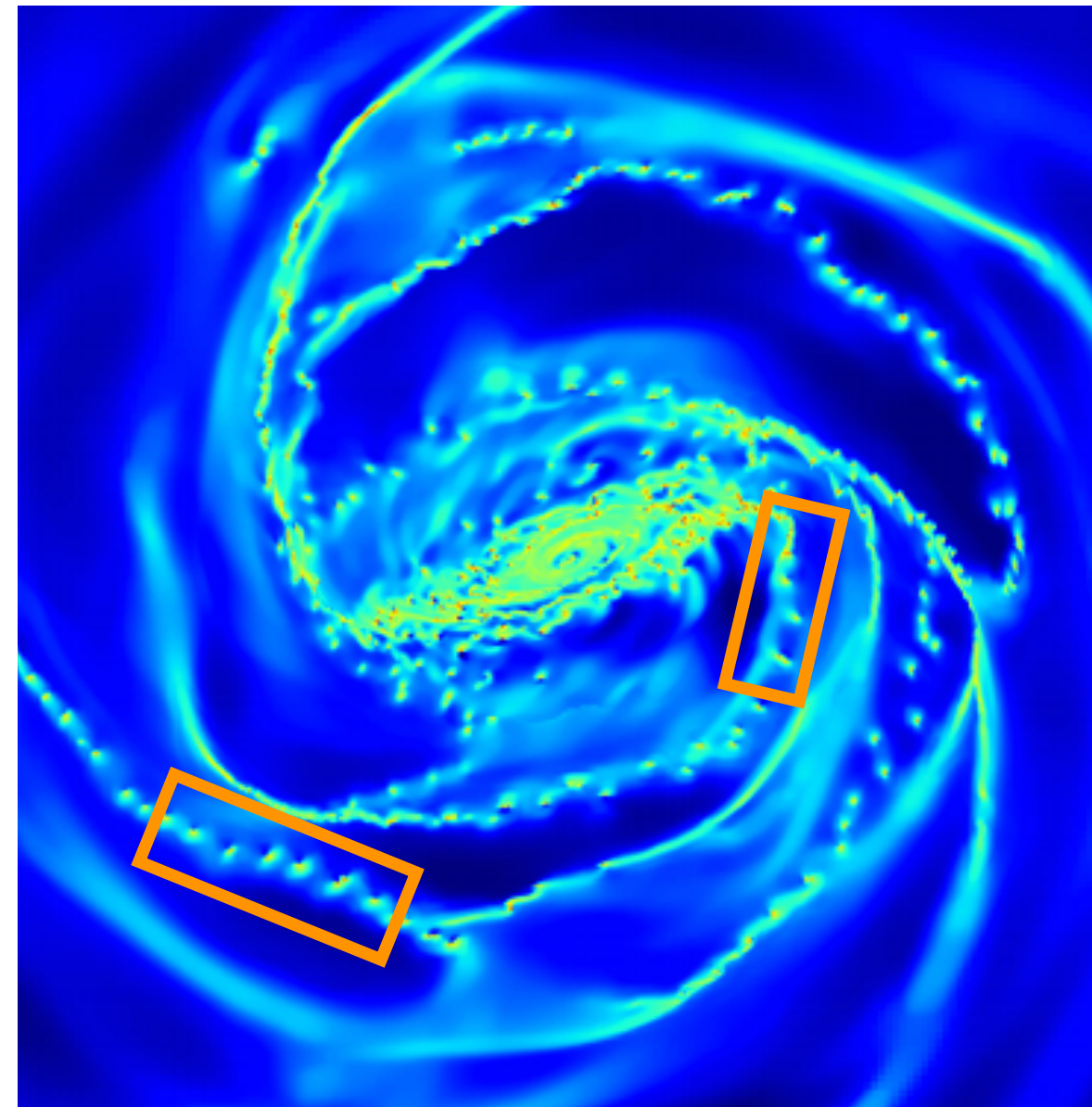
BEADS ON A STRING, SPURS

A same galaxy can host different structures along its spiral arms.

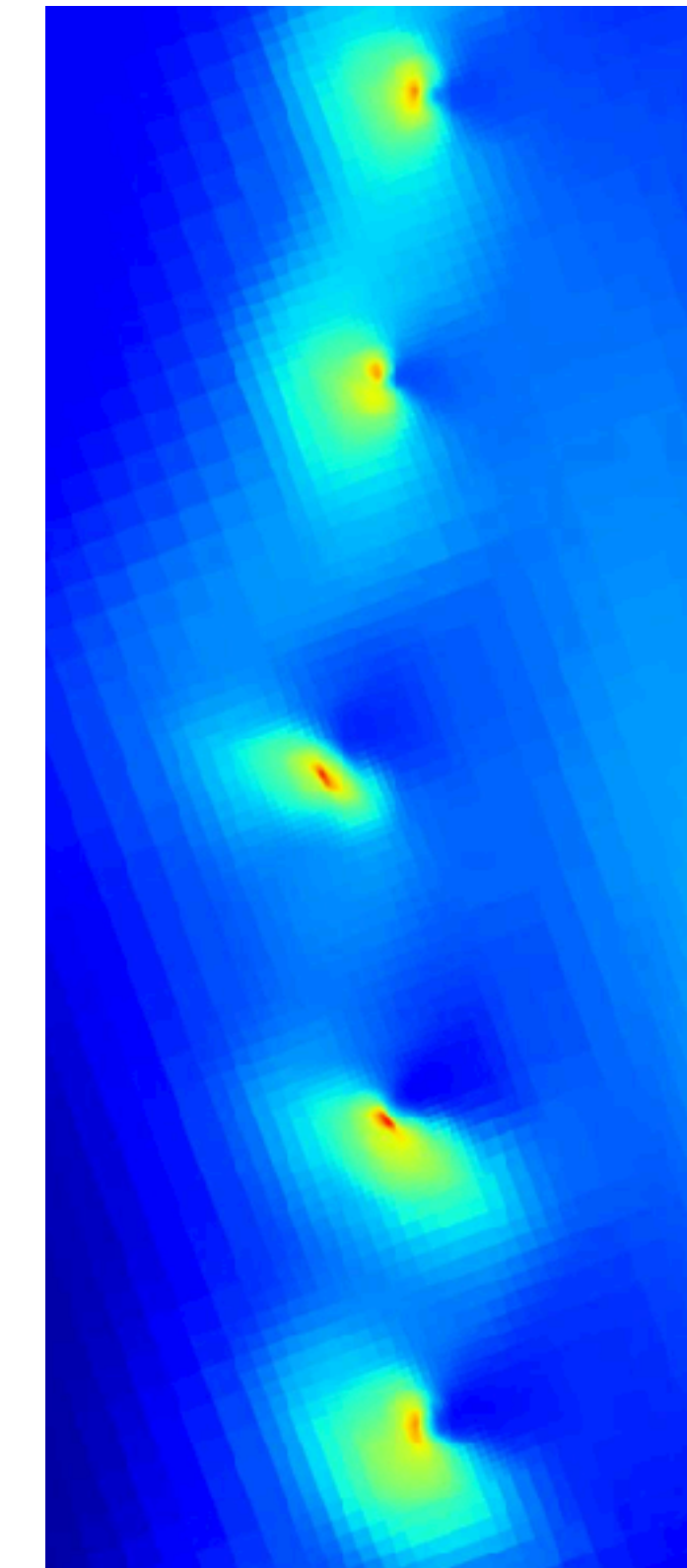
Clouds could be similar, but in very different environments.

Clouds in the inter-arm (e.g. feathers, spurs) survive the lack of compression from the arm

It questions the universality of cloud lifetime (~ 10 Myr). Still debated (it depends on the details of feedback prescriptions)



Beads on a string



Spurs

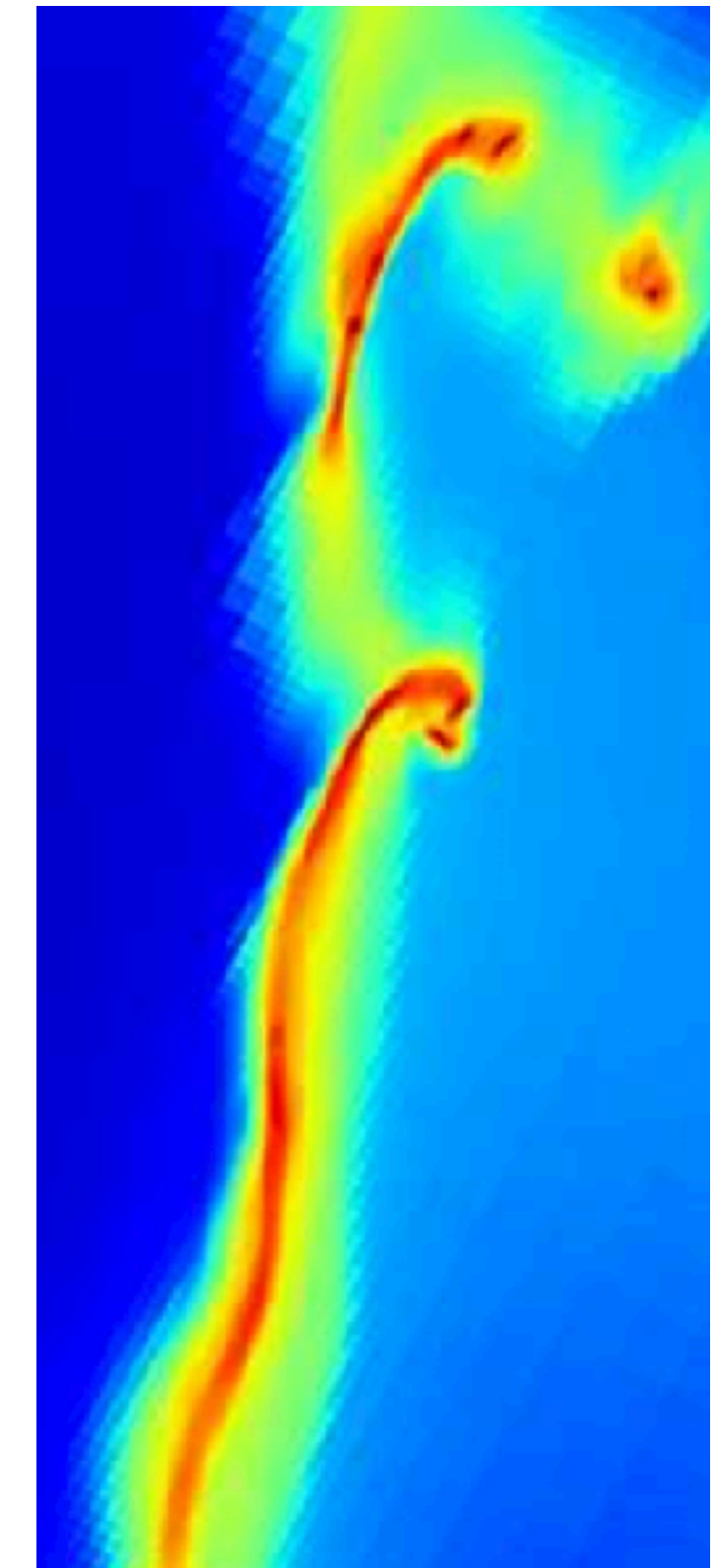
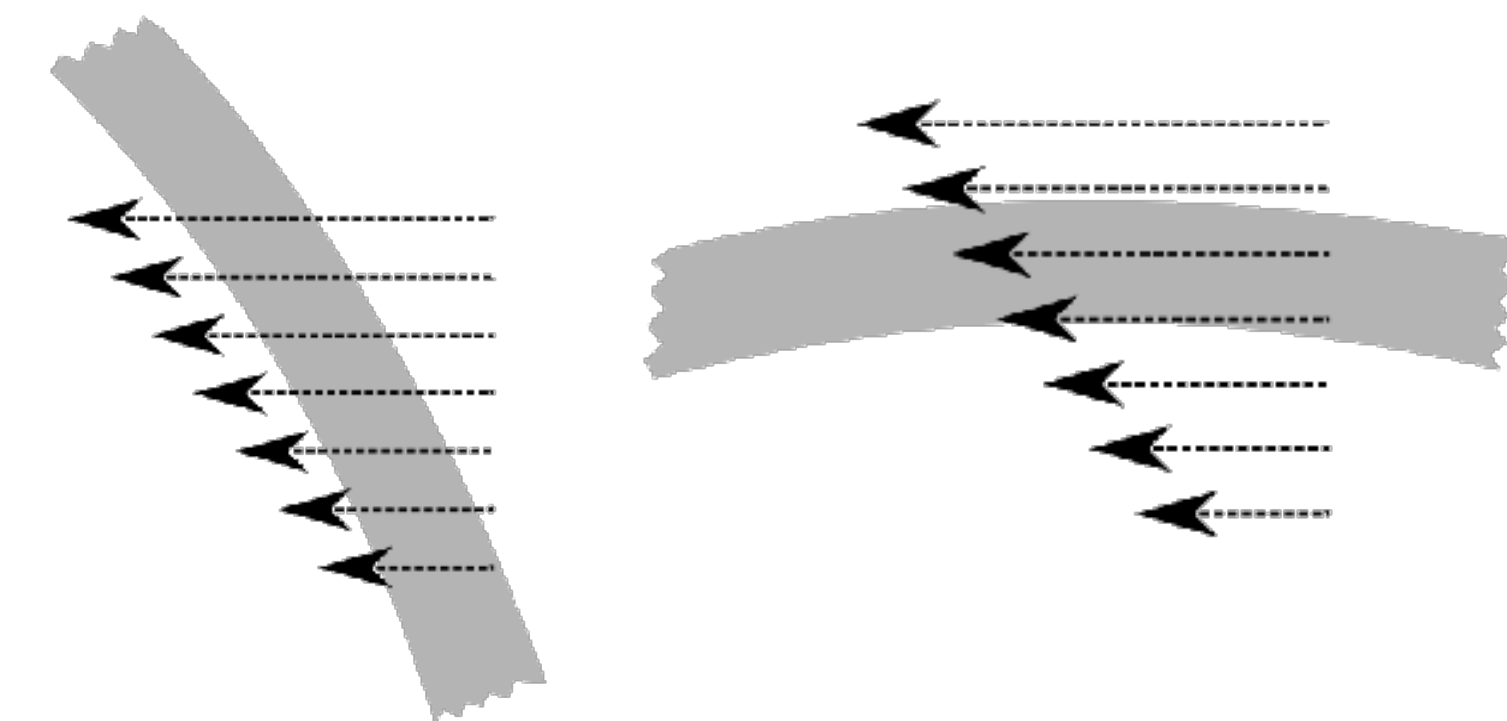


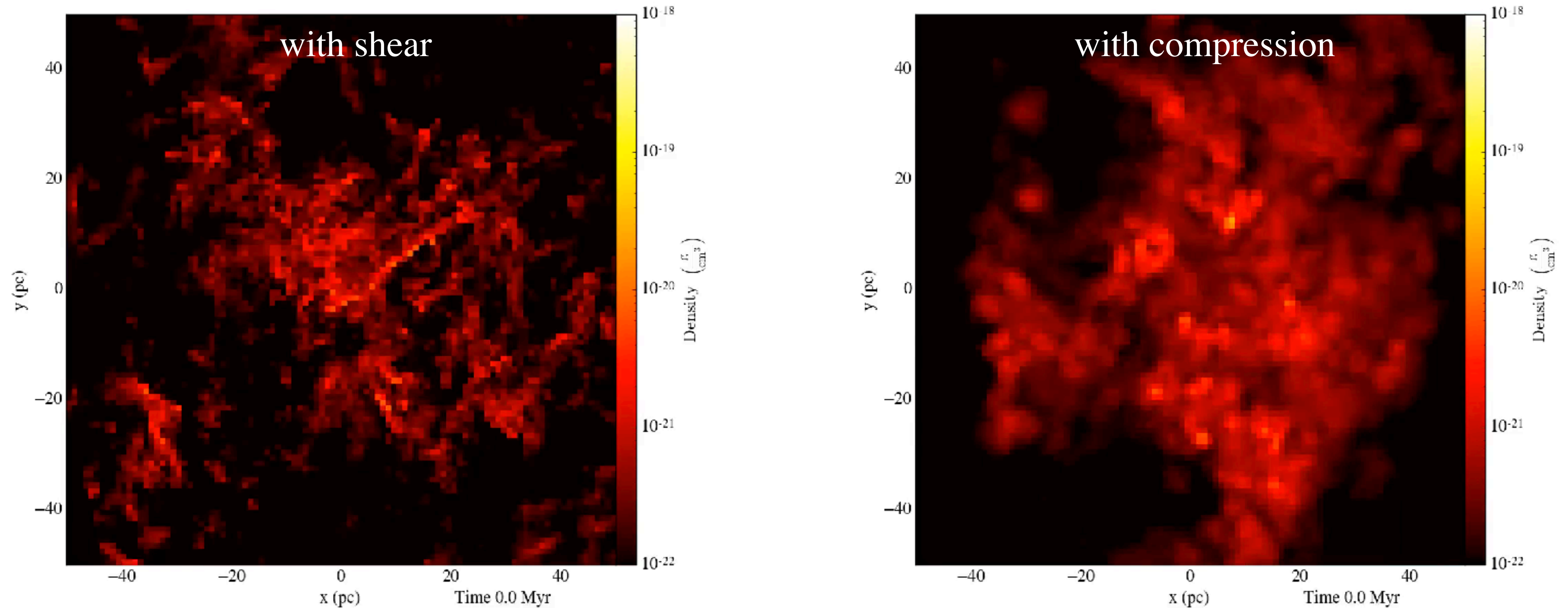
Fig: gas density along a spiral arm of a simulated Milky Way-like galaxy (top). A high pitch angle (i.e. arms being rather radial, left) leads to a small velocity difference (= weak shear) between the 2 sides of the arm. The arm can fragment into many clumps: beads on a string. A small pitch angle (right) yields a stronger velocity difference, and thus Kelvin-Helmholtz instabilities: spurs. Spurs are offset with respect to the main part of the arm. (Renaud et al. 2013, 2014)



LARGE SCALE DYNAMICS AND CLOUD EVOLUTION

kpc-scale dynamics sets the boundary condition for the evolution of clouds

Different boundary conditions lead to different outcome, time-scale, SFR etc.



Movies: simulations of a $10^5 M_{\odot}$ cloud with imposed shear (left) or compression (right), extracted from a galactic disk simulation. Without feedback (Rey-Raposo et al. 2015)

DIVERSITY OF SHEAR ENVIRONMENTS

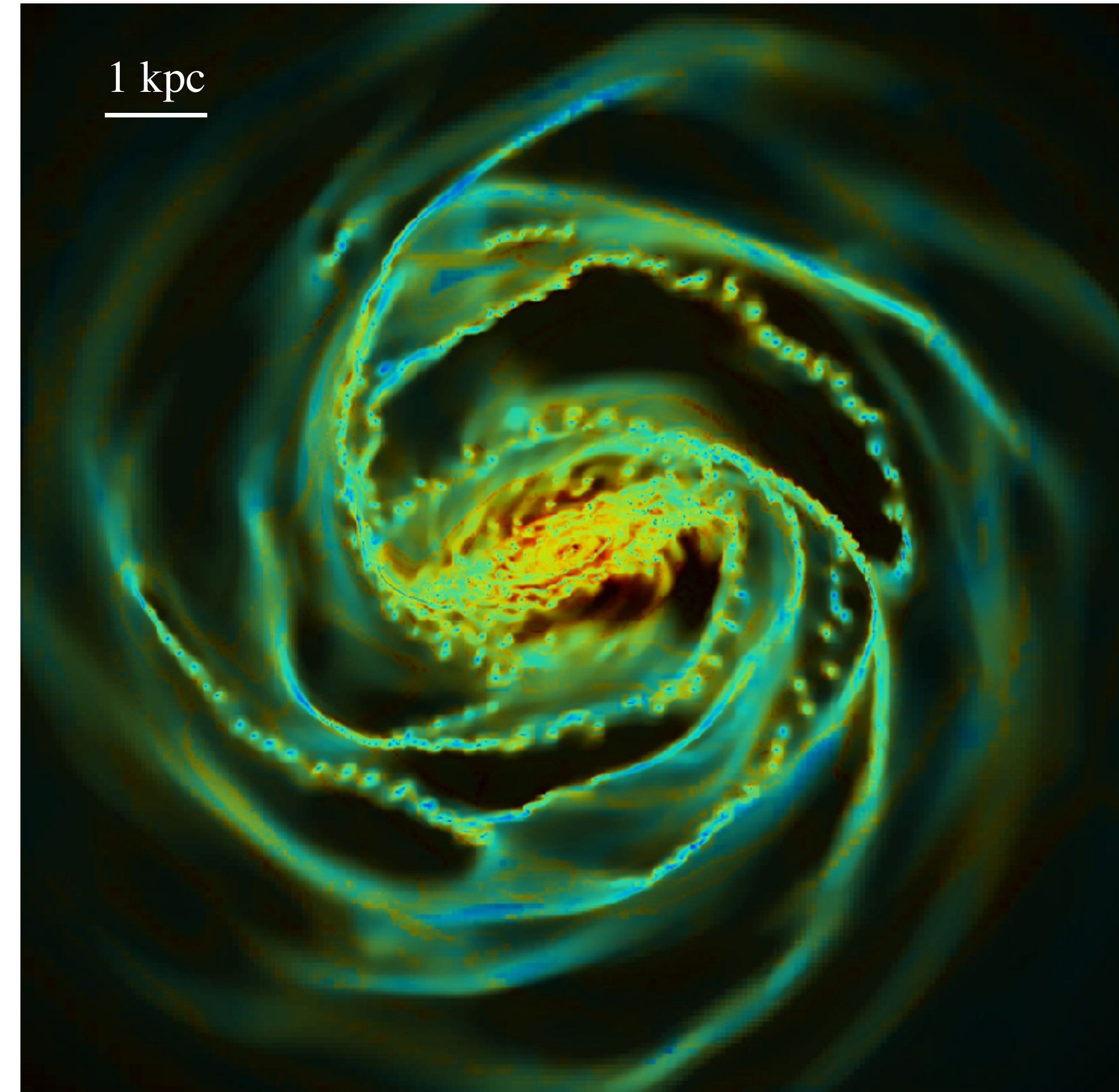
The galactic velocity curve (i.e. circular velocity vs. radius) inside the bar is steep \rightarrow strong shear

Shear smooths out overdensities like clouds

The gas stay dense, but without any central over-dense seed to collapse on \rightarrow star formation is slowed down (or even quenched)

E.g. in the central molecular zone (~ 300 pc), $\sim 10^7 M_{\odot}$ of molecular gas is found at high surface density, but the SFR is ~ 20 lower than expected (Morris et al. 1989, Longmore et al. 2013)

Fig: map of the shear force (normalized to self-gravity) from a simulation of a Milky Way-like galaxy. Shear the strongest near the galactic center, but the details are complex. (Emsellem et al. 2015)



weak strong

shear / self-gravity

BAR FORMATION

If $\Omega - \frac{\kappa}{2}$ is roughly constant over a wide range of radii, orbits in this range precess together.

epicycle frequency

If such orbits have an elongated shape, the shape is preserved in this radial range \rightarrow bar formation

Because $\Omega - \frac{\kappa}{2}$ is not perfectly constant, self-gravity must help to keep the bar together

The question is now: what makes these orbits in the first place?
(we don't have a complete answer to this)

Present-day disk galaxies have a high central mass concentration (e.g. bulge), i.e. a strong ILR, which does not favor the formation of a bar or spirals.

Extreme cases of this: S0 galaxies: the bulge is too big to allow for spirals

\rightarrow Strong bars must form and grow slowly, together with the central mass

Bars exert gravitational torques on matter and drive the gas inwards
(this can fuel an active galactic nucleus)

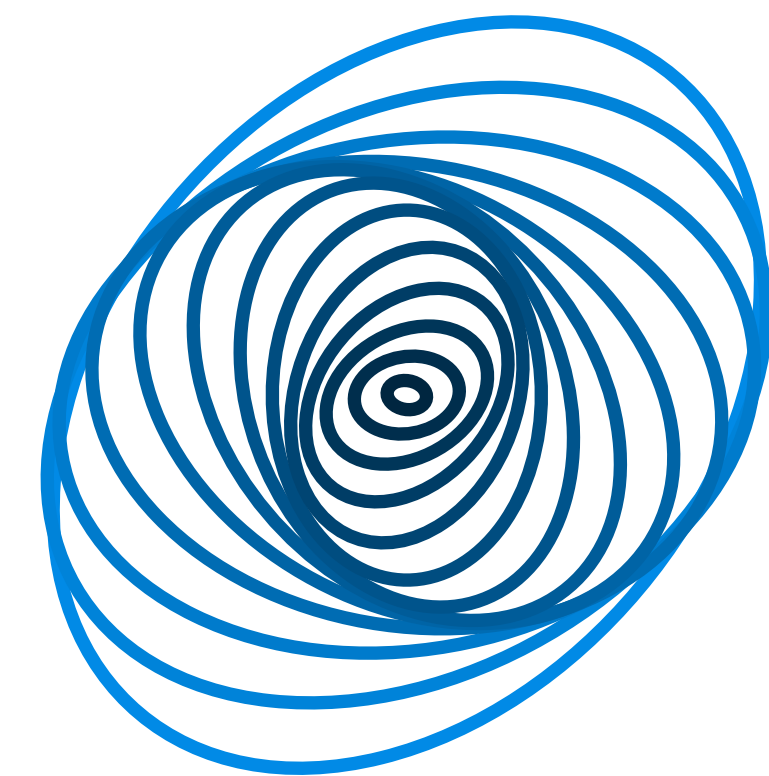


Fig: a spiral pattern appears with a simple shift in the phase of elongated orbits. It would be maintained with a roughly constant $\Omega - \kappa/2$

TIPS OF THE BAR

Gas can circulate along the bar
(on the so-called x_1 orbits)

For a Milky Way-like, it takes ~ 20 Myr
from one tip to the other

Tips of the bars are apocenters of these orbits
→ the mater slows down
→ traffic jam! (orbital crowding)

Connection with the spiral arm:
even more crowding!

Preferential location for cloud-cloud collisions

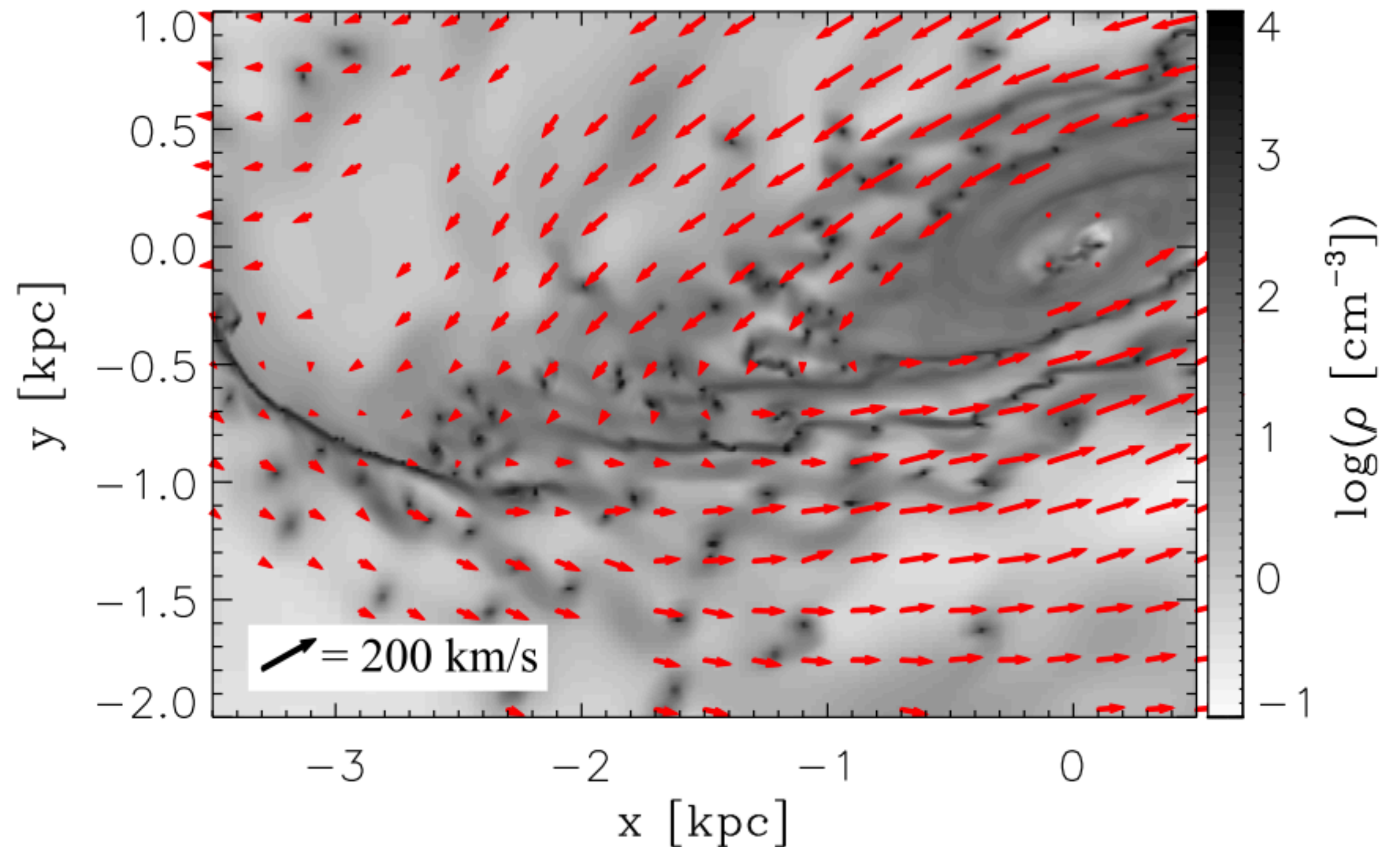


Fig: velocity field near the tip of the bar of a simulated Milky Way-like galaxy. The gas slows down at the tip. (Renaud et al. 2015)

CLOUD-CLOUD COLLISIONS

Collisions increase the gas density (e.g. shocks)

Similar physics as in galaxy mergers
(e.g. tidal tails can be detected)

It can lead to the formation of giant molecular associations
as observed at the tip of the Milky Way's bar (W43)

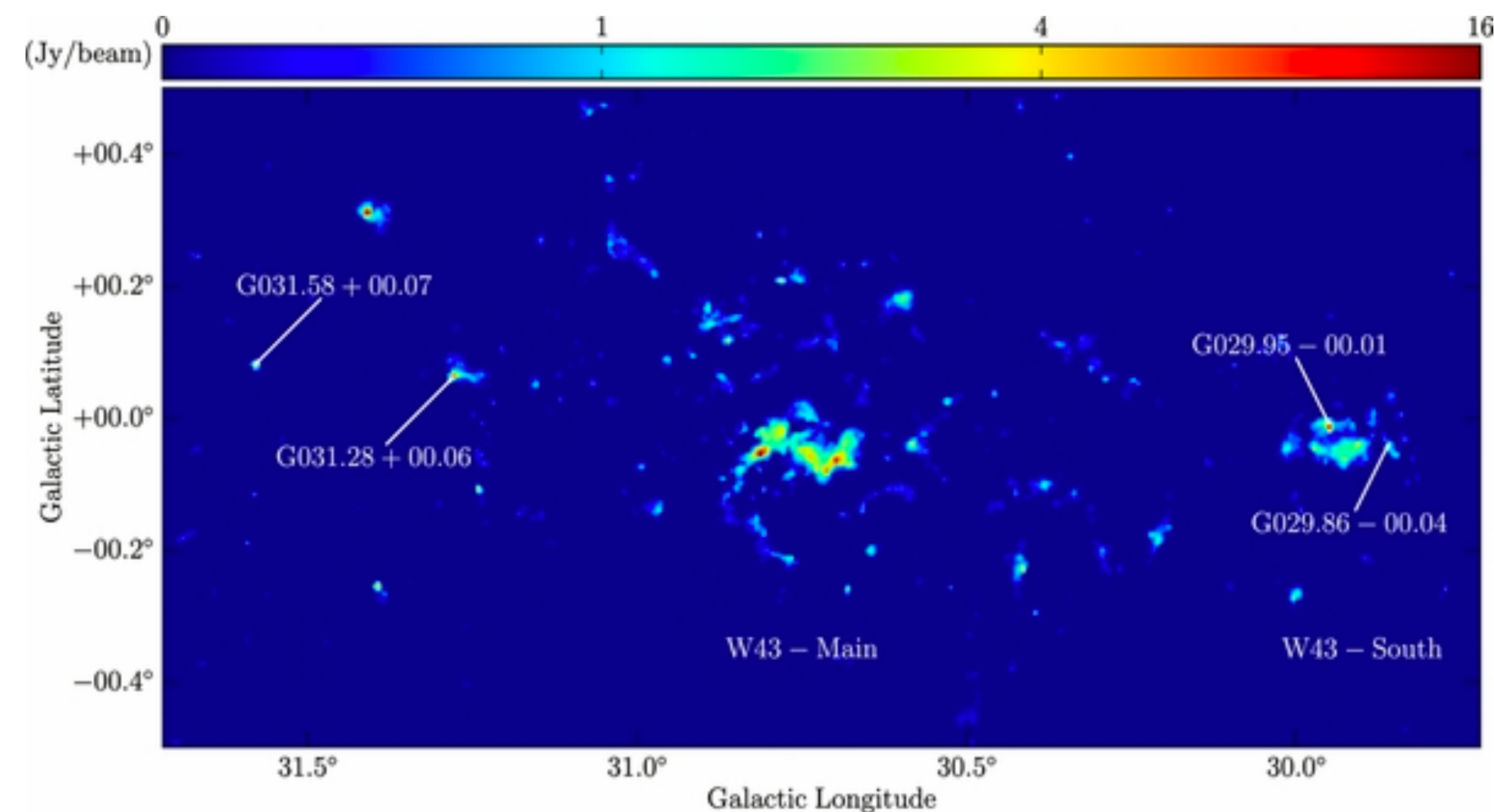


Fig: observations of CO in W43 (Zhang et al. 2014)

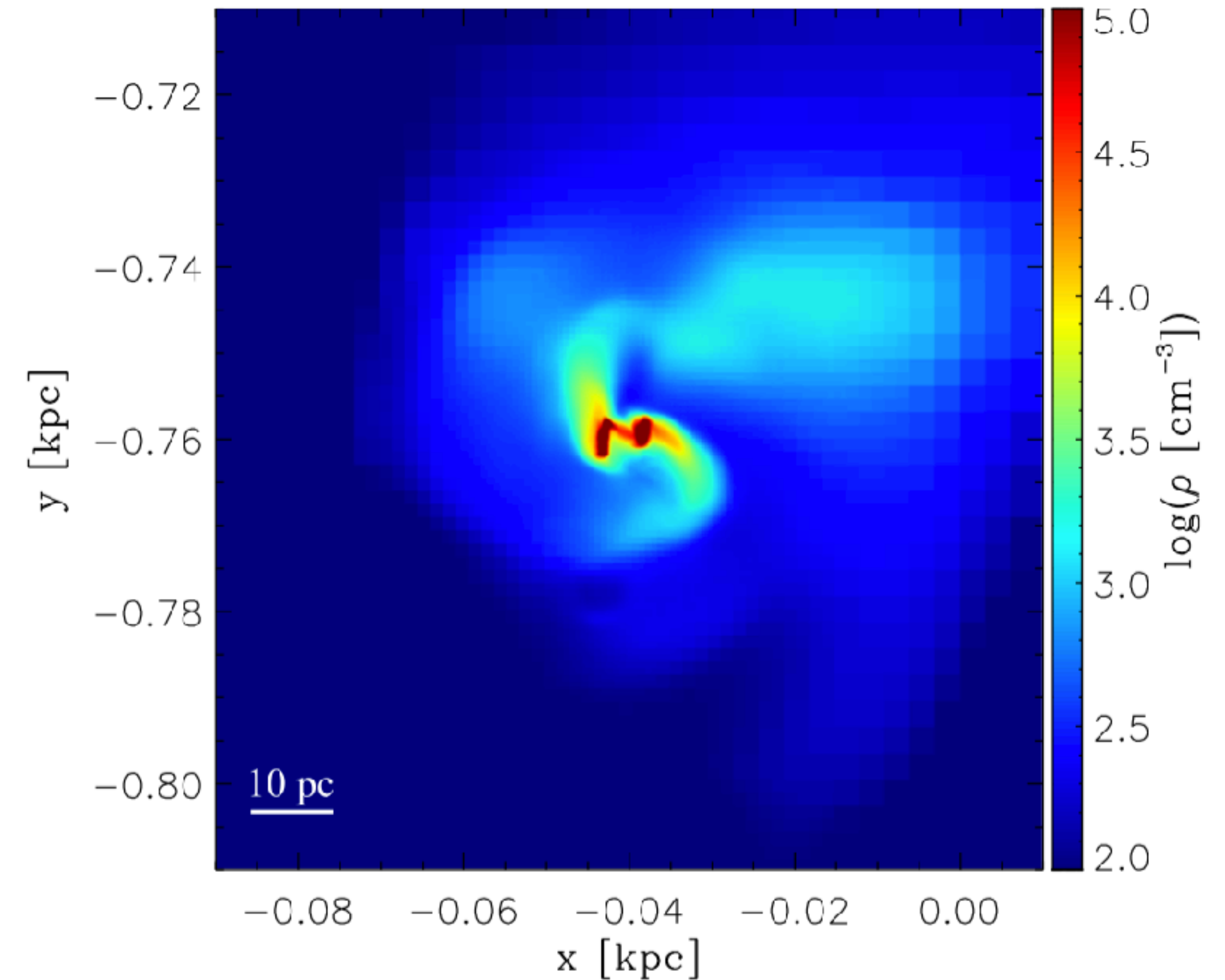


Fig: cloud-cloud collision at the tip of the bar of a Milky Way-like galaxy (Renaud et al. 2015)

INCREASE OF THE STAR FORMATION ACTIVITY

As interacting galaxies, cloud-cloud collisions can trigger star formation (Tan 2000, Inoue & Fukui 2013)

Star formation and young stars are preferentially found on the downstream side of the tip of the bar

The resulting association yields higher star formation efficiency than its progenitors and than typical clouds

Collisions can lead to the formation of massive stars (Takahira et al. 2014)

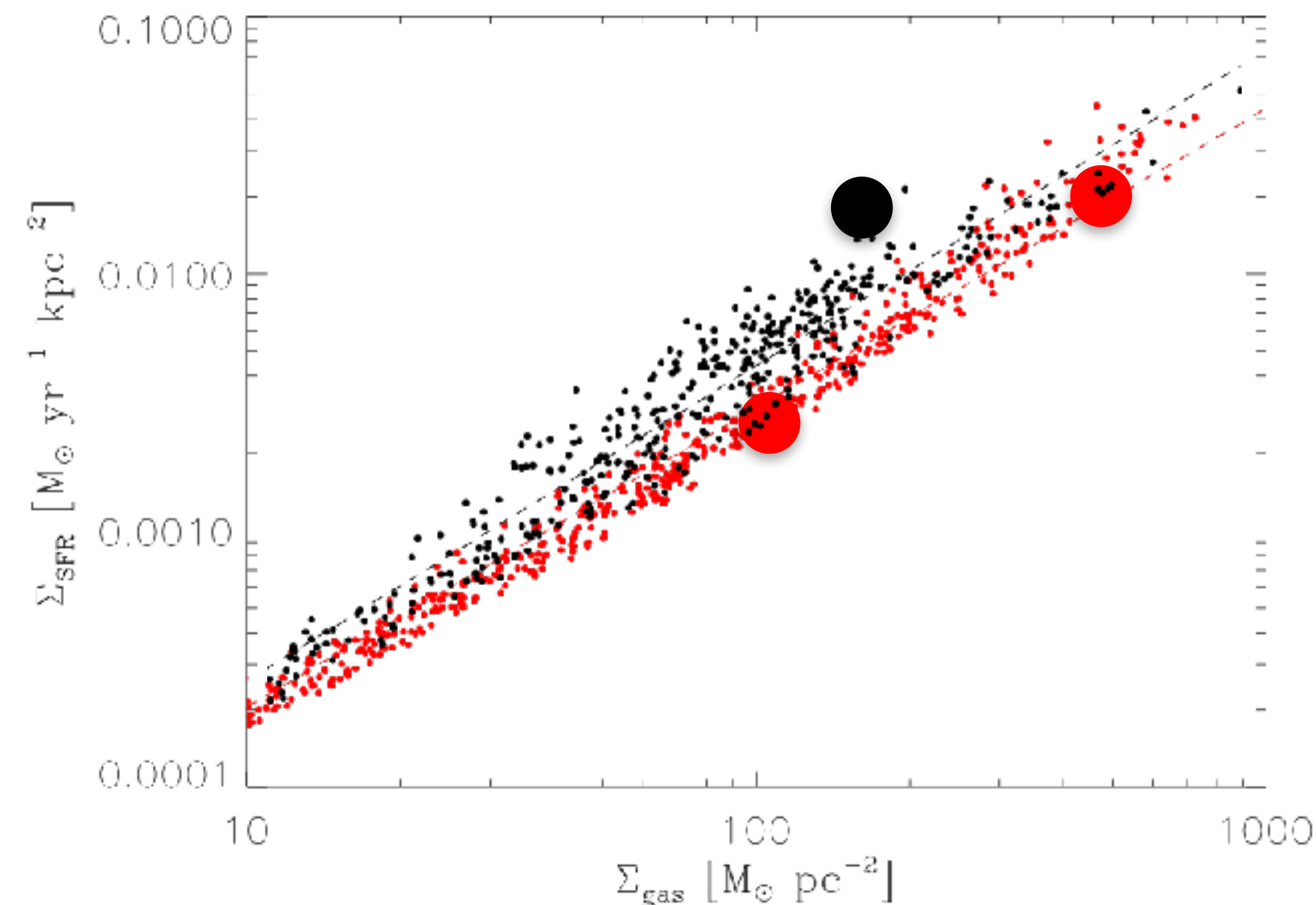
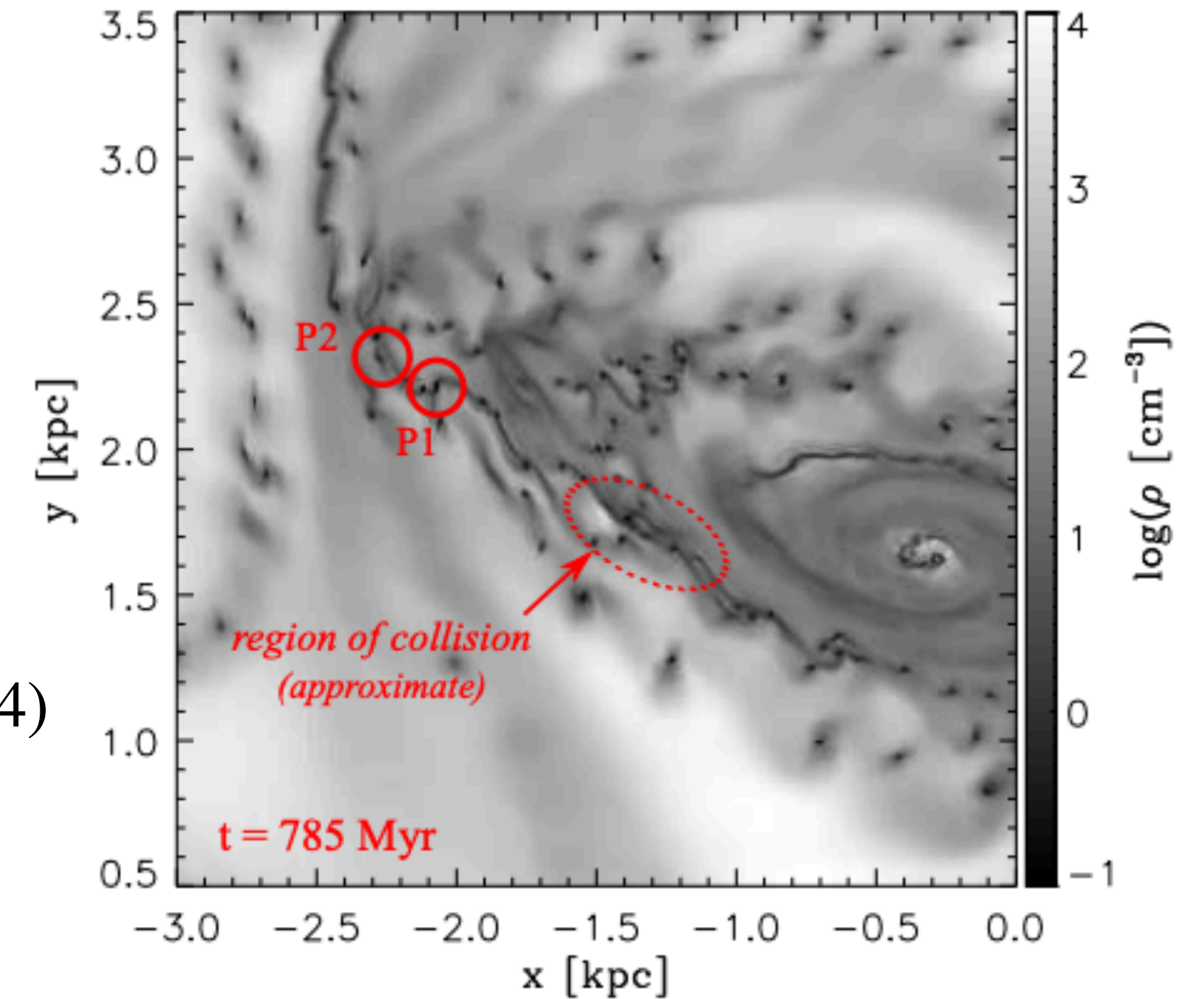


Fig: top: gas density at the tip of the bar in a Milky Way-like simulation. The clouds P1 and P2 will merge within a few Myr. Left: Kennicutt-Schmidt diagram of all molecular clouds in this simulation, highlighting progenitors of a cloud-cloud collision (large red circle) and their merger (large black circle). The merger lies above the bulk of all the other clouds (Renaud et al. 2015)

CLUMPY GALAXIES

At high redshift: high gas fraction: $f = \frac{M_{\text{gas}}}{M_{\star} + M_{\text{gas}}}$ ($\sim 50 - 60\%$ for Milky Way-like progenitors at $z \sim 1 - 2$)

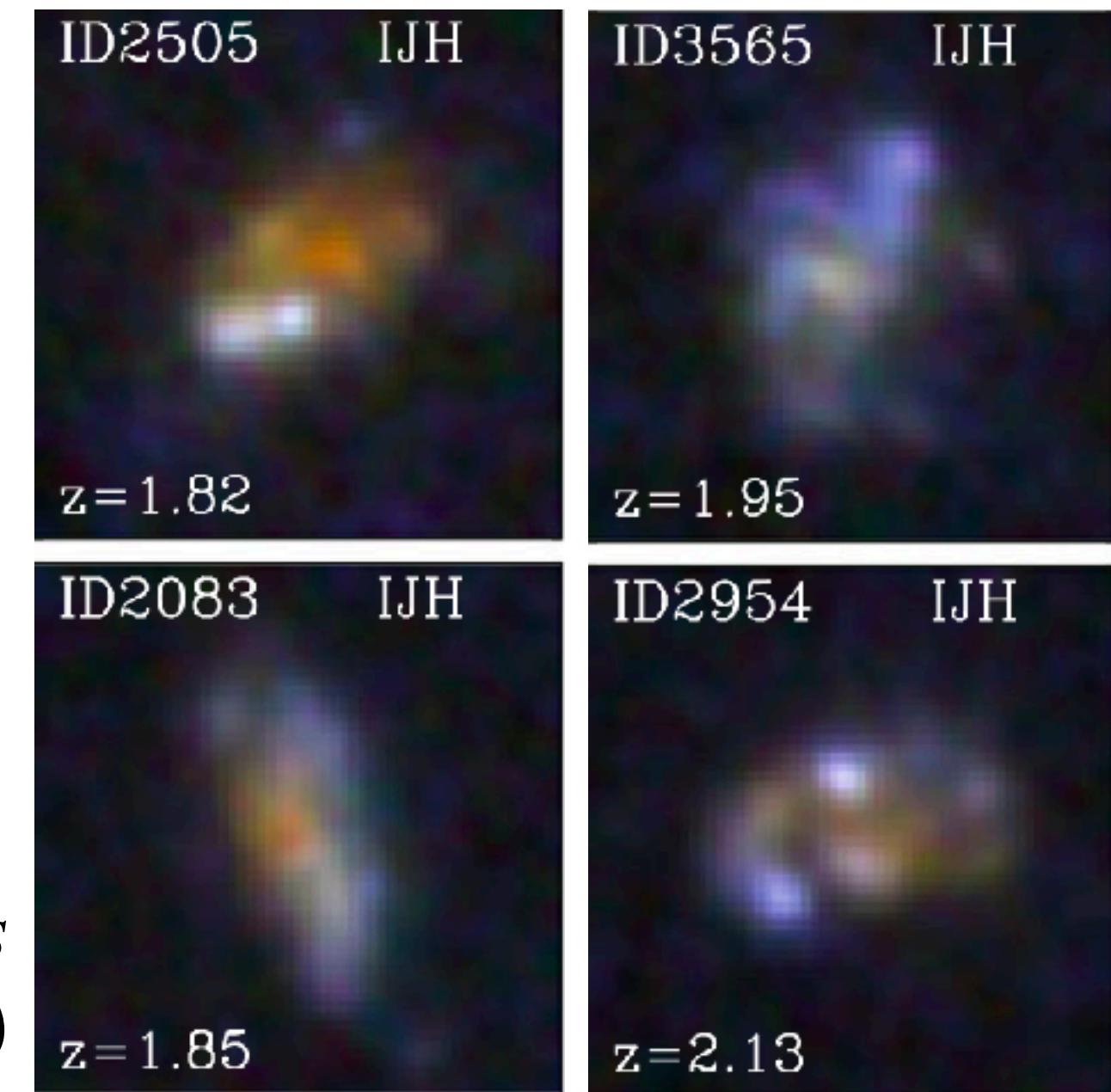
Turbulent ISM (Mach number: $\mathcal{M} \sim 10$)

Instabilities driven by the gas in the inter-clump medium lead to the formation of massive clumps ($10^{8-9} M_{\odot}$)

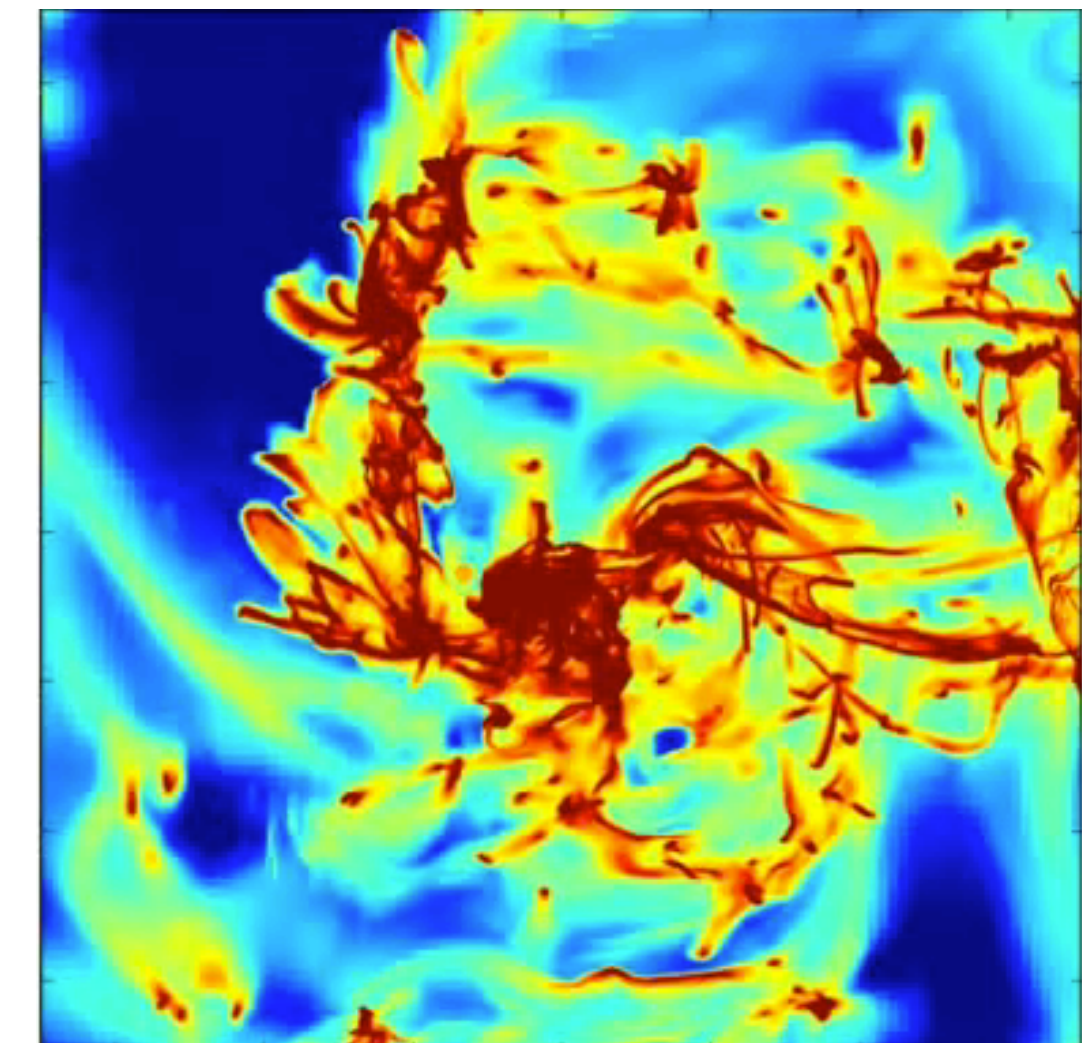
→ intense star formation (high SFR but average SFE) *Fig: observed clumpy galaxies (Wuyts et al. 2012)*

Feedback can be trapped in dense clumps
→ survival of clumps for > 100 Myr
→ long enough to spiral-in and contribute to bulge formation and BH growth

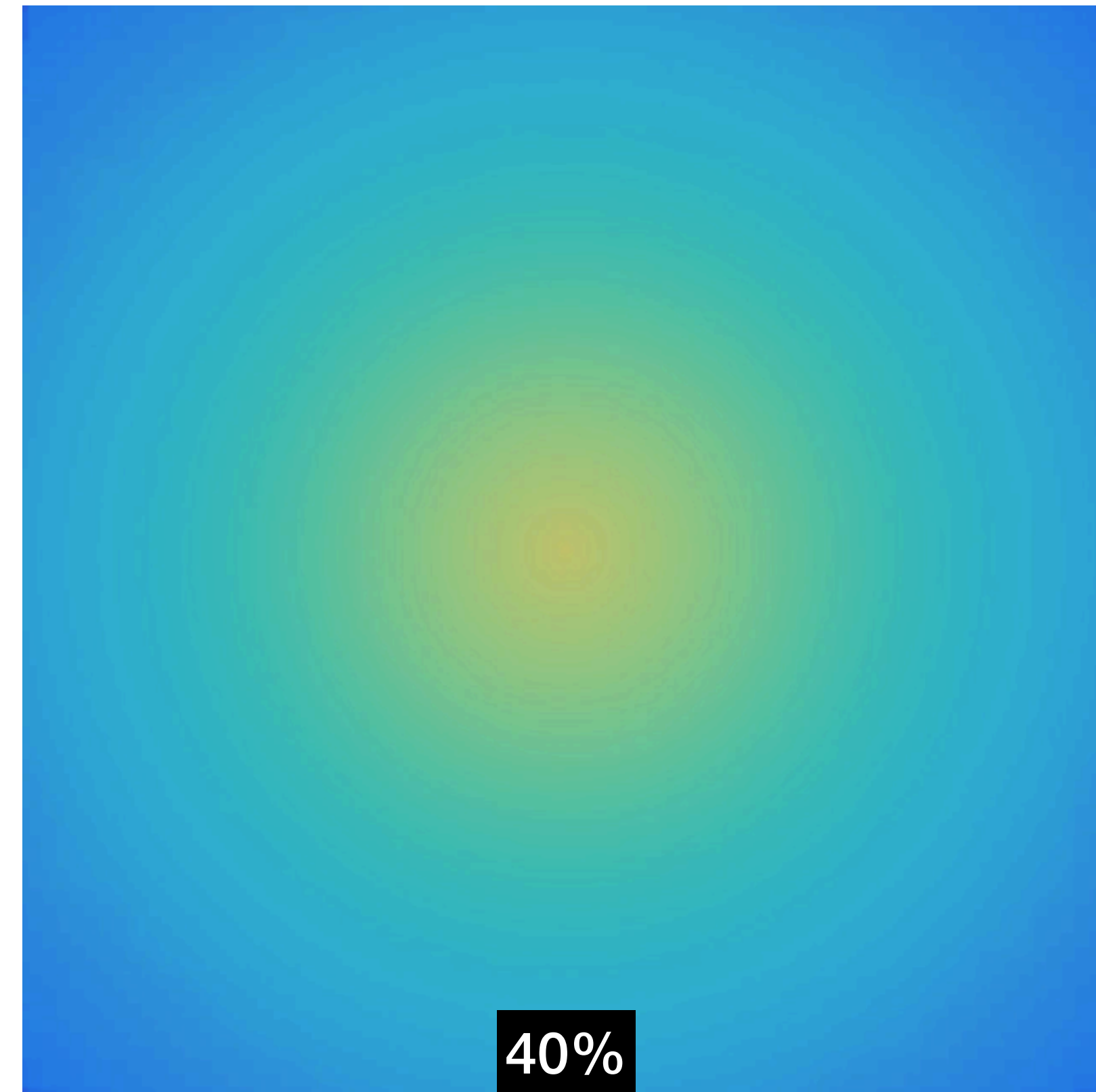
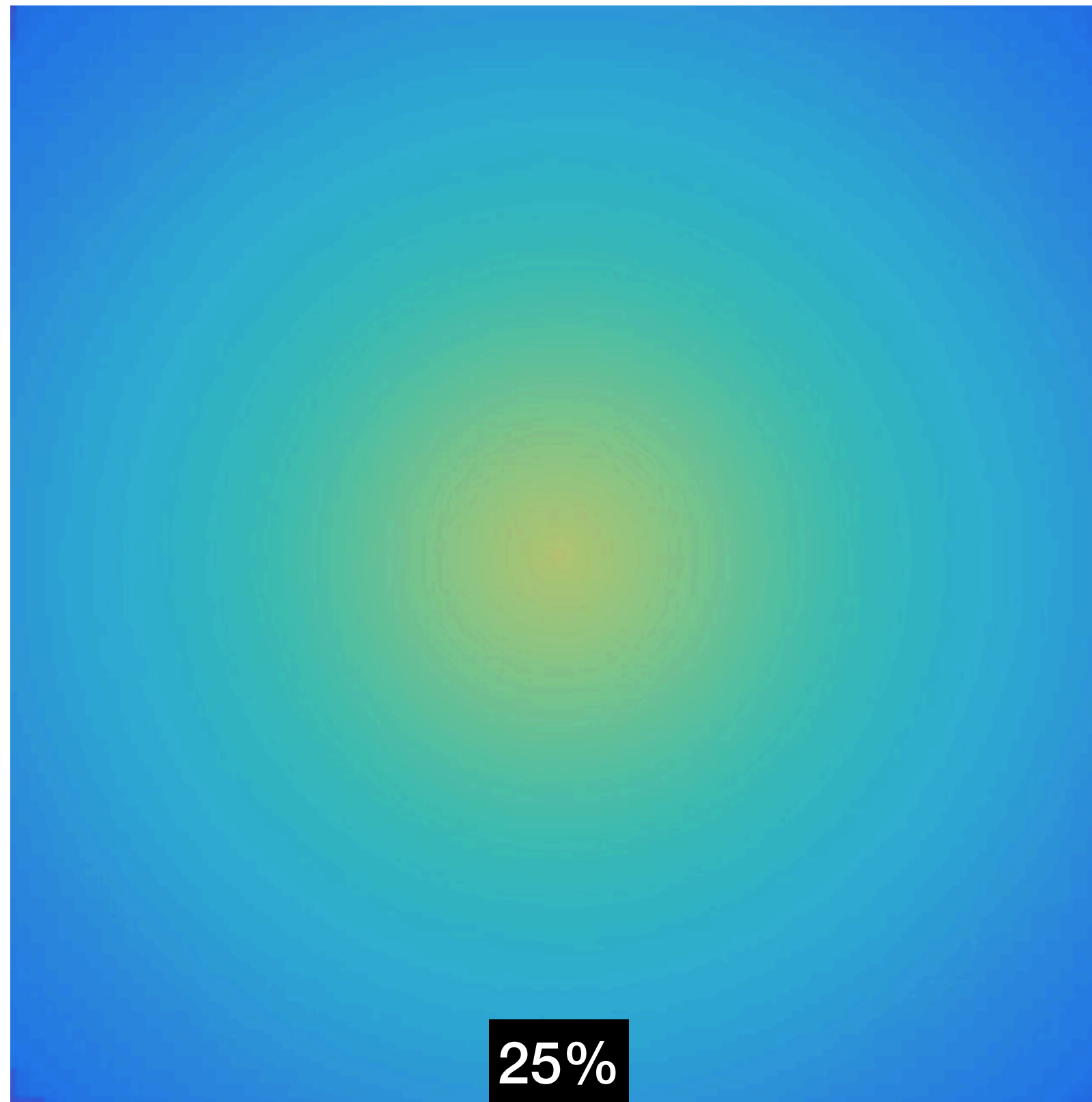
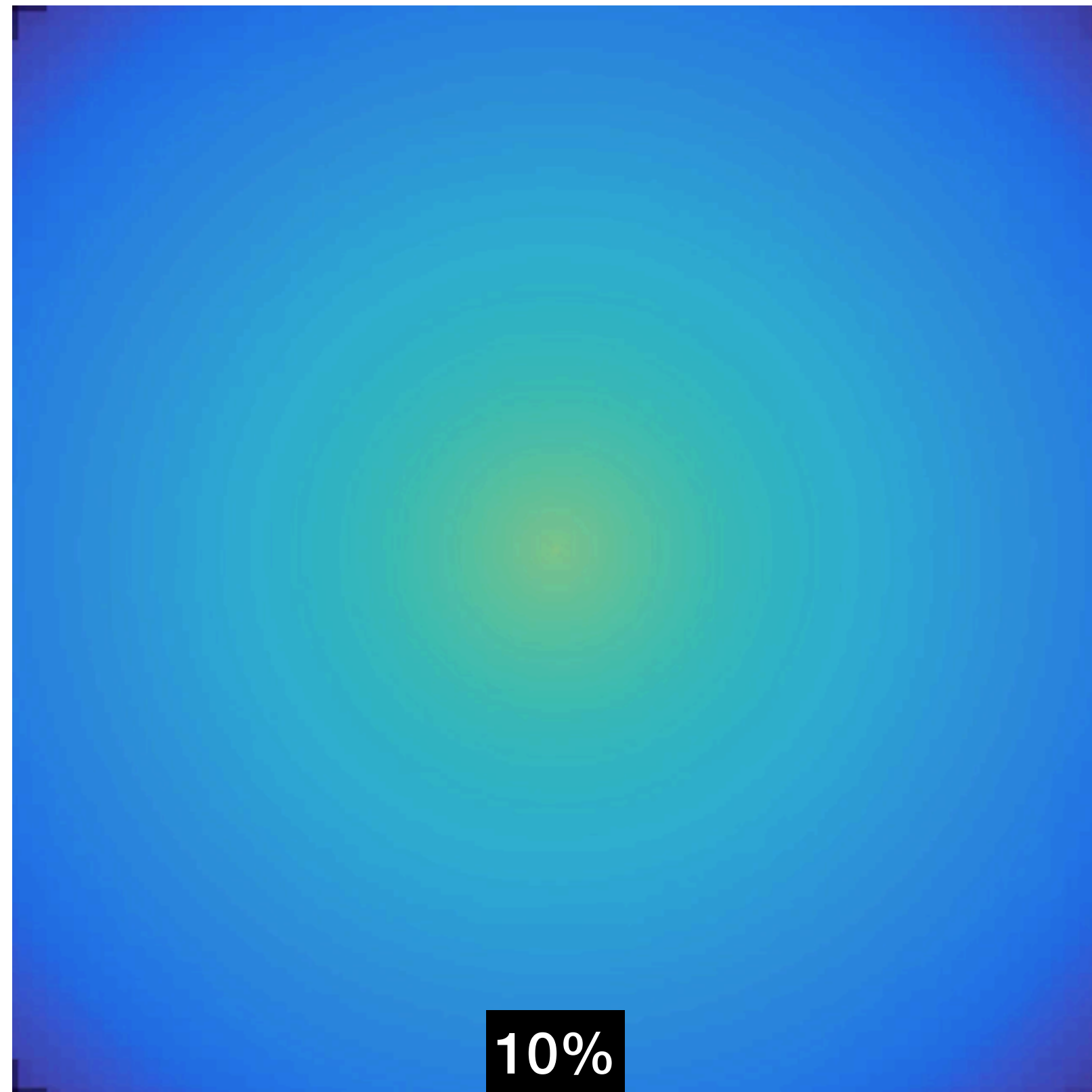
still debated but likely



Movie: gas density in a simulation of a clumpy galaxy



VARYING THE GAS FRACTION

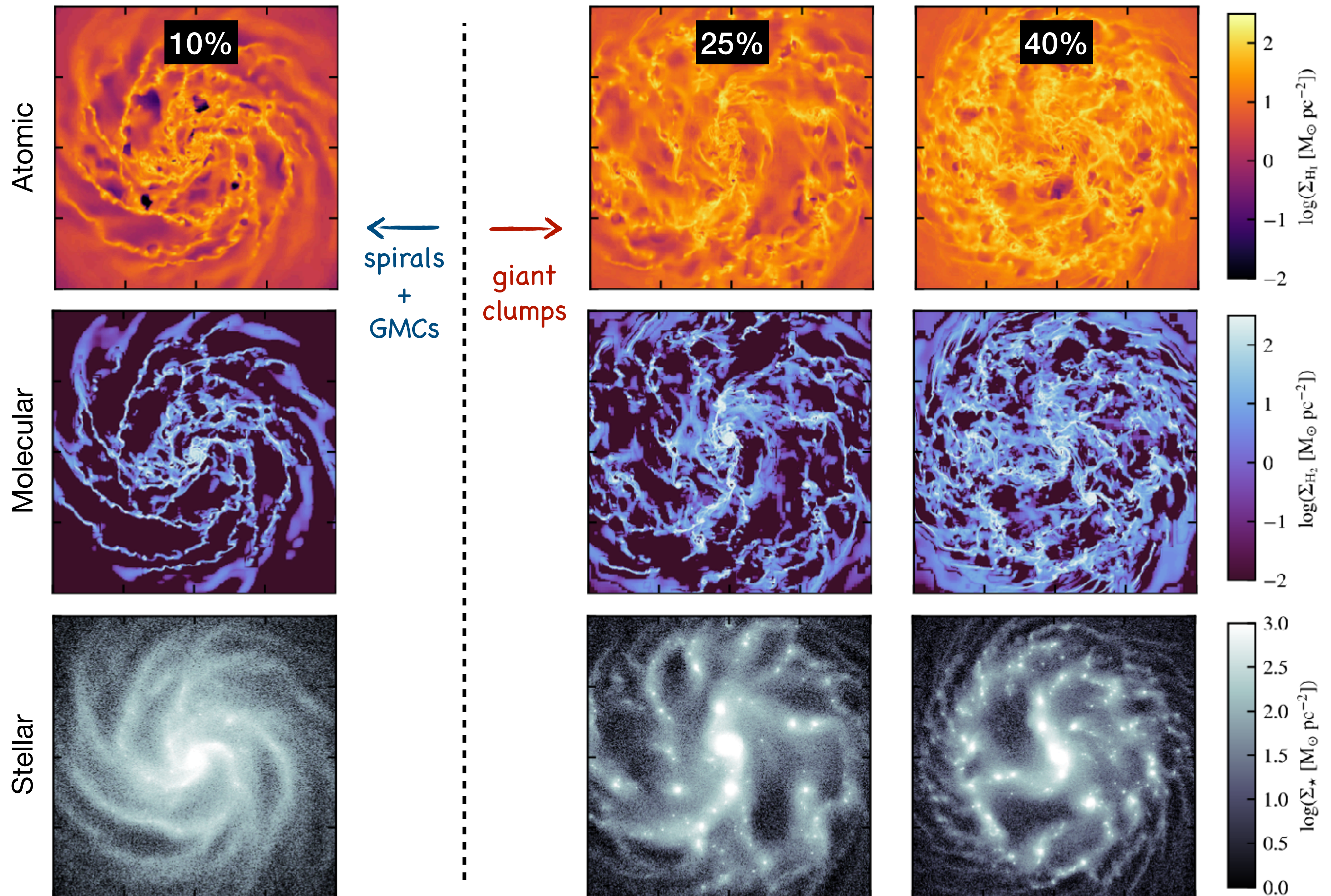


Movies: evolution of the gas density in simulations of isolated disks with different gas fractions. High gas fraction favor the onset of a different regime of instability, while low fractions maintain a disk regime, e.g. with spiral arms. The different structure of the ISM impacts the star formation activity (rate, efficiency). (Renaud et al. 2021c)

MORPHOLOGICAL EFFECTS OF VARYING THE GAS FRACTION

Fig: atomic, molecular, and stellar density of simulations of isolated disk galaxies with different gas fractions

When changing the gas fraction only, one move from a spiral structure, to a morphology dominated by massive clumps.
(Renaud et al. 2021c)



SUPPLEMENTARY MATERIAL

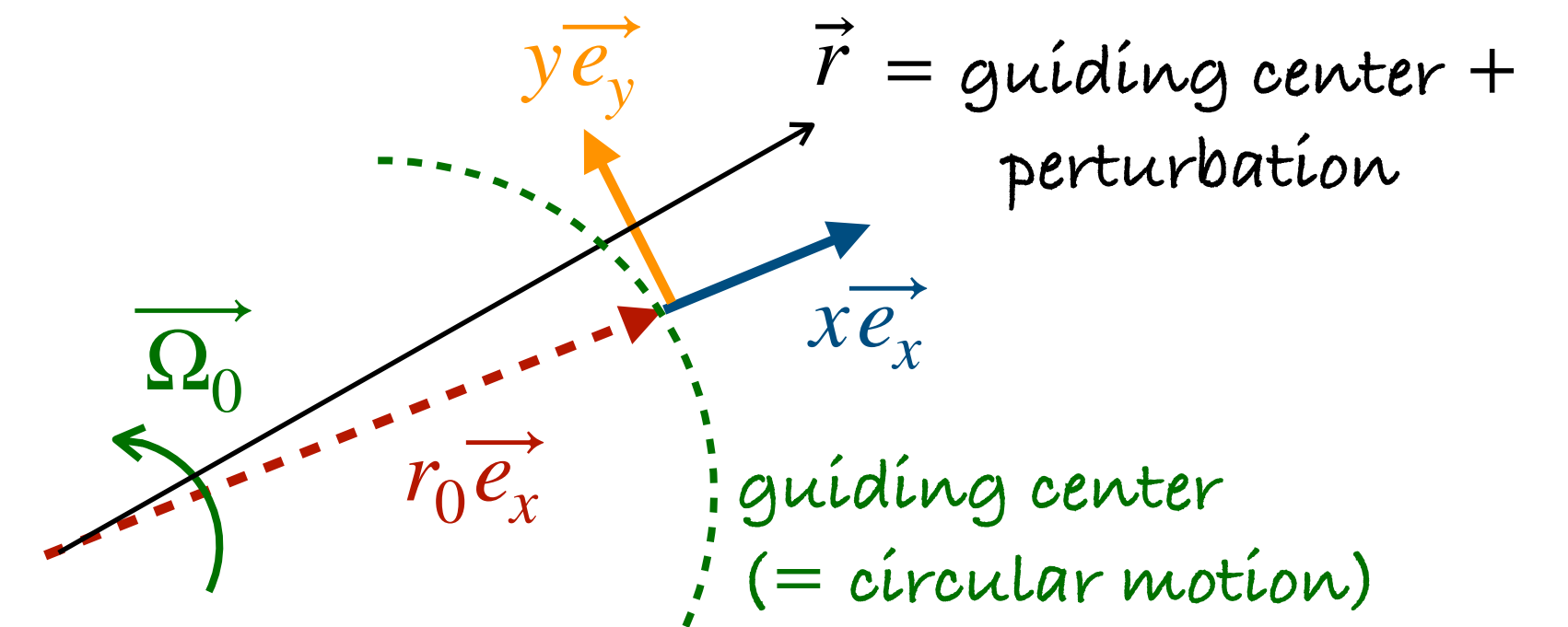
- Epicycle frequency
- Lindblad resonances
- Lane-Emden equation and the Bonnor-Ebert mass
- Jeans length and Jeans mass
- Jeans length including tides
- Virial theorem
- Safronov / Toomre Q parameter
- Romeo & Falstad Q parameter

EPICYCLE FREQUENCY (1/2)

Consider a perturbation from a circular orbit in a disk: the position is $\vec{r} = (r_0 + x)\vec{e}_x + y\vec{e}_y$

In the rotating reference frame (non-inertial), the equation of motion is

$$\frac{d^2\vec{r}}{dt^2} = \underbrace{-\vec{\nabla}\Phi}_{\text{gravity}} - \underbrace{2\vec{\Omega}_0 \times \vec{v}}_{\text{Coriolis}} - \underbrace{\vec{\Omega}_0 \times (\vec{\Omega}_0 \times \vec{r})}_{\text{centrifugal}}$$



We do a Taylor expansion of the gravitational force:

$$\vec{\nabla}\Phi = \Omega^2\vec{r} \approx \left(\Omega_0 + x \left. \frac{d\Omega}{dr} \right|_{r=r_0} \right)^2 \left[(r_0 + x)\vec{e}_x + y\vec{e}_y \right] \approx \left[\Omega_0^2 r_0 + \Omega_0^2 x + 2r_0 \Omega_0 x \left. \frac{d\Omega}{dr} \right|_{r=r_0} \right] \vec{e}_x + \Omega_0^2 y \vec{e}_y$$

$$\text{and } \frac{d^2x}{dt^2}\vec{e}_x + \frac{d^2y}{dt^2}\vec{e}_y \approx \left[-\Omega_0^2(r_0 + x) - 2r_0 \Omega_0 x \left. \frac{d\Omega}{dr} \right|_{r=r_0} \right] \vec{e}_x - \Omega_0^2 y \vec{e}_y + \underbrace{2\Omega_0 \frac{dy}{dt} \vec{e}_x - 2\Omega_0 \frac{dx}{dt} \vec{e}_y}_{\text{Coriolis}}$$

$$+ \underbrace{\Omega_0^2 (r_0 + x) \vec{e}_x + \Omega_0^2 y \vec{e}_y}_{\text{gravity}}$$

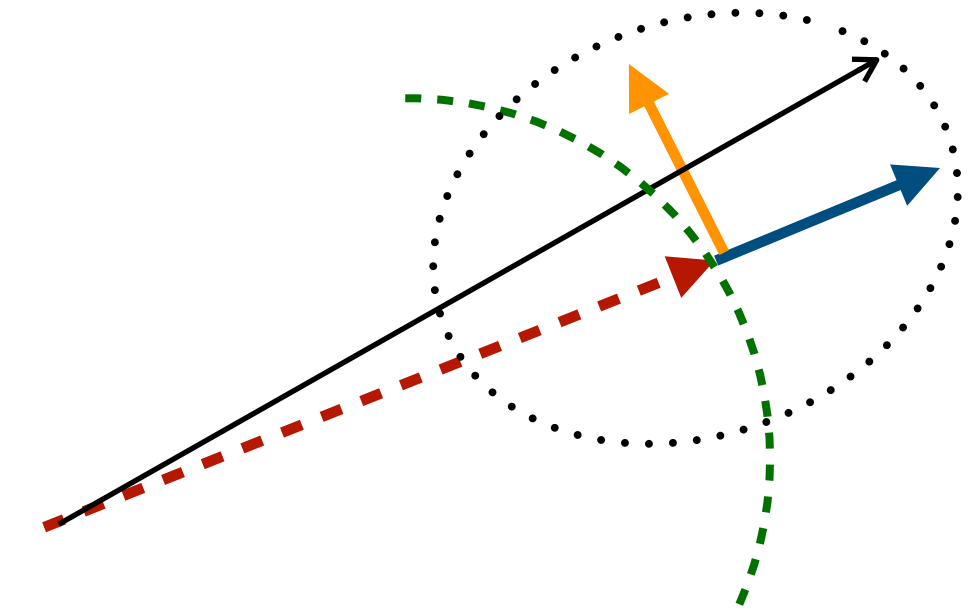
EPICYCLE FREQUENCY (2/2)

Possible solutions (as small oscillations around the guiding center):
 $x = x_0 \cos(\kappa t + \phi)$ and $y = y_0 \sin(\kappa t + \phi)$

$$\text{and then } \frac{d^2x}{dt^2} \approx -2r_0\Omega_0x \left. \frac{d\Omega}{dr} \right|_{r=r_0} + 2\Omega_0 \frac{dy}{dt} \quad \text{and} \quad \frac{d^2y}{dt^2} \approx -2\Omega_0 \frac{dx}{dt}$$

$$\text{which gives: } -\kappa^2 x_0 \cos(\kappa t + \phi) = -2r_0\Omega_0x_0 \cos(\kappa t + \phi) \left. \frac{d\Omega}{dr} \right|_{r=r_0} + 2\kappa\Omega_0y_0 \cos(\kappa t + \phi)$$

$$\text{and } -\kappa^2y_0 \sin(\kappa t + \phi) = 2\kappa\Omega_0x_0 \sin(\kappa t + \phi)$$



Therefore: $y_0 = -\frac{2\Omega_0}{\kappa}x_0$ and finally

$$\kappa^2 = \left(r \frac{d\Omega^2}{dr} + 4\Omega^2 \right)_{r=r_0}$$

κ is called the epicycle frequency

= frequency of the oscillations around a guiding center which is in circular motion

Special cases:

- solid-body: $\Omega = \text{cst} \rightarrow \kappa = 2\Omega$
- Kepler rotation: $\Omega = v_c/r = \sqrt{GM/r^3} \rightarrow \kappa = \Omega$

\rightarrow usually: $\Omega < \kappa < 2\Omega$

(at the position of the Sun: $\kappa \approx 1.4\Omega$)

RESONANCES

A resonance occurs when the orbital frequency of the star is an integer multiple of that of a forcing.

The forcing can be a rotating bar, and/or successive crests of spiral waves, and/or a triaxial halo, and/or a companion galaxy, ...

The frequency of the forcing is called the pattern speed: Ω_p

Thus, resonances occur for $\kappa = m(\Omega - \Omega_p)$ where m is an integer

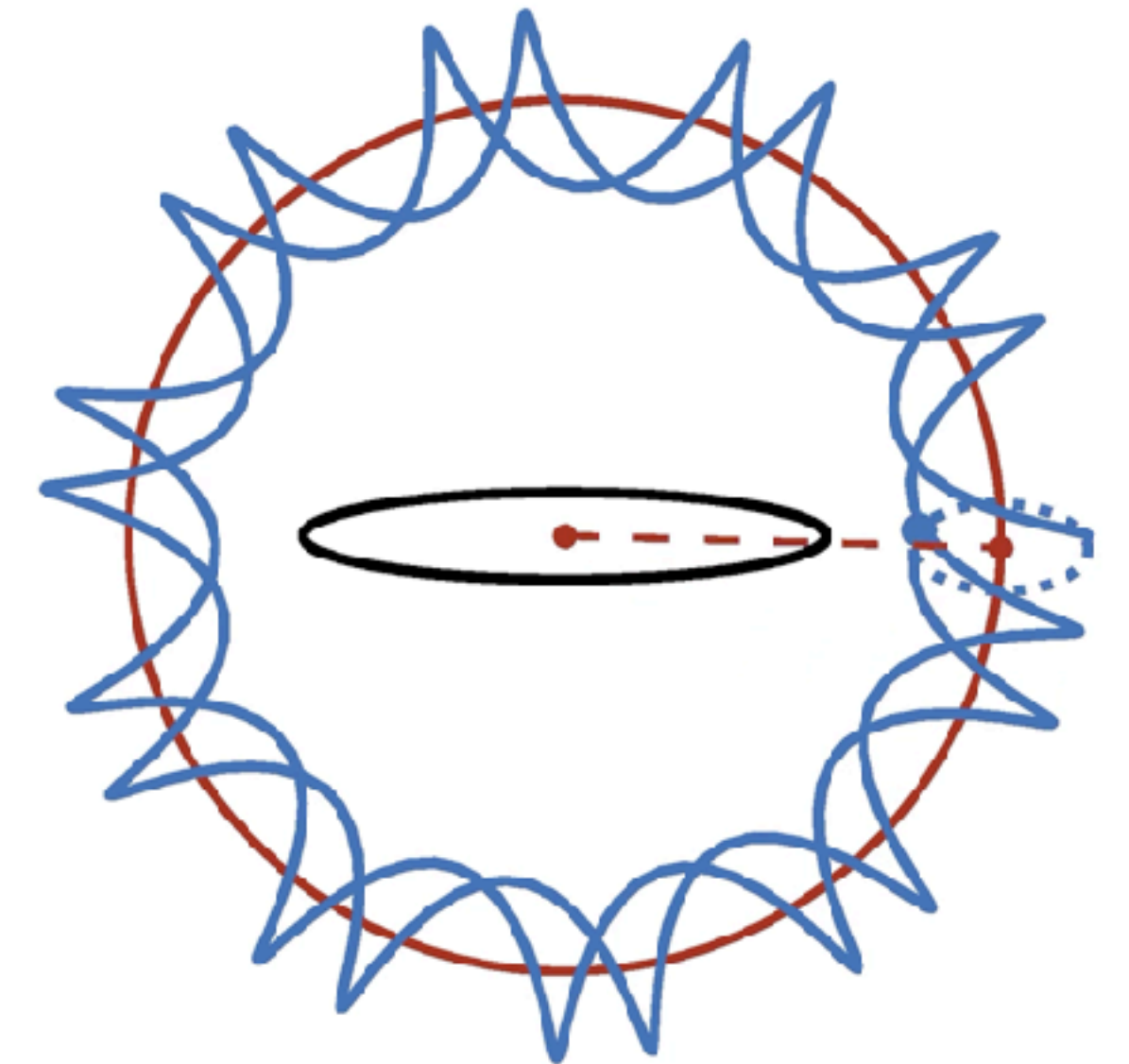
$m = \pm 2$ are a special set of resonances called Lindblad resonances

$|m| > 2$ also exist but have a smaller importance

Waves (e.g. spirals) are trapped in between resonances

If m is not an integer, the orbits are not closed, which induces a precession (and no resonance)

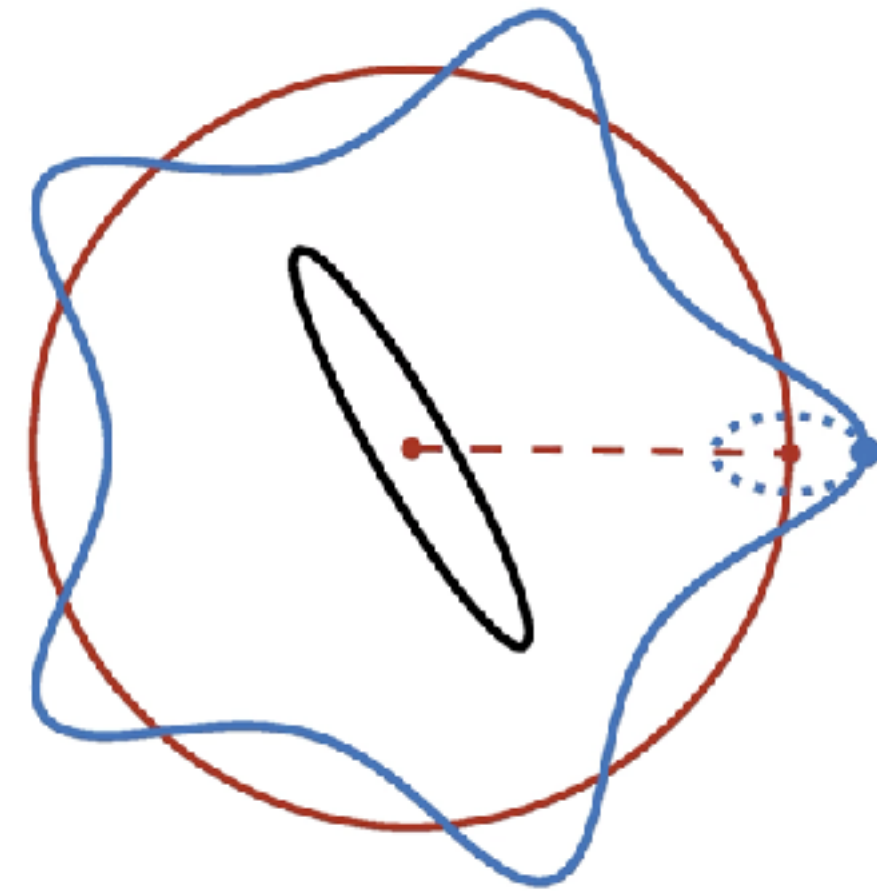
In real galaxies, there are several superimposed forcings and thus multiple pattern speeds.



Movie: epicycle in the rotating reference frame, with $\kappa = -10.3(\Omega - \Omega_p)$: the orbit is not closed, and thus it precesses

LINDBLAD RESONANCES (1/2)

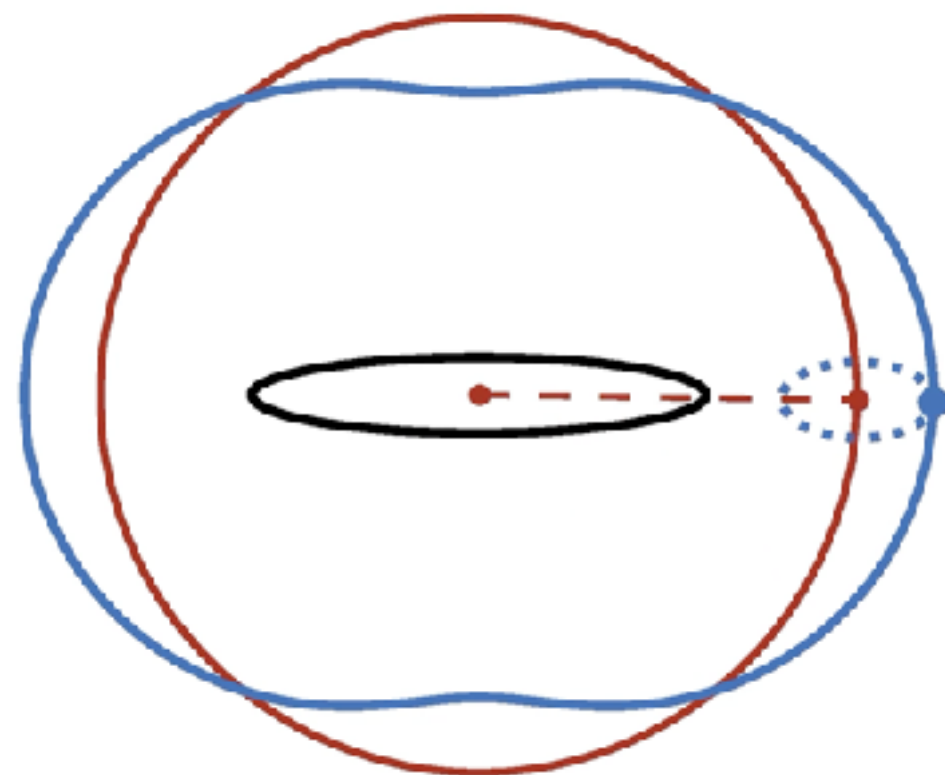
Consider an epicyclic motion in a barred galaxy



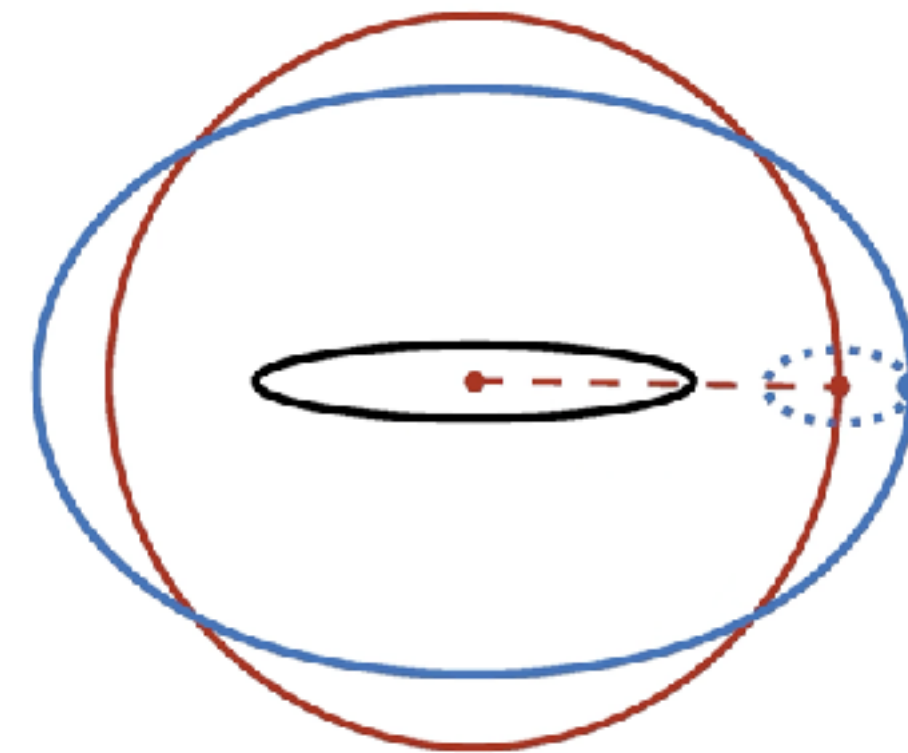
blue = star
red = guiding center
black = galactic bar
(here, $\kappa = 5\Omega$, for illustration only)

The bar has a velocity Ω_p
(here, $\Omega_p = \Omega/3$, for illustration)

Now, let's go to the reference frame of the bar:

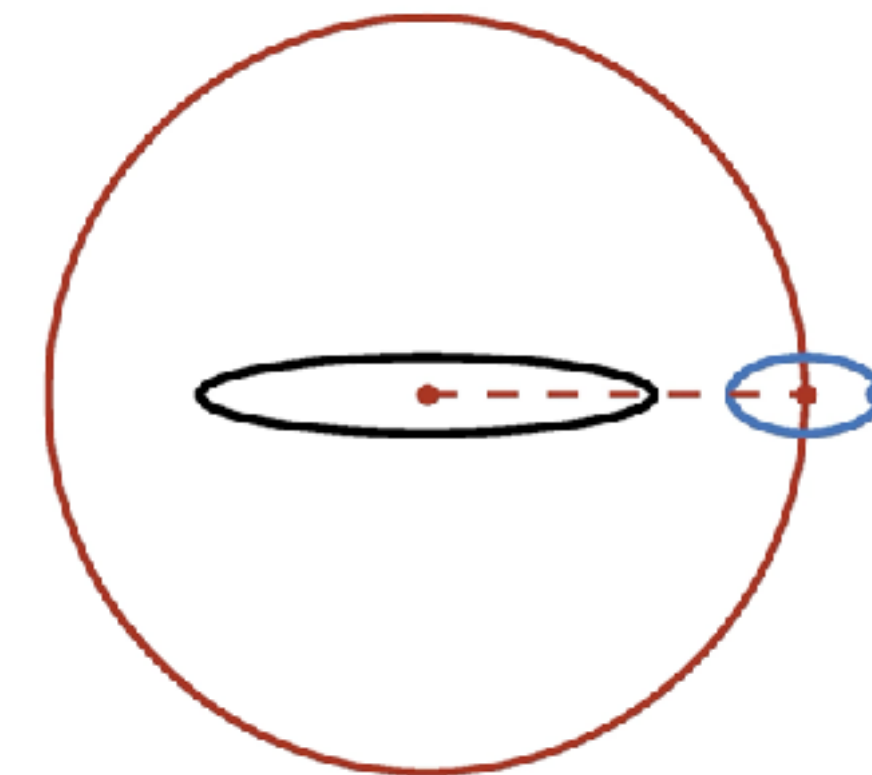


$\kappa = 2(\Omega - \Omega_p)$
→ inner Lindblad resonance (ILR)
i.e. $\Omega_p = \Omega - \frac{\kappa}{2}$



$\kappa = -2(\Omega - \Omega_p)$
→ outer Lindblad resonance (OLR)
i.e. $\Omega_p = \Omega + \frac{\kappa}{2}$

Same as ILR, but with a retrograde motion



Co-rotation:
 $\Omega_p = \Omega$
The star feels a steady potential from the bar

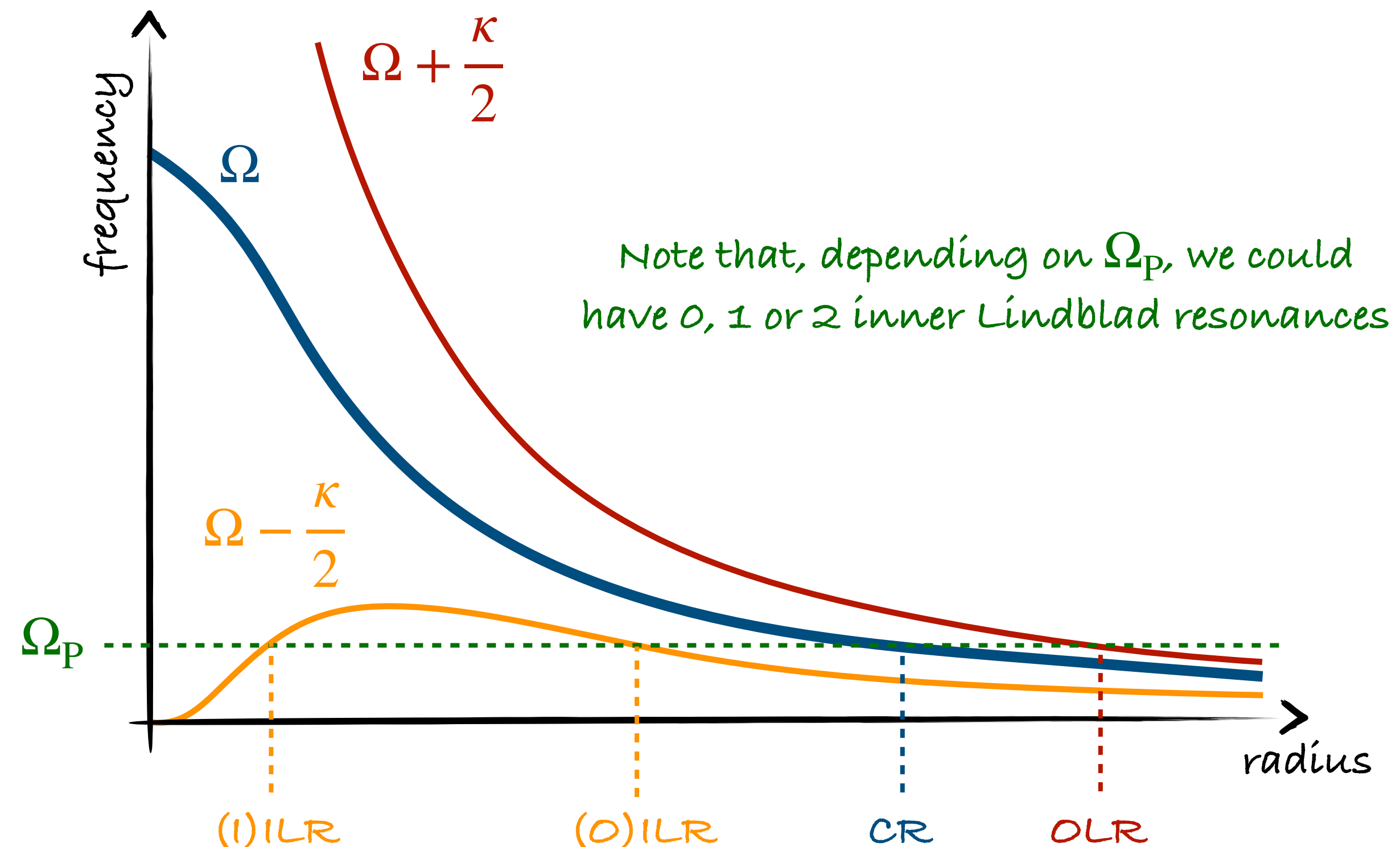
LINDBLAD RESONANCES (2/2)

With the velocity curve (or equivalently the potential) of the galaxy known, we can construct the frequency profile, i.e. $\Omega(r)$,

and compute $\kappa = \sqrt{r \frac{d\Omega^2}{dr} + 4\Omega^2}$

and plot, Ω and $\Omega \pm \frac{\kappa}{2}$ as functions of radius

For a given pattern speed Ω_p , we can find the radii of corotation and of Lindblad resonances



The effective potential (gravitational + non inertial terms) has barriers at the resonances
 → waves are trapped in between the Lindblad resonances

LANE-EMDEN EQUATION (1/3): THE SINGULAR ISOTHERMAL SPHERE

Consider a sphere of gas in hydrostatic equilibrium (pressure = gravity):

$$\frac{dP}{dr} = - \frac{Gm(< r)\rho}{r^2} \quad (\text{note that } \rho \text{ depends on } r)$$

The equation of state of an ideal gas gives $P = nk_{\text{B}}T = c_s^2\rho$ and thus $\frac{r^2}{\rho} \frac{d\rho}{dr} = - \frac{G}{c_s^2} m(< r)$

with the mass distribution being: $m(< r) = \int \rho dV = \int_0^r 4\pi r^2 \rho dr$ (in spherical symmetry), i.e. $\frac{dm}{dr} = 4\pi r^2 \rho$

Taking the derivative WRT r , we get the Lane-Emden equation: $\frac{1}{r^2} \frac{d}{dr} \left(\frac{r^2}{\rho} \frac{d\rho}{dr} \right) = - \frac{4\pi G\rho}{c_s^2}$

A simple solution is $\rho \propto r^{-2}$, i.e. a singularity at $r = 0$. This is called the singular isothermal sphere.

(The exact solution is $\rho = \frac{c_s^2}{2\pi Gr^2}$)

Unphysical, but simple and regularly used.

LANE-EMDEN EQUATION (2/3): THE BONNOR-EBERT SPHERE

Non-singular solutions exist if we impose boundary conditions: a finite central density: $\rho(r = 0) = \rho_c$ and the equilibrium with an external pressure $P(r = r_e) = P_e = c_s^2 \rho(r = r_e)$

This solution of a cloud of isothermal gas confined by external pressure is called a Bonnor-Ebert sphere.

Let's change variables: $\rho = \rho_c \exp(x)$ and $r = y \sqrt{\frac{c_s^2}{4\pi G \rho_c}}$

The new differential equation reads $\frac{1}{y^2} \frac{d}{dy} \left(y^2 \frac{dx}{dy} \right) + \exp(x) = 0$

Introducing $w = y^2 \frac{dx}{dy}$, we get $\frac{dw}{dy} = -y^2 \exp(x)$, and these 2 first order ODEs can be solved numerically.

LANE-EMDEN EQUATION (2/3): THE BONNOR-EBERT MASS

The mass enclosed by a Bonnor-Ebert sphere is $m(< r) = \int_0^r 4\pi r^2 \rho dr = 4\pi \rho_c \left(\frac{c_s^2}{4\pi G \rho_c} \right)^{3/2} \int_0^y y^2 \exp(x) dy$

Combined with the Lane-Emden equation and integrating for the total mass (i.e. up to $r = r_e$), we get

$$M = \frac{c_s^3}{\sqrt{4\pi G^3 \rho_c}} \left(y^2 \frac{dx}{dy} \right)_{y=y'_e}$$

The form of the right-hand side term implies that unstable conditions exist.

Gravity overcomes internal pressure when the mass of the cloud exceeds a certain value (found numerically):

$$M \gtrsim M_{\text{BE}} = 1.18 \frac{c_s^4}{\sqrt{G^3 P_e}}$$

M_{BE} is the Bonnor-Ebert mass, used as a criterion for stability against collapse.

JEANS LENGTH AND MASS

Consider a density perturbation ρ_1 in a homogeneous medium of density ρ with the speed of sound c_s . We consider only self-gravity and pressure forces.

The perturbation is unstable if its wavelength is larger than the Jeans length: $\lambda_J = \sqrt{\frac{\pi c_s^2}{G\rho}}$

or equivalently if the mass involved is larger than the Jeans mass: $M_J = \frac{\pi^{5/2} c_s^3}{6G^{3/2} \rho^{1/2}}$

For instance: a cloud above this mass ("*important gravity*") will collapse and form stars (when ignoring external forces)

The Jeans and Bonnor-Ebert masses are very similar and relate to comparable stability criteria:

$$M_J \approx 2.92 \frac{c_s^3}{\sqrt{G^3 \rho}} \quad \text{and} \quad M_{\text{BE}} \approx 1.18 \frac{c_s^3}{\sqrt{G^3 \rho}} \quad (\text{using } P_e = c_s^2 \rho)$$

JEANS LENGTH AND MASS (1/2)

Apply Euler equations to a perturbation density ρ_1 in a homogeneous medium of density ρ . The linearized equations are

- (1) Continuity $\frac{\partial \rho_1}{\partial t} + \rho \nabla v_1 = 0$
- (2) Force $\rho \frac{\partial v_1}{\partial t} = -\rho \nabla \phi_1 - \nabla P_1$
- (3) Poisson's equation $\nabla^2 \phi_1 = 4\pi G \rho_1$
- (4) Equation of state
(barotropic here) $P_1 = c_s^2 \rho_1$

*Details on where this comes from in
Binney and Tremaine (2008)
about the "Jeans swindle"*

Time derivative of (1): $\frac{\partial^2 \rho_1}{\partial t^2} + \rho \frac{\partial \nabla v_1}{\partial t} = \frac{\partial^2 \rho_1}{\partial t^2} + \rho \nabla \left(\frac{\partial v_1}{\partial t} \right) = 0$

Divergence of (2), combined with (4): $\rho \nabla \left(\frac{\partial v_1}{\partial t} \right) = -\rho \nabla^2 \phi_1 - c_s^2 \nabla^2 \rho_1$

The above-two combined with (3): $\frac{\partial^2 \rho_1}{\partial t^2} = 4\pi G \rho \rho_1 + c_s^2 \nabla^2 \rho_1$

JEANS LENGTH AND MASS (2/2)

The solutions of the differential equation $\frac{\partial^2 \rho_1}{\partial t^2} = 4\pi G \rho \rho_1 + c_s^2 \nabla^2 \rho_1$ are $\rho_1(x, t) \propto \exp [i (kx - \omega t)]$

When injecting into the equation: $(-i\omega)^2 \rho_1 = 4\pi G \rho \rho_1 + c_s^2 (ik)^2 \rho_1$
 $-\omega^2 \rho_1 = 4\pi G \rho \rho_1 - c_s^2 k^2 \rho_1$
 $\omega^2 = c_s^2 k^2 - 4\pi G \rho$ which is the dispersion equation of the perturbation

The perturbation grows (i.e. we have an instability instead of an oscillation) if $\omega^2 < 0$, i.e. $c_s^2 k^2 < 4\pi G \rho$

In term of wavelength $\lambda = \frac{2\pi}{k}$ we get $\lambda^2 > \frac{\pi c_s^2}{G \rho}$ which defines the Jeans length $\lambda_J = \sqrt{\frac{\pi c_s^2}{G \rho}}$

In term of mass: $M_J = \frac{4}{3} \pi \rho \left(\frac{\lambda_J}{2} \right)^3 = \frac{\pi^{5/2} c_s^3}{6 G^{3/2} \rho^{1/2}}$ (λ_J is the "diameter" of the unstable region)

JEANS CRITERION INCLUDING TIDES

In the Jeans formalism, we study the propagation of a perturbation in a homogeneous Universe

In reality, a non-flat gravitational potential induces tides, which alter the stability criteria

The Jeans criterion can be modified to include tidal effects:
(Jog 2013, 2014, Mondal & Chakraborty 2015)

$$M_{\text{Jeans}} \propto \frac{1}{(1 - \lambda)^{3/2}} \left(\frac{v_s^2}{G\rho^{1/3}} \right)^{3/2}$$

internal pressure

correction term for the tides

self-gravity

With classical tides: $\lambda > 0$

It goes with pressure and acts as a support against collapse

With compressive tides: $\lambda < 0$ (see Renaud et al. 2008, 2009)

It goes with self-gravity and favors collapse

VIRIAL THEOREM

For a system in isolation, in a stationary state of equilibrium:

$$E_{\text{kin}} = -\frac{E_{\text{pot}}}{2} \quad \text{also often written:} \quad 2K + W = 0$$

Therefore, for a virialized system:

$$E = E_{\text{kin}} + E_{\text{pot}} = \frac{E_{\text{pot}}}{2} = -E_{\text{kin}}$$

Being virialized is not the same as being in equilibrium (see the derivation on the next slides)

VIRIAL THEOREM (1/5)

The moment of inertia of a system made of N particles is $I = \sum_i m_i r_i^2$

Its time derivative is $\frac{dI}{dt} = 2 \sum_i m_i r_i \frac{dr_i}{dt} = 2 \sum_i m_i r_i v_i$

The quantity $Q = \frac{1}{2} \frac{dI}{dt}$ is called the virial.

The time derivative of the virial is $\frac{dQ}{dt} = \sum_i m_i (v_i^2 + r_i a_i) = \sum_i m_i v_i^2 + \sum_i r_i \sum_{j \neq i} F_{ij}$
 $\Rightarrow \sum_i m_i v_i^2 + \sum_i \sum_{j < i} r_{ij} F_{ij}$

This step is explained in 2 different ways on the next 2 pages.

VIRIAL THEOREM (2/5)

Explanation #1 for the double sum:

$$\sum_i r_i \sum_{j \neq i} F_{ij} = \sum_i r_i \left(\sum_{j < i} F_{ij} + \sum_{j > i} F_{ij} \right) = \sum_i \sum_{j < i} r_i F_{ij} + \sum_i \sum_{j > i} r_i F_{ij} \quad (\text{we split the innermost sum})$$

About the last term: $\sum_i \sum_{j > i} r_i F_{ij} = \sum_j \sum_{i < j} r_i F_{ij}$ (we inter-change the sums)

$$= \sum_i \sum_{j < i} r_j F_{ji} \quad (\text{we change the name of the indexes, nothing else})$$

$$= - \sum_i \sum_{j < i} r_j F_{ij} \quad (\text{from Newton's 3rd law})$$

Back to the first line: $\sum_i r_i \sum_{j \neq i} F_{ij} = \sum_i \sum_{j < i} r_i F_{ij} - \sum_i \sum_{j < i} r_j F_{ij}$

$$= \sum_i \sum_{j < i} (r_i - r_j) F_{ij} = \sum_i \sum_{j < i} r_{ij} F_{ij}$$

VIRIAL THEOREM (3/5)

Explanation #2 for the double sum:

$$\begin{aligned} \sum_i r_i \sum_{j \neq i} F_{ij} &= \\ &= r_1 (F_{12} + F_{13} + F_{14} + \dots) + r_2 (F_{21} + F_{23} + F_{24} + \dots) + r_3 (F_{31} + F_{32} + F_{34} + \dots) + \dots \\ &= r_1 (F_{12} + F_{13} + F_{14} + \dots) + r_2 (-F_{12} + F_{23} + F_{24} + \dots) + r_3 (-F_{13} - F_{23} + F_{34} + \dots) + \dots \\ &= [F_{12}(r_1 - r_2) + F_{13}(r_1 - r_3) + F_{14}(r_1 - r_4) + \dots] + [F_{23}(r_2 - r_3) + F_{24}(r_2 - r_4) + \dots] + [F_{34}(r_3 - r_4) + \dots] + \dots \\ &= [F_{12}r_{12} + F_{13}r_{13} + F_{14}r_{14} + \dots] + [F_{23}r_{23} + F_{24}r_{24} + \dots] + [F_{34}r_{34} + \dots] + \dots \\ &= \sum_i \sum_{j < i} r_{ij} F_{ij} \end{aligned}$$

VIRIAL THEOREM (4/5)

Suppose that the force attracts the particles as the inverse power q of the their distance:

$$F_{ij} = -\frac{k}{r_{ij}^q} \quad (\text{for gravitation, } q=2)$$

The potential energy of this force is $U_{ij} = -\int F_{ij} dr = -\frac{k}{(q-1)r_{ij}^{q-1}}$

and thus $r_{ij}F_{ij} = -\frac{k}{r_{ij}^{q-1}} = (q-1)U_{ij}$

Back to the virial: $\frac{dQ}{dt} = \sum_i m_i v_i^2 + \sum_i \sum_{j<i} (q-1)U_{ij} = 2E_{\text{kin}} + (q-1)E_{\text{pot}}$

When Q is constant (see what it means on the next page), and for the gravitation force ($q=2$):

$$\frac{dQ}{dt} = 0 \implies E_{\text{kin}} = -\frac{E_{\text{pot}}}{2}$$

VIRIAL THEOREM (5/5)

The time average of a quantity X is $\langle X \rangle = \lim_{\tau \rightarrow \infty} \frac{1}{\tau} \int_0^\tau X dt$

Applied to the derivative of Q , we get $\langle \frac{dQ}{dt} \rangle = \lim_{\tau \rightarrow \infty} \frac{1}{\tau} \int_0^\tau \frac{dQ}{dt} dt = \lim_{\tau \rightarrow \infty} \frac{Q(\tau) - Q(0)}{\tau}$

This is equal to zero if Q takes finite values, which typically means a bound system with regular motions. This leads to the virial theorem.

In principle, we can only apply this when averaging over infinite time ($\tau \rightarrow \infty$). But for large N systems we can invoke the ergodic principle:

Averaging over an infinite time $\lim_{\tau \rightarrow \infty} \frac{1}{\tau} \int_0^\tau dt$ is equivalent to averaging over many objects $\lim_{N \rightarrow \infty} \frac{1}{N} \sum_N$

and therefore, $E_{\text{kin}} = -\frac{E_{\text{pot}}}{2}$ when the energies are the averages over many particles (e.g. star clusters, galaxies)

THE SAFRONOV / TOOMRE Q PARAMETER

Local instability criterion for an axisymmetric thin disk

The disk is stable to axisymmetric perturbations (only!)

$$\text{for } Q \equiv \frac{\kappa C_s}{\pi G \Sigma_0} > 1 \text{ (for gas) or } Q \equiv \frac{\kappa \sigma_R}{3.36 G \Sigma_0} > 1 \text{ (for stars)}$$

It's comparable (but not equivalent) to Jeans' criterion
for 3D waves (pressure vs. gravity)

In stellar + gaseous disks, we need a mix of the gas and stellar Q
which evolves with the gas fraction (several theoretical propositions)

In practice, instabilities are often seen even for $Q \gtrsim 2$, because of
assumptions in the formalism, and because of non-axisymmetric effects

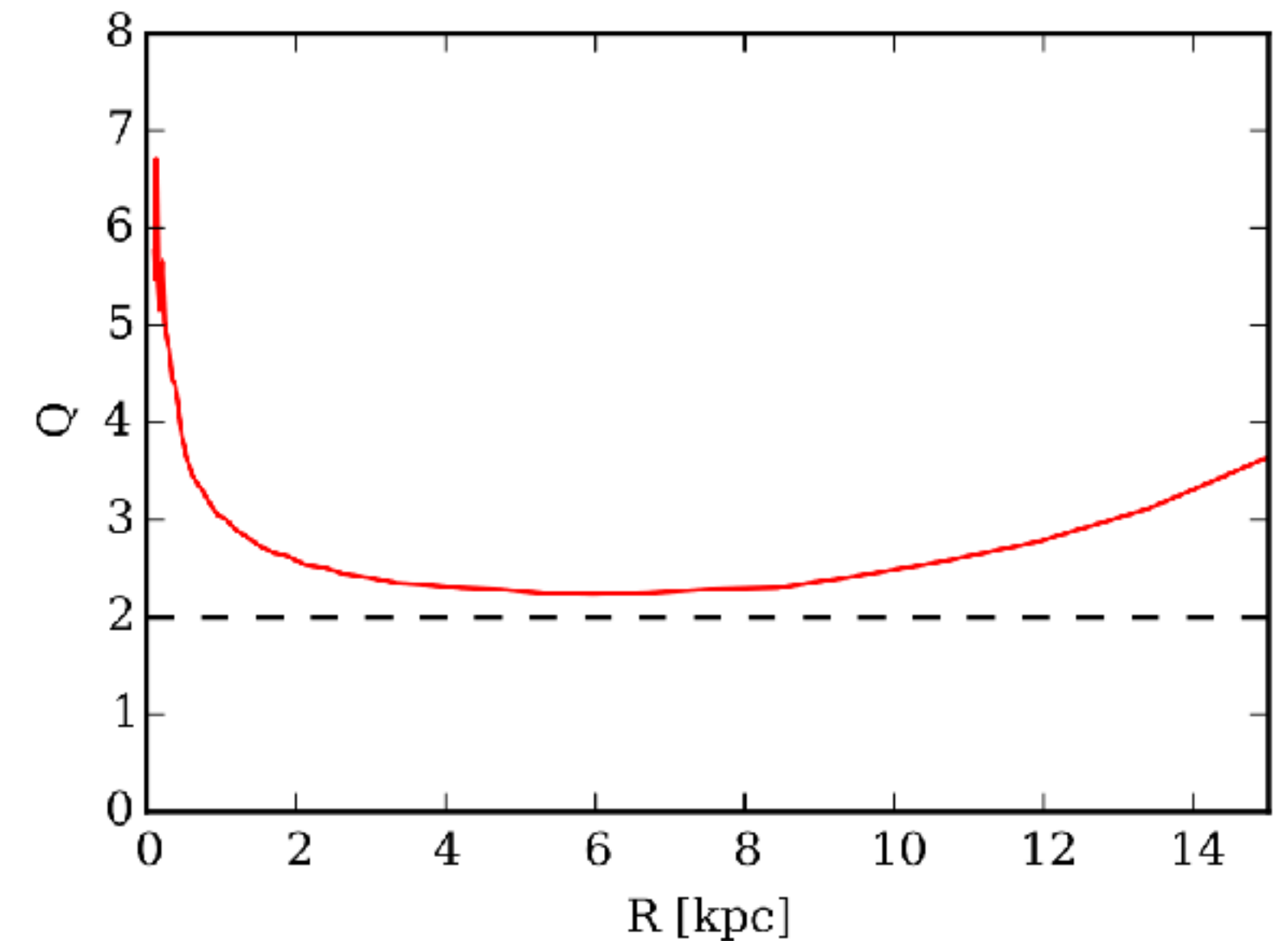


*Fig: example of a radial profile
of Toomre Q
(Semczuk et al. 2016)*

THE ROMEO & FALSTAD (2013) STABILITY PARAMETER

Limitations of the Safronov / Toomre Q parameters:

- does not account for more than one component (stars *or* gas)
- relies on the razor thin disk approximation: $kh \ll 1$
(i.e. perturbation scale \gg disc scale-height))

It does not have a predictive power on real galaxies

Alternative: the Wang & Silk (1994) parameter: $Q_{\text{WS}} = \left(\frac{1}{Q_{\star}} + \frac{1}{Q_{\text{g}}} \right)^{-1}$

But it does not account for the mutual effect of the components on each others, nor for different weights of the components

Better alternative: the Romeo & Falstad (2013) parameter:

- sum over the components
- weight the Toomre parameters with a correction factor (W / T)

(see an application to simulated disk galaxies in Renaud et al. 2021c)

how different from the
most unstable component

$$Q_{\text{RF}} = \left(\sum_i \frac{1}{Q_i} \frac{W_i}{T_i} \right)^{-1}$$

disc
thickness